Division of Plastic, Aesthetic and Reconstructive Surgery
Department of Surgery
Medical University of Graz

Local alterations in scars

or

Contributing factors to hypertrophic scar formation – implementation of a novel Duroc pig model

Dissertation
submitted for the degree of
Doctor of Medical Science (Dr. scient. med.)
at the
Medical University of Graz

by
Priv.-Doz. Dr. med. Sebastian P. NISCHWITZ

under the supervision of
Univ.-Prof. Dr. med. Lars-Peter KAMOLZ, MSc.

2023

"Progress is impossible without change,
and those who cannot change their minds cannot change anything."

George Bernard Shaw

Statutory Declaration

I hereby declare that this thesis is my own original work and that I have fully acknowledged by name all of those individuals and organizations that have contributed to the research for this thesis.
Due acknowledgement has been made in the text to all other material used. Throughout this thesis and in all related publications I followed the "Guidelines of the Medical University of Graz on Good Scientific Practice".

Graz, 14th August 2023 Sebastian P. Nischwitz

Disclosures

Parts of this thesis have been published similarly or identically in (Nischwitz, S.P.; Fink, J.; Schellnegger, M.; Luze, H.; Bubalo, V.; Tetyczka, C.; Roblegg, E.; Holecek, C.; Zacharias, M.; Kamolz, L.-P.; et al. The Role of Local Inflammation and Hypoxia in the Formation of Hypertrophic Scars—A New Model in the Duroc Pig. Int. J. Mol. Sci. 2023, 24,316. https://doi.org/10.3390/ ijms24010316.), which is hereby referenced [1]. There may be congruencies in content or form in this work that are not explicitly marked. Even though great care was taken to reference this publication when appropriate, it is not completely excluded that certain passages have been unintentionally overlooked.

It is hereby confirmed that (a) the authors of the above-mentioned publication are the sole copyright holders due to open access publication and (b) all co-authors agree to the use of the data obtained within this project in the present doctoral thesis.

Institutional Review Board approval

The Federal Ministry Republic of Austria, Education, Science and Research (BMBWF-66.010/0116-V/3b/2019) approved the animal study protocol. No patient or human data was involved in this study, waiving the need for informed consent and/or ethics committee approval.

Funding Information and Conflict of Interest

This project (and thereby this resulting doctoral thesis) was funded by the Medical University of Graz and JOANNEUM RESEARCH Forschungsgesellschaft mbH (Graz, Austria). While conducting the experimental part of the project, I was an employee of the Division of Plastic, Aesthetic and Reconstructive Surgery, Department of Surgery, Medical University of Graz and COREMED – Center for Regenerative Medicine and Precision Medicine at JOANNEUM RESEARCH Forschungsgesellschaft mbH. The scientific work for this project in my role as a student of the Medical University of Graz did not collide with my duties as employee of the aforementioned institutions; it was conducted in compliance with the guidelines of good scientific practice. The funding parties did not influence the data and results of this project. No conflict of interest is to be reported.

Contributions

The following people have supported this doctoral thesis through their expertise in alphabetical order:

- DI Dr. Thomas Birngruber [1]
- Kaddour Bounab [2]
- Dr. med. vet. Vladimir Bubalo and his team [3]
- Julia Fink, BSc, MSc [4]
- Christian Holecek [1]
- Univ.-Prof. Dr. med. Lars-Peter Kamolz, MSc [4,5,6]
- Ass.-Prof. Mag. Dr. rer. nat. Petra Kotzbeck [4,5,7]
- Priv.-Doz. Dr. scient med. Dr. med. univ. Hanna Luze [4,5]
- Univ.-Prof. Mag. pharm. Dr. rer. nat. Eva Roblegg [8]
- Mag. Dr. med. univ. Marlies Schellnegger [4,5]
- Univ.-Prof. Dr. med. univ. Stephan Spendel [5]
- Mag. pharm. Dr. rer. nat. Carolin Tetyczka [8]
- Dr. med. univ. Martin Zacharias [9]

[1] HEALTH – Institute for Biomedicine and Health Sciences, JOANNEUM RESEARCH Forschungsgesellschaft mbH, Graz, Austria

[2] Division of Endocrinology and Diabetology, Department of Internal Medicine, Medical University of Graz, Graz, Austria

[3] Biomedical Research Unit, Medical University of Graz, Graz, Austria

[4] COREMED – Center for Regenerative Medicine and Precision Medicine, JOANNEUM RESEARCH Forschungsgesellschaft mbH, Graz, Austria

[5] Division of Plastic, Aesthetic and Reconstructive Surgery, Department of Surgery, Medical University of Graz, Graz, Austria

[6] Research Unit for Safety and Sustainability in Health Care, Medical University of Graz, Graz, Austria

[7] Research Unit for Tissue Regeneration, Repair and Reconstruction, Medical University of Graz, Graz, Austria

[8] Department of Pharmaceutical Technology and Biopharmacy, Institute of Pharmaceutical Sciences, University of Graz, Graz, Austria
[9] Diagnostic and Research Institute of Pathology, Medical University of Graz, Graz, Austria

Thomas Birngruber and Stephan Spendel supported this project with valuable input as part of the dissertation committee. Kaddour Bounab was responsible for sample handling and histological slide preparation, which trained pathologist Martin Zacharias has then analyzed. Vladimir Bubalo and his team were responsible for animal handling and well-being. Julia Fink performed the gene expression analysis. Christian Holecek was a valuable help during the experimental phase, as were Julia Fink, Hanna Luze, and Marlies Schellnegger. Hanna Luze and Marlies Schellnegger have also assisted in organizational issues and project administration. Eva Roblegg and Carolin Tetyczka were managing the ointment preparation. Lars-Peter Kamolz and Petra Kotzbeck supervised the project and gave valuable input in all project phases.

Publications

Parts of this thesis were similarly or identically published in:

- S.P. Nischwitz, J. Fink, M. Schellnegger, H. Luze, V. Bubalo, C. Tetyczka, E. Roblegg, C. Holecek, M. Zacharias, L.-P. Kamolz, P. Kotzbeck.
  The Role of Local Inflammation and Hypoxia in the Formation of Hypertrophic Scars—A New Model in the Duroc Pig.
  Int. J. Mol. Sci. 2023, 24, 316.
  doi: 10.3390/ ijms24010316.

Additional publications that originated from the preparational work of this project:

- S. Rössler, S.P. Nischwitz, H. Luze, J.C.J. Holzer-Geissler, R. Zrim, L.-P. Kamolz.
  In Vivo Models for Hypertrophic Scars-A Systematic Review.
  Medicina (Kaunas). 2022, 58(6):736.
  doi: 10.3390/medicina58060736.

- S.P. Nischwitz, K. Rauch, H. Luze, E. Hofmann, A. Draschl, P. Kotzbeck, L.-P. Kamolz.
  Evidence-based therapy in hypertrophic scars: An update of a systematic review.
  Wound Repair Regen. 2020 Sep;28(5):656-665.
  doi: 10.1111/wrr.12839.

Conference contributions

- S.P. Nischwitz.
  Hypoxia or inflammation – Which is the driving force of pathologic scarring?
  IMCAS Americas; JUL 2023; Cartagena de Indias, Colombia.

- S.P. Nischwitz.
  Wound oxygenation or inflammation - Where lies the future of scar therapy?
  IMCAS ASIA; JUN 2023; Bangkok, Thailand.

- S.P. Nischwitz, H. Luze, T. Rappl, L.-P. Kamolz.
  The Hypertrophic Scar: An Unwanted Problem After Surgery – The Evidence Behind Its Treatment.
  ISAPS World Congress; SEP 2022; Istanbul, Turkiye.

- S.P. Nischwitz, M. Schellnegger, J. Fink, H. Luze, V. Bubalo, P. Kotzbeck, S. Spendel, L.-P. Kamolz.
  Establishment of a hypertrophic scar model and the role of inflammatory processes in the Duroc pig.
  19th European Burns Association Congress; SEP 2022; Turin, Italy.

- S.P. Nischwitz, M. Schellnegger, J. Fink, H. Luze, V. Bubalo, P. Kotzbeck, T. Birngruber, S. Spendel, L.-P. Kamolz.
  PorcScar - Ein neues Modell der Hypertrophen Narbe am Duroc-Schwein.
  63. Chirurgenkongress, Östereichische Gesellschaft für Chirurgie; JUN 2022; Graz, Austria.

- S.P. Nischwitz, H. Luze, T. Rappl, L.-P. Kamolz.
  Evidence-based therapy of hypertrophic scars.
  IMCAS World Congress; MAY 2022; Paris, France.

- S.P. Nischwitz, M. Schellnegger, J. Fink, H. Luze, V. Bubalo, P. Kotzbeck, T. Birngruber, S. Spendel, L.-P. Kamolz.
  PorcScar: Etablierung eines Modells der hypertrophen Narbe und die Rolle inflammatorischer Prozesse am Duroc-Schwein.
  39. Jahrestagung der Deutschsprachige Arbeitsgemeinschaft für Verbrennungsbehandlung. JAN 2022; Zurich, Switzerland.

- S.P. Nischwitz, L.P. Kamolz.
  Moderne Verbandsmaterialien: Mehr als nur eine Wundabdeckung – Neues aus der Forschung und Entwicklung.
  Jahrestagung der Deutsche Gesellschaft für Verbrennungsmedizin, Arbeitskreis das schwerverletzte Kind. MAY 2021; Stuttgart, Germany.

Acknowledgments

First, I am very grateful to the Medical University of Graz and the Doctoral School of Molecular Medicine as well as JOANNEUM RESEARCH Forschungsgesellschaft mbH for giving me the opportunity to conduct scientific research in a highly relevant field by providing funding and infrastructure for this project.

My next and foremost thank you is to the department chair and my supervisor Prof. Dr. Lars-Peter Kamolz, MSc, for the project allocation, the excellent opportunities to work on it, and the formidable supervision and support, not only in terms of this project but as a mentor during my scientific and clinical career.

I am also very grateful for the help and input from my co-supervisors in the dissertation committee, Prof. Dr. Stephan Spendel and DI Dr. Thomas Birngruber, for their valuable input and the necessary freedom that was needed to conduct this research.

A special thanks goes to the responsible team of COREMED with Mag. Dr. Petra Kotzbeck as team leader for the provision of resources, their invaluable help and advice, and conduction of laboratory work.

My sincere gratitude is also expressed towards the subjects of this study, towards Dr. Vladimir Bubalo and his team, who always looked out for them, and to my partner who taught me a lot and went the extra mile to make sure they enjoyed their life.

I would also like to express my appreciation to all the methodology experts, researchers and assistants who are too many to be named, located at various departments who contributed to this work and without whom, this project would not have been possible.

Last, but not least, I thank my partner, my family & friends and everyone who supported me for their perpetual support & help; you have my deepest respect for bearing with me during these last few years.

Table of Contents

List of Figures

List of Tables

List of Abbreviations

+	-	intensity of characteristic
+/-	-	standard deviation
++	-	intensity of characteristic
+++	-	intensity of characteristic
*	-	$p < 0.05$
**	-	$p < 0.01$
***	-	$p < 0.001$
****	-	$p < 0.0001$
3D	-	three dimensional
3R	-	Replacement, Reduction, Refinement
ACTA2	-	gene coding for alpha smooth muscle actin
ANOVA	-	analysis of variance
ASPS	-	American Society of Plastic Surgeons
BW	-	full-thickness burn wound
BWR	-	full-thickness burn wound induced with resiquimod
C	-	control biopsies
CO_2	-	carbon dioxide
COL1	-	gene coding for collagen 1
COL3	-	gene coding for collagen 3
e.g.	-	*exempli gratia* – for example
ECM	-	extracellular matrix
et al.	-	*et alia* – and others
FT	-	full-thickness excisional wound
FTR	-	full-thickness excisional wound induced with resiquimod
HIF1a	-	gene coding for hypoxia-inducible factor 1 alpha
HIF-1α	-	hypoxia-inducible factor 1 alpha
HPF	-	high power field
HSPA4	-	heat shock protein family A member 4
HTS	-	hypertrophic scar (in Table 1)

i.e.	-	*id est* – that is
IL6/8/10	-	gene coding for interleukin 6/8/10
IL-6/8/10	-	interleukin 6/8/10
LPS	-	lipopolysaccharides
MMP	-	matrix metalloproteinase
MMP1	-	gene coding for matrix metalloproteinase 1
NIR	-	Near Infrared Perfusion Index
PCR	-	polymerase chain reaction
PDGF	-	platelet-derived growth factor
R+	-	Resiquimod-induced
R-	-	Non-induced
RNA	-	ribonucleic acid
SMAD3	-	mothers against decapentaplegic homolog 3
TGF-ß	-	transforming growth factor beta
TGFB1-3	-	gene coding for transforming growth factor beta 1-3
TLR	-	toll-like receptor
TNF-α	-	tumor necrosis factor alpha
TO	-	tissue oxygenation
VEGF	-	vascular endothelial growth factor
vs.	-	versus
VSS	-	Vancouver Scar Scale
w/w	-	weight per weight
YWHAZ	-	tyrosine 3-monooxygenase/tryptophan 5-monooxygenase activation protein zeta (housekeeping gene)

Zusammenfassung

Hintergrund: Hypertrophe Narbenbildung stellt nach wie vor eine große Herausforderung dar, insbesondere nach Verbrennungen. Die meisten Behandlungsmethoden weisen eine unzureichende Evidenz auf, nicht zuletzt, da die Pathophysiologie nur unvollständig verstanden ist. Um genauere Zusammenhänge zu verstehen, sind bei heterogenen Prozessen wie Narben präklinische Modelle erforderlich. Das Duroc-Schwein hat sich als eines etabliert, welches zum Menschen vergleichbare hypertrophe Narben bildet. Dieses Projekt diente zur Untersuchung der Narbenbildung nach induzierter Entzündung, der Beobachtung von lokalen Unterschieden in Narben unterschiedlicher Ätiologie und der Einführung eines Modells zur standardisierten Narbenbildung nach prolongierter Entzündung.

Methoden: Vier verschiedene Wundtypen wurden auf dem Rücken von sechs Duroc-Schweinen erzeugt: Vollhautwunden, allschichtige Verbrennungswunden und Versionen dieser beiden, die einen zusätzlichen Entzündungsschub durch Resiquimod erhielten. In den folgenden fünf Monaten wurden klinische Bewertungen mittels Scores und Bildgebung, die Messung der Gewebsoxygenierung mittels Hyperspektralbildgebung, eine histologische Beurteilung sowie Genexpressionsanalysen an mehreren Zeitpunkten durchgeführt.

Ergebnisse: Alle vier Wundtypen bildeten deutliche Narben. Sowohl Verbrennungswunden als auch beide Arten von induzierten Wunden führten zu signifikant höheren Narbenscores. Die Induktion durch Resiquimod spiegelte bei beiden induzierten Wundtypen die Entzündungsreaktion nach Verbrennungen wider und klang in Vollhautwunden etwas früher ab als in Verbrennungswunden. Eine relative Hypoxie in den drei Wundtypen korrelierte stark mit dem endgültigen Narbenscore. Die Genexpressionsanalyse bestätigte diese Hypoxie, zeigte aber nur geringe Veränderungen bei den Remodellierungsparametern. Induzierte Vollhautwunden zeigten die stärkste Entzündungsreaktion mit histologischen Merkmalen hypertropher Narben, wie auch die beiden Arten von Verbrennungswunden.

Schlussfolgerung: Wir konnten erfolgreich die Basis für ein neues Modell für hypertrophe Narben kreieren. Verschieden Wundtypen führten zu lokalen Unterschieden der Narben im Duroc-Schwein. Erhöhte Entzündungen und Hypoxie, verursacht durch Verbrennungen oder Resiquimod, führten zu intensiveren Narben. Künftige Studien sind erforderlich, um die genaue Pathophysiologie der pathologischen Narbenbildung weiter zu untersuchen und das Modell weiter zu verbessern.

Abstract

Background: Hypertrophic scarring still poses a major challenge, especially after burns. Most treatment modalities lack evidence, not least because the pathophysiology is incompletely understood. A persistent inflammatory response throughout the healing process appears to be the triggering factor in pathologic scarring. To properly understand pathophysiology in heterogeneous phenomena like scars, models are required. Many scar models exist, but the Duroc pig has emerged as one with similar hypertrophic scars to humans. This project's objectives were to investigate the mechanisms of scar formation following prolonged inflammation, observe differences in various scar etiologies, and to introduce a method for creating standardized hypertrophic scars by induction of prolonged inflammation.

Methods: Four distinct wound types were inflicted on the backs of six Duroc pigs: excisional full-thickness and burn wounds, and versions of both of these that had an additional inflammation boost induced by resiquimod for six days. Throughout the subsequent five months, clinical evaluation by scores and imaging, tissue oxygenation as measured by hyperspectral imaging, histologic assessment, and gene expression analyses were carried out at several different time points.

Results: All four wound types resulted in distinct scars. Burn wounds, and both types of induced wounds resulted in significantly higher scar scores. The induction by resiquimod mimicked the inflammatory response after burns in both induced wound types and subsided slightly earlier in excisional wounds than in burn wounds. Relative hypoxia was seen in all three wound types as compared to full-thickness wounds in hyperspectral imaging. Gene expression analysis confirmed these hypoxic conditions but revealed only low alterations concerning remodeling parameters. Hypoxia in early wound stages correlated with the final scar score; this correlation was also shown for inflammation during wound healing, but lower. Resiquimod-induced full-thickness wounds showed the highest number of inflammatory cells and the histologic hallmarks of hypertrophic scars, similar to both types of burn wounds.

Conclusion: Various wound etiologies on the Duroc pig were used to find local alterations in scars. We successfully created a new model for hypertrophic scarring. Increased inflammation and hypoxia caused by burns and resiquimod resulted in more severe scars. Future studies are needed to further investigate the exact pathophysiology of pathologic scarring and to advance the model for preclinical testing.

1 Introduction

This introductory section summarizes basic information and maps the current state of research necessary for understanding this thesis as a whole. While a conscious decision has been made not to merely summarize textbook knowledge, information that may appear redundant to some readers is included. In order to provide the reader with a self-contained understanding of all the essential aspects of this work, this content has been outlined without going into too much detail where possible.

1.1 Human skin

1.1.1 Anatomy & Physiology

The skin is the biggest organ in the human body, with a surface area of up to $2m^2$ [2,3]. In addition to the macroscopic division into hair-bearing and hairless skin, histologically, it is divided into epidermis and dermis. Roughly summarized, the epidermis is a barrier against physical, chemical, and biological impacts, while the dermis is primarily responsible for the biomechanical properties of the skin [4,5]. Recent findings have suggested that the hypodermis, which consists of adipose tissue, has inherent characteristics different from "regular" subcutaneous adipose tissue, leading to the hypodermis being considered part of the skin (by some authors) [3,4]. Age, sex, and the individual anatomical location with its functional requirements and difficulties all affect the detailed anatomy, including thickness and development of the sublayers of the skin [6].

The epidermis is the outermost layer of the skin, consisting mainly of keratinocytes and lacking any blood vessels. Keratinocytes are firmly connected by desmosomes and tight junctions, forming a resistant barrier against environmental influences - the epithelium. The epidermis is further divided into five layers from outside to inside: *stratum corneum*, *stratum lucidum* (only present in hairless skin), *stratum granulosum*, *stratum spinosum,* and *stratum basale* [5]. This layered distinction explains the formation of new epithelium with cells wandering from the *stratum basale* upwards, differentiating into the finally nucleus-less keratinocytes that can be visible as shed and flaky skin. Other cell types interwoven in between the keratinocytes scaffold are Langerhans cells (antigen-presenting cells), Merkel cells (pressure receptors), and melanocytes (production of melanin) [7,8].

The layer beneath the epidermis is the dermis. Firmly connected to the epidermis via the epidermal-dermal junction, it consists mainly of connective tissue [9]. Collagen-producing fibroblasts and fibrocytes are the predominant cells in this layer, responsible for preserving structural integrity and mechanically resilient skin properties. Alongside collagen, elastic fibers, proteoglycans, and other molecules form the extracellular matrix (ECM). The dermis is differentiated into *stratum papillare* and *stratum reticulare.* While the first is composed of rather loose connective tissue and is mainly responsible for epidermal support and nutrition as well as tactile sensation by Meissner's corpuscules, the latter (lower) *stratum reticulare* contains a dense network of reticular, elastic, and collagen fiber and determines the skin's biomechanical properties like elasticity and strength [4,10,11].

With about 75% of the dry weight of skin, collagen is the main component of the dermis [12].

Collagen molecules form thin collagen fibrils of about 15-130nm that in turn form larger fibrils (2-20µm). Currently, around 30 different collagen subtypes are known; however, not all types are capable of collagen fibril formation [13]. Collagen fibrils usually consist of a mixture of multiple types of collagen rather than being composed exclusively of a single type. Depending on subtypes, fibrillar formation, the complexity of cross-linking, and mineralization content, the different connective tissues of the body are composed. Collagen types 1 and 3 are predominantly found in the skin [14]. The dense reticular dermis shows a higher ratio of collagen 1 to 3 than the loose papillary dermis (with type 1 still being the main component). The ratio of these two subtypes also changes throughout a human's life, shifting to a more pronounced presence of collagen 1 in adult skin compared to fetal skin [15,16]. After collagen fibers, elastin is the second most common component of the dermis. It is predominantly responsible for the recoiling capacity of skin after being stretched [10,17]. Overstretching or "aged" elastin reduces recoiling capacity explaining skin's laxity with age [18]. The third component – summarizing all remaining substances of the dermis – is the ground substance. It does not directly contribute to biomechanical properties but rather serves as a linking substance that allows binding, water storage, support, and intercellular exchange [19]. It is, therefore, a leading contributor to tissue lubrication during movements and responsible for the orientation of collagen fibers.

The orientation of collagen fibers is clinically relevant, as it determines the direction of the so-called *Langer* lines or cleavage lines [17]. Surgical incisions along these lines show

reduced tension on the wound edges (compared to incisions orthogonal to these lines), better healing and ultimately resulting in more inconspicuous scars. Skin incisions and any other trauma exceeding the biomechanical capacity of the skin lead to a wound, defined as a disruption of the skin's continuity.

1.1.2 Wound Healing

Wound healing describes the process of restoring skin's continuity. The physiological regulation of wound healing is a complex process that depends on many different cell types and mediators interacting on many levels [20–23]. Since regeneration is very limited in humans, wound healing is accomplished by multiple processes, such as epithelial, endothelial, and fibroblastic cell proliferation and collagen production, ultimately resulting in a scar. Wound healing itself is a continuous process, but it can be broadly categorized into three phases: hemostasis and inflammation phase (sometimes considered as two separate phases), proliferation phase, and remodeling phase [20,22]. However, it is important to note that a wound may be in more than one phase simultaneously, as healing may not progress at the same rate in all parts of the wound.

Immediately after injury, the hemostasis and inflammation phase begins with the induction of coagulation and hemostasis. The primary goal of this mechanism is to prevent hemorrhage and consecutive organ failure. In addition, the coagulum forms a scaffold over which migrating cells are guided during wound healing [22]. An interplay of endothelial cells, platelets, coagulation cascade, and fibrinolysis regulate hemostasis. Small vessels are usually damaged if the skin is injured, constricting the vessel wall's smooth muscle cells. As part of this constriction, there is a deposition and activation of platelets, which stick together in the leak area, causing the initial reduction in bleeding. Subsequently, hypoxia and acidosis in the wound environment lead to relaxation so that an initially stagnant bleeding can start again [21]. In addition to these cellular hemostatic processes, plasmatic hemostasis is activated via the extrinsic and intrinsic pathways. Here, the initial coagulation of platelets is supported by fibrin, which is deposited in the wound area, beginning the process of actual wound healing. Platelets also contain essential growth factors (e.g. Platelet-derived growth factor (PDGF), Transforming growth factor beta (TGF-β)) and cytokines (e.g. Interleukin (IL)-6, IL-8), which act as promoters in wound healing by attracting neutrophil granulocytes, macrophages, endothelial cells, and fibroblasts [21,22].

This attraction initiates the actual inflammation phase, which aims to establish a competent immune response against microorganisms invading through the damaged barrier. The neutrophil granulocytes are the initial core cells of this phase and begin to phagocytose microorganisms, foreign bodies, and damaged tissue [24]. This is a crucial process since wounds that are heavily colonized/infected or where damaged/poorly-vascularized tissue is prevalent will not heal [25].

The actual immigration of neutrophil granulocytes begins approximately one day after injury. Once the initial "wound cleansing" has been accomplished by the neutrophil granulocytes, macrophages are attracted via additional chemokines. The granulocytes then become apoptotic and themselves are phagocytosed by the macrophages. This takes place approximately 48 - 72 hours after injury. Macrophages play a crucial role in wound healing, as they have a significantly longer lifespan than neutrophilic granulocytes, thus maintaining the "clean wound" and serving as a reservoir for further cytokines and growth factors [26]. Subsequently, additional lymphocytes migrate, supporting the defense against foreign substances and altered endogenous cells. The lymphocytes arrive later in the wound than granulocytes and macrophages and are responsible for a rather long-term immune modulation [27].

After hemostasis and a competent immune defense are established in the wound area, the wound will enter the proliferation phase and begin tissue repair. Macroscopically, granulation tissue will form at this time. This phase begins approximately three days after wounding and lasts about two weeks if undisturbed. The main players in this phase are migrating fibroblasts, responsible for building a new extracellular matrix to replace the initial fibrin scaffold [22]. Fibroblasts are able to differentiate and express a myofibroblast phenotype that can contract and thereby reduce wound size [28]. However, the fibroblasts and myofibroblasts are already stimulated to proliferate at the time of wounding by the release of TGF-β and PDGF. When the immune defense is then established, they receive the signal to migrate. Once in the wound, they produce procollagen 1 and 3 (precursor proteins of collagen 1 and 3), as well as other matrix components, such as fibronectin or proteoglycans, which are incorporated on-site [21]. The resulting extracellular matrix allows additional cells to migrate, thus reinforcing the process. In addition to the build-up of the extracellular matrix, another crucial aspect is the production of new blood vessels, which occurs continuously throughout the wound healing process. Growth factors such as Vascular endothelial growth

factor (VEGF) are secreted and thus ensure that the wound area is supplied with the above-mentioned cells via the formation of new vessels, and thus that wound healing progresses [21]. While in the beginning, there is blood supply only at the wound edges, this process explains how the center of a wound, which is initially not supplied with blood, can subsequently heal.

When enough extracellular matrix is built up, fibroblasts transform into myofibroblasts. These myofibroblasts subsequently attach to the surrounding proteins and then exert contractile forces, resulting in the contraction of the wound and the stabilization of its structural integrity [28]. This ultimately results in the maturation of granulation tissue consisting of macrophages, proliferating fibroblasts, collagen, fibrinogen, fibronectin, and other building blocks, thereby decreasing the density of blood vessels and creating the conditions for scar formation [22]. In addition to the above mechanisms, epithelialization is another aspect of the proliferation phase. This process begins shortly after wounding and is also triggered by the release of growth factors [21]. Epithelial cells migrate from intact skin, i.e., the wound margin, and attach to the underlying granulation tissue, which is initially provisional and later stable. When the wound cover is closed, the layer thickness is reinforced, and the basement membrane is constructed [29].

The final phase of wound healing is the remodeling phase. It is responsible for transforming the initial wound closure into stable scar tissue and lasts until approximately one year after wounding or longer [22]. However, after about three to four weeks, a plateau phase is reached, from which remodeling is less active than it was at the beginning [30]. Like the other phases of wound healing, remodeling is controlled by regulatory mechanisms, all of which aim to establish and maintain a balance between degradation and synthesis of cells and matrix, allowing normal wound healing with an inconspicuous and stable scar. This is controlled in particular by matrix metalloproteinases (MMP), which are enzymes produced by neutrophil granulocytes, fibroblasts, and macrophages that are responsible for collagen degradation while fibroblasts accomplish the buildup [31]. While the initial collagen scaffold is somewhat disorganized and jumbled, remodeling creates an ordered and interwoven scaffold. Additionally, remodeling entails the breakdown of fibronectin and the removal of fibroblasts and macrophages. This is accompanied by an increase in the diameter of collagen fibers, which increases the tissue's tensile strength [30]. It is worth noting, however, that despite these changes in scar tissue, it typically only reaches a maximum of 80% of the tensile strength observed in uninjured skin [32]. The remodeling process is terminated with the cessation of

capillary production, which decreases blood flow and, thus, metabolism in the wound area. If the process is undisturbed, the final result is a mature scar with reduced cell and vessel numbers and high tear resistance.

1.1.3 Specifics of Burn Wound Healing

A special situation challenging the regular processes of wound healing is a burn wound. Burns are regarded as thermal injuries that occur due to elevated temperatures that human skin cannot withstand without suffering damage. The epidermis, dermis and deeper tissues experience coagulative necrosis as a result. The extent of the damage is influenced by the temperature, the length of exposure, and the skin's relative resistance related to its thickness [33,34]. For contextual reasons, only burns exceeding the epidermis are dealt with in this section, as burns confined to the epidermis heal without scarring.

The local burn may be divided into three intensity zones [35]: the coagulation zone is the core region (often the area of direct contact). Cells are irrevocably destroyed in this region. The surrounding region is known as the zone of stasis, where cell metabolism has either decreased significantly or stopped entirely (yet the cells are still alive). The zone of hyperemia, where perfusion and metabolism remain unaltered and even elevated, is located in the periphery. A few days later, the cells in the stasis zone may have succumbed to the burn's harmful effects, leading to necrosis. This development is called burn wound progression, which leaves just two zones (necrotic and alive) [35,36]. The alive zone (including the hyperemic peripheral zone) usually recovers, and the cells regain their physiological function.

In contrast to incisional wounds, which are commonly vertical in orientation, burn wounds are typically significantly bigger and show a horizontal component. If certain body surface areas are exceeded during a burn, it can culminate in systemic burn illness [37]. Compared to other acute wounds, the heat results in initial sterility and reduced blood loss due to its coagulation impact. Secondarily, they become more vulnerable to infections, because of the extensive necrosis and breakdown of the skin barrier, as well as the patient’s often compromised immune system.

Protein denaturation is the principal destructive process in burns [38]. In response to this harmful process, inflammatory mediators are promptly activated. Peptidases and oxidants, which encourage tissue necrosis, further damage the endothelial cells, which are already vulnerable. Edema develops as a result of damaged endothelial cells [39]. Even with proper

fluid resuscitation, edema may become more pronounced the more serious the burn and, therefore, the endothelial damage (depth, area, and inflammatory response). This might lead to hypovolemic conditions boosting neutrophil and xanthinoxidase activity, which in turn causes a rise in potentially harmful byproducts [40,41]. Thereby, a vicious circle is instituted, further worsened by an increased histamine buildup that may eventually result in a systemic burn disease with systemic complications that can cause multiple organ failure and death [42,43].

The reasons why the inflammatory phase in burns might be seen as aberrant compared to the wound healing process in incisional wounds include the mechanisms mentioned earlier. These also lead to a longer healing time during which bacterial colonization and/or infection occur, further hampering the physiological mechanisms of wound healing. Despite the eventual healing of wounds, the persistence of inflammatory cells in burn wounds and the prolonged elevation of pro-inflammatory cytokine levels years after the initial trauma provide evidence for the enduring nature of the inflammatory phase [44,45].

1.2 Scars

While the previous section provided a fundamental understanding of wound healing, the subsequent section delves into a more comprehensive examination of the intricate physiological processes involved in advanced wound healing (scar formation). It also highlights the unanswered concerns that still remain in the field of scar research and investigates the practical applications of this information in therapeutic settings.

1.2.1 Pathologic scar – definition and physiology

Scars are the human body's unavoidable consequence of dermal wounding. Once wounds are fully epithelialized, they enter the remodeling phase. The components that make up the ECM are then transformed, with synthesis being reduced but not totally stopped [30]. Collagen 1, the primary structural protein in healthy, unwounded dermis, gradually replaces collagen 3, the principal kind of collagen found in granulation tissue [46]. This remodeling results in more stable scars. However, the remodeled collagen 1 is organized in bundles in contrast to a basket weave arrangement in normal, unharmed dermis. Finally, elastin, which is not present in granulation tissue, starts to reappear [47,48]. Despite collagen remodeling and elastin fibers reappearing, the elastic and mechanical properties of uninjured skin are never fully regained owing to the altered structure and function of collagen and elastin. A delicate equilibrium between profibrotic and antifibrotic processes is characteristic of the remodeling phase, with scar maturation being concluded by an ultimate reduction of (myo-)fibroblast and vascular cells [49,50].

As wound healing and scar formation are highly complex and interwoven, alterations and influencing forces in any wound healing phase may lead to pathologic scarring [51,52]. While the exact pathways leading to pathologic scarring are still discussed and not completely elucidated, the current understanding is that, ultimately, pathologic scars result from an altered ratio of collagen production to collagen degradation [50,52].

There are three basic categories of pathologic scarring. If collagen degradation surpasses collagen production relative to a regular scar, atrophic scars result [53]. They appear as small skin dimples and are the usual sequelae of locally confined inflammatory diseases like *acne vulgaris*. Atrophic scars rarely cause somatic health problems but can be an often-underappreciated stigma for affected persons. In case of collagen production being the dominating parameter, two other types of pathologic scars can develop: hypertrophic scars and

keloids [54]. With these two types being the outcome of collagen overproduction, they are considered two different entities by most authors. While hypertrophic scars are confined to the region of the trauma, keloids show a horizontal growth pattern exceeding the borders of the trauma. They also express histological differences and show different behaviors. Additionally, a genetic component has been detected for the occurrence of keloids, which could not be confirmed in hypertrophic scars [55]. As a result, keloids are far more common among Asian and Sub-Saharan African populations than in people of Caucasian heritage. Despite these differences, some authors consider them successive stages of the same pathology [56–58].

From a clinical point of view, hypertrophic scars can result from adequate trauma and are specifically common after burns (up to 90% depending on the literature, compared to about 30% after incisional trauma) [59–61]. Keloids can form after non-adequate trauma, like mosquito bites in predisposed people. Clinically, both entities manifest as elevated, firm areas that appear reddish, accompanied by itching and/or pain. In cases where these pathological scars occur over joints, there is a risk of developing contractures [62]. Given that they are frequently seen in medical settings and that most publications and authors treat keloids and hypertrophic scars as separate entities, this project and thesis specifically focus on hypertrophic scars while excluding keloids from the scope of this investigation.

While the exact mechanisms and reasons for pathologic scar formation have not been elucidated yet, many theories and discoveries point to inflammation as a crucial factor [59]. The ifs, whens, and hows of said inflammation, however, remain to be completely revealed. In the following, some important information about the pathophysiology for the understanding of this thesis is highlighted.

1.2.1.1 Inflammation

An extended inflammatory phase increases fibroblast activity, promoting increased fibrosis. Among various inflammatory modulators, pro-inflammatory cytokines, such as IL-6, IL-8, and anti-inflammatory IL-10, have been identified as relevant factors [59,63]. Notably, fetal wounds usually heal without scarring [64,65], and it was shown that diminished IL-6 was found in that context [66]. Experiments using IL-6 to induce inflammation have shown increased scarring parameters, while using IL-10 has reduced scarring in mice models [67–69]. These findings are further supported by another study that introduced mast cells (which ultimately lead to IL-6 induction) to a fetal wound healing model and resulted in more severe

scarring as well [70]. Another pro-inflammatory factor modulating scar formation is Tumor necrosis factor alpha (TNF-α), which has been shown to increase MMP-1 activity, thus reducing fibrosis [34,71]. However, TNF-α has also been shown to express tissue-specificity, and increased expression has been demonstrated in hypertrophic scars in other models [72–74]. The specific role of TNF-α is yet not fully understood and appears to be influenced by co-factors [72,73,75].

Recent evidence suggests that the intensity of the inflammatory response and the type of inflammatory response are responsible for pathologic scar formation [52,76,77]. It has been shown that different expression patterns of T-helper cells as a subset of the long-remaining lymphocytes led to either profibrotic [78,79] or antifibrotic [80] wound healing due to the respective cytokine release behavior [81]. As these findings primarily see the inflammatory response as the driving force of fibrosis, many treatment modalities focus on inflammatory modulation. Furthermore, they provide an explanation for the increased prevalence of pathologic scarring in burns compared to surgical trauma, as stated above, since thermal trauma produces significantly higher levels of local and systemic inflammation [82–84].

Other relevant molecules in fibrosis are toll-like receptors (TLRs). TLRs are a set of highly conserved molecules that enable the innate immune system to detect pathogen-associated molecular patterns and endogenous necrosis-derived waste products [85]. They serve as activators of the innate immune system but are increasingly linked to the transition from normal wound healing responses to fibrosis in various organs and tissues [85,86]. Several TLRs are involved in immune defense, including TLR2 and TLR4, which bind lipopolysaccharides (LPS; a form of bacterial toxins) to identify gram-positive and gram-negative bacteria, respectively [87]. The mechanism of fibrosis in the skin and several other tissues is not thoroughly researched. Still, in the liver, LPS directly stimulates TLR4-dependent fibrosis, targeting fibroblast precursors that produce chemokines to activate macrophage-like Kupffer cells. This causes uncontrolled TGF-β-mediated increased deposition of extracellular matrix and the development of liver fibrosis [88–90]. TLRs are also present in dermal fibroblasts. Hence their activation might contribute to dermal scarring [91]. The LPS-mediated reaction has been used in several studies to induce inflammation successfully [92,93]. However, the ability to bind to TLRs depends on the composition of LPS [94], which is why a specific activation of TLRs independent of the substrates-composition might yield more predictable and stable results. Recently, a delayed-healing model was

successfully developed by using said specific TLR7/8 activation using the immunomodulatory TLR agonist resiquimod [95]. The specific TLR activation, mediated by resiquimod and its precursor Imiquimod, is used to treat several dermatologic conditions and was also applied in inflammatory skin models, e.g. psoriasis [96]. *In vitro*, data showed similar inflammatory responses regarding monocyte activation and cytokine expression when using the specific TLR7/8 agonist or LPS [97]. However, further research on the TLR-dependent inflammatory response and scarring is necessary.

1.2.1.2 Remodeling

Alongside liver fibrosis, another fibrotic disease that researchers tried to transfer knowledge from is pulmonary fibrosis. Among other reasons, the lack of satisfactory results from strong immunoinflammatory therapy in pulmonary fibrosis has prompted researchers to explore additional targets that may contribute to the development of hypertrophic scarring [52,98,99]. With its crucial implications in practically all phases of wound healing, TGF-β has been designated as a worthy target point for further research [50,52,100]. There are several TGF-β subtypes, of which TGF-β1 and TGF-β2 have been identified as the main profibrotic and TGF-β3 as the main antifibrotic isoform in mammals [101]. All three isoforms compete for the same receptors leaving the concentration and ratio a predominant variable for the occurrence of a hypertrophic scar [101]. Several studies have confirmed the pro-/antifibrotic effects of the isoforms and the presence thereof in pathologic scars [102–104]. Additionally, using TGF-β antibodies has significantly decreased scar hypertrophy in a rabbit ear [105] as well as a mouse model [106,107].

Therefore, dysregulation of these three isotypes leads to an increased fibroblast activity and also an improved growth-factor receptor environment, ultimately leading to an overproduction of ECM and consecutively to abnormal scar growth [108].

As another important factor in remodeling, MMPs have been identified. MMPs are a group of enzymes that are involved in the breakdown of dermal and ECM proteins. The main enzyme identified to break down collagen 1 is MMP-1, and to break down collagen 3, which is overexpressed in hyperplastic scars compared to collagen 1, MMP-13 [109]. While there are theories about differences in hypertrophic scar and keloid MMP expression profiles [76], it was shown that MMP-1 expression is significantly higher and MMP-13 expression significantly lower in human keloid fibroblasts compared to normal skin [110]. Despite MMPs being a

relevant player in skin fibrosis and a noteworthy target point, MMP expression is at least partly controlled by TGF-β [76]. While MMPs, like TGF-β, are an indispensable part of wound healing, a cumulative disturbance in the balance of construction (mainly mediated by TGF-β) and breakdown (mediated, among other co-factors, by MMPs) may result in disrupted wound healing and consecutively a hypertrophic scar.

1.2.1.3 Mechanical stress

When looking at the "macroscopic" or clinical aspects influencing the development of hypertrophic scars, mechanical stress has emerged as a significant parameter. Mechanical stress refers to the physical force exerted on the skin and underlying tissues during the wound healing process. This force can originate from various sources, such as muscle contractions, stretching of the skin, or movement of the affected body part.

The presence of mechanical stress during the healing process can impact the development of hypertrophic scars by influencing the equilibrium between collagen production and degradation. When a healing wound is subjected to mechanical stress, it can increase the production of collagen and other ECM proteins necessary for scar tissue formation. However, if the mechanical stress is excessive, it can lead to an overproduction of collagen and ECM proteins, resulting in the formation of a hypertrophic scar. Additionally, mechanical stress can also affect the activity of enzymes that break down ECM proteins, such as MMPs. If mechanical stress is excessive, it can lead to an imbalance in the activity of MMPs and their inhibitors, resulting in hypertrophic scar formation. It is also postulated that this mechanical stress leads to local inflammation by mechanosensitive nociceptors (nerve fibers). If these nociceptors are triggered, a somatic sensation of "tension" is produced, leading to cellular reactions as if actual tension was put on a wound. Mechanical stress has been shown to result in higher inflammation in numerous preclinical and clinical studies [111–114]. The underlying mechanisms of this mechano-signaling have been identified for certain pathways, while others remain speculative and require further investigation [115].

1.2.1.4 Hypoxia

The absence of oxygen, or hypoxia, is crucial to the inflammatory response. The initiation of the inflammatory phase is characterized by the recruitment of white blood cells and other immune cells to the site of the problem. These cells are highly dependent on the presence

of oxygen for their normal functioning. In cases where oxygen is deficient in a particular location, it can trigger a cascade of events that intensify the inflammatory response. Due to a lack of blood flow, the tissue around a wound may become hypoxic. This may upregulate hypoxia-inducible factor 1-alpha (HIF-1α), a protein that reacts to changes in oxygen levels. Upregulation of HIF-1α is associated with the activation of a wide range of inflammatory response genes, including IL-8 and other leukocyte-attracting cytokines. In addition, it promotes wound healing by stimulating angiogenesis. The recruitment of immune cells to the affected area releases pro-inflammatory cytokines and chemokines, further amplifying the inflammatory response. As a result, healing is facilitated by the formation of new blood vessels, increased blood flow, and reduced hypoxia.

However, prolonged hypoxia can lead to an overproduction of collagen and other ECM proteins, leading to a hypertrophic scar. Additionally, hypoxia also affects the activity of MMPs, which again can lead to an imbalance between these enzymes and their inhibitors, resulting in excessive degradation of ECM proteins and the formation of a hypertrophic scar.

While most scar research focused on direct remodeling and inflammatory pathways, recent developments also investigated hypoxia as a possible variable [75] since it has long been known to be a relevant aspect of wound healing and myofibroblast differentiation [116,117].

Some data imply that hypoxic environments are related to hyperplastic scar development [118,119], and it was shown that hypoxia generates a pro-fibrotic state through the TGF-β1/SMAD3 (Mothers against decapentaplegic homolog 3) pathway [120].

1.2.3 Hypertrophic scar treatment

There are several different treatments available for hypertrophic scars. However, it is to note that the evidence behind each one varies, and many treatment modalities are rather eminence- than evidence-based. Some of the most popular modalities are summarized below.

Pressure therapy, which involves the application of constant pressure to the scar, has been shown to be effective in reducing the thickness and improving the appearance of hypertrophic scars. The pressure helps to prevent the overgrowth of collagen and promote the alignment of collagen fibers, resulting in a flatter and less visible scar.

Silicone gels, sheets, and creams have also effectively reduced the symptoms and appearance of hypertrophic scars. These products work by hydrating the scar tissue, which can

help to reduce itching and discomfort, and by creating a barrier on the skin that can help to reduce the amount of collagen produced.

Corticosteroids have been used as injections or topical creams to reduce inflammation and the overproduction of collagen in hypertrophic scars. They work by decreasing the activity of the fibroblasts, the cells responsible for producing collagen.

Laser therapy, such as pulsed dye laser therapy, has been used to reduce the redness, thickness, and itchiness of hypertrophic scars. It works by targeting the blood vessels that feed the scar tissue and by breaking down the collagen in the scar. Carbon dioxide (CO_2)-lasers, on the other hand, are ablative and reduce scar thickness and have also been shown to reduce pain sensation and erythema and improve skin elasticity.

1.2.3.1 The evidence behind hypertrophic scar treatment

In preparation for this thesis, a systematic review was conducted to explore the various treatment modalities currently available for hypertrophic scars [121]. For this review, scientific medical databases have been screened for clinical trials investigating the effect of postulated treatment modalities. These trials have been categorized according to their level of evidence as defined by Evans *et al.*, respectively, the American Society of Plastic Surgeons [122,123]. In concordance with earlier investigations and opinions [124–126], only a limited number (nine) of scientifically sound studies were found in the last ten years. Four of these nine studies investigated the effect of intralesional triamcinolone and/or fluorouracil infiltrations [127–130], and four investigated the effect of topical creams/gels (enalapril/silicone/"lotion") or pressure therapy/massage [131–134]. One of the nine studies investigated the effect of the CO_2 laser. The highest evidence could be found for intralesional anti-inflammatory therapy with triamcinolone and/or fluorouracil. The studies dealing with topical treatment showed some positive results; however, the conclusion of the topical therapy studies of that review could be "to do anything is better than nothing", since these therapies do not harm and the effects are rather contained. Since only one study dealt with the CO_2 laser [135], insufficient scientifically robust evidence exists to derive definitive recommendations for its usage. Although both the intervention and control groups showed some encouraging outcomes, the possibility of randomization bias limited the study's overall significance.

1.2.3.2 Emerging and coming treatment modalities

While the current evidence for existing treatment modalities for scars remains limited, researchers have begun exploring novel modalities that hold the potential to alleviate the burden of scars in the future. Although several substances have been tested, no level of evidence I study has been conducted as of the writing of this thesis.

One of these treatment options is the use of botulinum toxin A. The postulated mechanism is an inhibition of TGF-β1 and consecutive fibroblast reduction [136]. This neurotoxin further paralyzes the surrounding musculature, thus reducing tension on the scar. Its use has been shown to ameliorate scars [137–139].

Another possible emerging therapy is the use of stem cells. Due to their vast potential, they can exert immunomodulatory and antifibrotic effects [140,141], thus improving pathologic scars. One approach that has shown promise in addressing these effects is using an amniotic membrane as stem cell providing skin transplant dressing, which is associated with faster re-epithelialization and wound healing [142,143]. Considering that delayed wound healing is a significant determinant in the development of hypertrophic scars [144], it has been observed that applying an amniotic membrane reduces the incidence of hypertrophic scars following burns [145]. A second approach possibly relating to these effects is fat grafting. Although the mechanism is unknown, it is hypothesized that adipose-derived stem cells possess biological properties that can alleviate cutaneous fibrosis [146,147]. This is attributed, at least in part, to their angiogenic and antiapoptotic capabilities [146,147]. These stem cells exert a modulatory effect on a series of growth factors, thereby enhancing angiogenesis and influencing vessel density, collagen orientation, and the granulation process. Collectively, these cellular actions have the potential to contribute to improved scar appearance [148,149].

With TGF-β1 continuing to be one of the most important therapeutic targets for hypertrophic scarring, the selective inhibition of TGF-β1 represents a potential treatment strategy. This could be achieved by, for instance, antioxidants or Shikonin, an active component isolated from Chinese herbs, whose efficacies have been proven *in vitro* already, with *in vivo* results still pending [150,151].

Ultimately, to date, there is no one size fits all for treating hypertrophic scars. Many uncertainties in pathophysiology, as well as working mechanisms of treatment modalities, remain that do not allow a uniform solution. These shortcomings of modern medicine are not last caused by the current lack of an ideal model that represents standardized hypertrophic

scars [152,153]. With hypertrophic scars presenting in a multitude of phenotypes in considerable heterogeneity, a standardized *in vivo* scar model is indispensable for a deeper understanding of pathophysiology and exploration of potential working points [154]. The following sections introduce some of the available models, including their shortcomings.

1.2.3 Hypertrophic scar models

Models are crucial in scar research as they allow scientists to explore the formation and progression of scars in a controlled and systematic manner. By creating scar models, researchers can investigate the underlying mechanisms involved in scar formation, explore the impact of different factors and interventions, and assess the efficacy of potential treatments.

Scar research utilizes various models, including *in vitro*, *in vivo*, and *in silico* models. The selection of the optimal model for a specific investigation should be based on the model's unique characteristics and the intended study objectives. *In vitro* models may be utilized to determine the many processes involved in scar formation and for high-throughput drug development investigation. On the other hand, preclinical *in vivo* models are often employed to investigate phenotypical scar development and create novel treatment strategies. *In silico* models are the most recent entity. These models are used to digitally simulate cell behavior and interaction on a computer. While they are certainly a promising tool for future research, they a) lack the physical properties of biological models, b) rely on data from *in vivo*/*in vitro* experiments, and c) are a relatively new concept whose full potential has yet to be explored.

1.2.3.1 In vitro models

The first *in vitro* models used cell monolayer cultures. Then, co-cultures of different cell lines (keratinocytes and fibroblasts) were introduced. Despite their speed, simplicity, and low cost, the cell monolayer cultures lack a scar's three dimensional (3D) macroscopic fibrotic tissue structure. This rendered them physiologically irrelevant [155]. Adding collagen or fibrin gel to the 3D environment created a more realistic scar phenotype [156]; allowing fibroblasts to make their own matrix mimics *in vivo* conditions [157]. Organotypic skin equivalents were developed when it was discovered that epidermal keratinocytes and dermal fibroblasts govern extracellular dermal matrix formation via substantial interaction [155]. These 3D organotypic skin models containing keloid fibroblasts and normal skin-derived keratinocytes can imitate and investigate pathologic scar development [158]. However, without circulating biomarkers, these models

cannot be used to generate novel treatment regimens, nor can they display the whole *in vivo* process of scar formation.

The most recent *in vitro* development suggests that subcutaneous fat-derived mesenchymal stromal cells may be employed to create a tissue-engineered hypertrophic scar model: The van den Broek *et al.* model involves the creation of a reconstituted epidermis using typical healthy human keratinocytes, which is then placed on a dermal matrix with subcutaneous fat [159]. This model has several hypertrophic scar features, such as increased collagen 1 production, contraction, and epidermal thickness, and allows significant parameters to be found and confirmed with therapy procedures. Despite advances in these models, they only depict hypertrophic scar formation produced by severe damage (e.g. burns) that exposes adipose tissue. These models cannot simulate hypertrophic scarring after wound closure or mild damage.

1.2.3.2 In vivo models

Even with all the progress seen with *in vitro* models, they still cannot properly replicate the complex dynamics and intricacies of the living organism (yet). Consequently, researchers often resort to *in vivo* models [160]. However, it is important to differentiate between human and animal models. On the one hand, human models are ethically challenging to justify and are mostly limited to *ex vivo* models, making any kind of standardization difficult. On the other hand, animal models should always adhere to the 3R framework – Replacement, Reduction, and Refinement: Ideally, animal experiments should be *replaced* with alternative modalities whenever possible. If replacement is not possible or feasible, the number of animals used should be *reduced* to the lowest reasonable extent, and the conditions for the animals should always be *refined* to ensure natural and agreeable conditions [161,162].

Various animal species, including mice, rats, dogs, guinea pigs, rabbits, and pigs, have been used in scar research so far [160]. However, the use of dogs and guinea pigs as animal models is limited to only a few reports, despite their similarities to human hypertrophic scars [160,163,164]. Ethical considerations and adherence to the 3R have prevented their widespread use [160,163,164]. In contrast, rodents are more commonly employed in scar research. In rodent models, reddish and elevated scars with collagen nodules are considered a typical hypertrophic scar criterion, but they lack the same size and thickness as troublesome hypertrophic scars in humans, since wound size is restricted to body size. Furthermore,

experiments in mice and rats are limited to a single scar per animal, necessitating a high number of animals to generate valid data. The rabbit appears to be a useful animal for generating hypertrophic scars. However, it should be noted that wound healing mechanisms differ between rodents, rabbits, and humans. In rodents and rabbits, wound closure usually occurs through contraction of the *panniculus carnosus*, a subcutaneous muscle layer that humans do not possess. Interestingly, it was discovered that rabbit ear wounds heal through granulation and not through contraction, just like human wounds do. However, the rabbit ear's underlying cartilage can affect how a wound heals, making this model not ideal as well.

The animal with the highest transferability to human skin wounds is the pig. It was shown that wound healing studies show a concordance of 78% with human wound healing, while small mammals only reach 53%, and *in vitro* studies 57% [165]. While the first studies with the red Duroc pig forming distinct hypertrophic scars were published in 1976 [166], the results were hard to reproduce [167–170]. Several studies have since then used the red Duroc pig as their preferred animal to produce hypertrophic scars in different ways, yet no gold standard exists for a hypertrophic scar model. The review conducted in preparation for this project by Rössler *et al.* summarizes the advantages and disadvantages of the available *in vivo* models, as shown in Table 1.

Table 1: *Available in vivo models for hypertrophic scarring (adapted from [160]).*

Model (animal)	**Wound method**	**Histological features of human hypertrophic scar**	**Multiple scars per animal**	**Transferability to human**	**Easy availability and low costs**	**Critique**
Nude mouse model (mouse)	Human skin graft and incision or burn	Yes	No	Low	Yes	Requires human skin grafts, impeded immune system
Bleomycin model (mouse)	Implantation of bleomycin pump	Yes	No	Low	Yes	Requires special Bleomycin pumps, scar evolves by drug delivery and not by injury
Mechanical stress model (mouse)	Incision and stretching device	Yes	No	Low	Yes	Requires special stretching devices and continuous control for their adequate positioning
Rat tail model (rat)	Incision and stretching device	Yes	No	Low	Yes	Requires special stretching device and continuous control
Rabbit ear model (rabbit)	Incision or burn	Yes	Yes	Low	Yes	Cartilage could influence scar formation
Duroc model (pig)	Incision or burn	Yes	Yes	High	No	Flat scars without redness
Large White model (pig)	Burn	Not clear	Yes	High	No	No collagen nodules
Coal tar model (guinea pig)	Incision and coal tar treatment	Yes	Yes	Low	Yes	High mortality
Hairless dog model (dog)	Incision	Yes	Yes	Unclear	No	Carnivore with fangs and claws

Research Objective

Hypertrophic scars are still a significant burden, especially after burns. Despite advances in the insights of pathophysiology, there are many unanswered questions. The therapy of pathologic scars is also rather eminence- than evidence-based. These shortcomings might be – among others – due to the lack of an appropriate and reproducible model producing standardized hypertrophic scars.

This project aimed to investigate local alterations in scars of different etiologies and to develop a new model for standardized hypertrophic scars. To accomplish this, insights from previous research were transferred to this project: Burn and full-thickness skin wounds were produced on Duroc pigs, of which in some hyperinflammation was induced by TLR7/8 activation. Wound healing and scar formation were then observed clinically, microscopically, and with imaging devices. Additionally, gene expression analyses were conducted.

This setup was established to acquire further insights into the scarring process and provide a model allowing the development of targeted treatment modalities in future research.

2 Material and Methods

The responsible authority, the Federal Ministry Republic of Austria, Education, Science and Research (BMBWF-66.010/0116- V/3b/2019), reviewed and approved all animal work. The study's timeframe is depicted in Figure 1 – the procedures are explained thereafter. Parts of the methods are described in [1] which is hereby referenced.

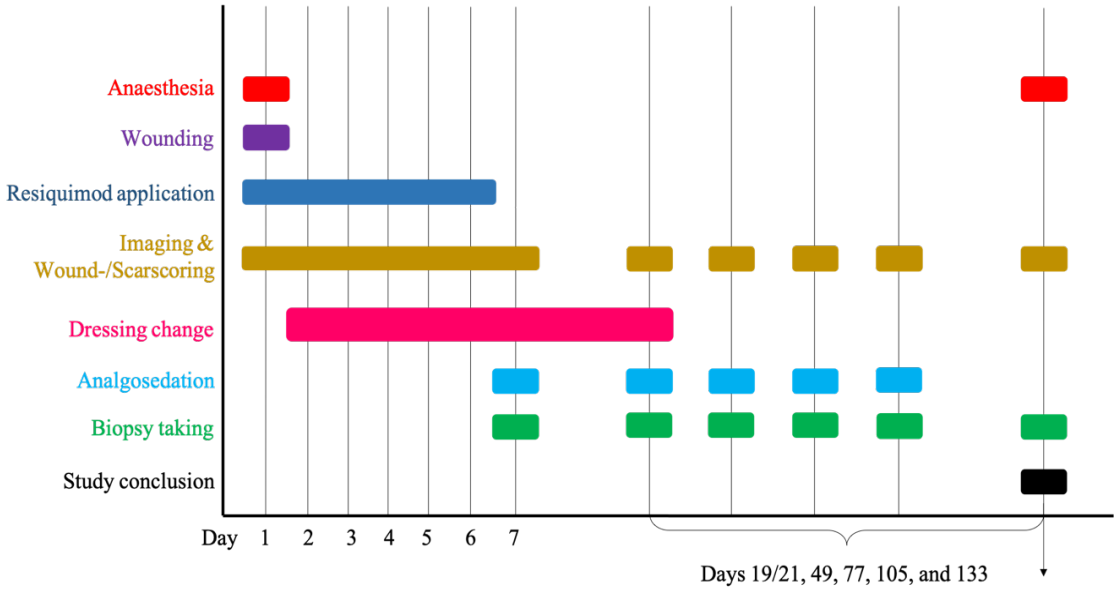

Figure 1: *Depiction of the study course. The study took 133 days for each pig. All wound manipulations were conducted under anesthesia or analgosedation. Resiquimod was applied to the wounds for six consecutive days. Dressing changes were performed until complete re-epithelialization. Imaging, visual assessment, and biopsy taking were performed on the respective days throughout the study course.*

2.1 Animals

For this research project, six male, castrated, purebred Duroc pigs were used. Due to logistical reasons, two project series with three pigs each have been conducted. The second series of three pigs had to be purchased from a different breeder because the first one went out of business due to the coronavirus pandemic 2019. All animals were between eight and twelve weeks old and were acclimatized in the research facility at least two weeks before the start of the experiments. The median weight of the six pigs was 15.6 kg (range: 8.5 – 25.0 kg) at the beginning of the experiments. The pigs' housing and handling were carried out in a species-appropriate manner with an enriched environment and food and water *ad libitum*. Veterinarians and/or veterinary-qualified personnel were available and present around the clock.

2.1.1 Medical care

All study-related activities have been conducted under analgosedation to create a stress-reduced environment. For wounding, the pigs have been anesthetized and intubated by professional veterinarians. The following drugs have been used for these procedures: 0.5 mg/kg midazolam (Midazolam Accord, Accord Healthcare Limited, Devon, UK), 10 mg/kg ketamine (Ketasol, Graeub, Bern care Limited, Devon, UK), 0.2 mg/kg butorphanol (Butomidor, Richter Pharma AG, Vienna, Austria) and 2 mg/kg azaperone (Stresnil, Elanco GmbH, Bad Homburg vor der Höhe, Germany). Additionally, Isofluran (1-2%) was used for anesthesia. Throughout the duration of the project, pain medication was administered using fentanyl patches ranging from 25 to 50 µg/h, tailored to individual requirements, when not in surgery.

2.1.2 Wounding

The animals' backs were shaved the day before the wounding, and the pigs were fasted 12h before the procedure. All animals except for one received eight wounds on their back located on bilateral flanks paramedian with at least 6 cm in between wounds in deep anesthesia. The sixth pig only received four wounds due to its smaller size and weight (8.5 kg). All wounds measured 3x3 cm and were planned and positioned using an exact stencil. Half of the wounds have been caused by full-thickness excision (FT, four wounds and two wounds for the sixth pig) using a #10 blade scalpel, and the other half have been caused by a full-thickness burn (BW, four wounds and two wounds for the sixth pig). The full-thickness burns were administered using 3x3 cm stainless-steel cuboids that had been heated to ~200°C (+/- 10°C) in a drying oven and put onto the pig's skin by its own weight for 30 seconds. The cuboid's temperature was verified immediately before application using the FLIR One® Pro for iOS Attachment for iOS Smartphones (FLIR Systems, Inc., Wilsonville, OR, USA).

To avoid confounding effects owing to the wound location (localized more cranially/caudally), different wound localizations have been applied to the animals (see Figure 2). While both described wound types were full-thickness wounds, excisional wounds will in the following be meant by full-thickness wounds (FT) except when stated otherwise.

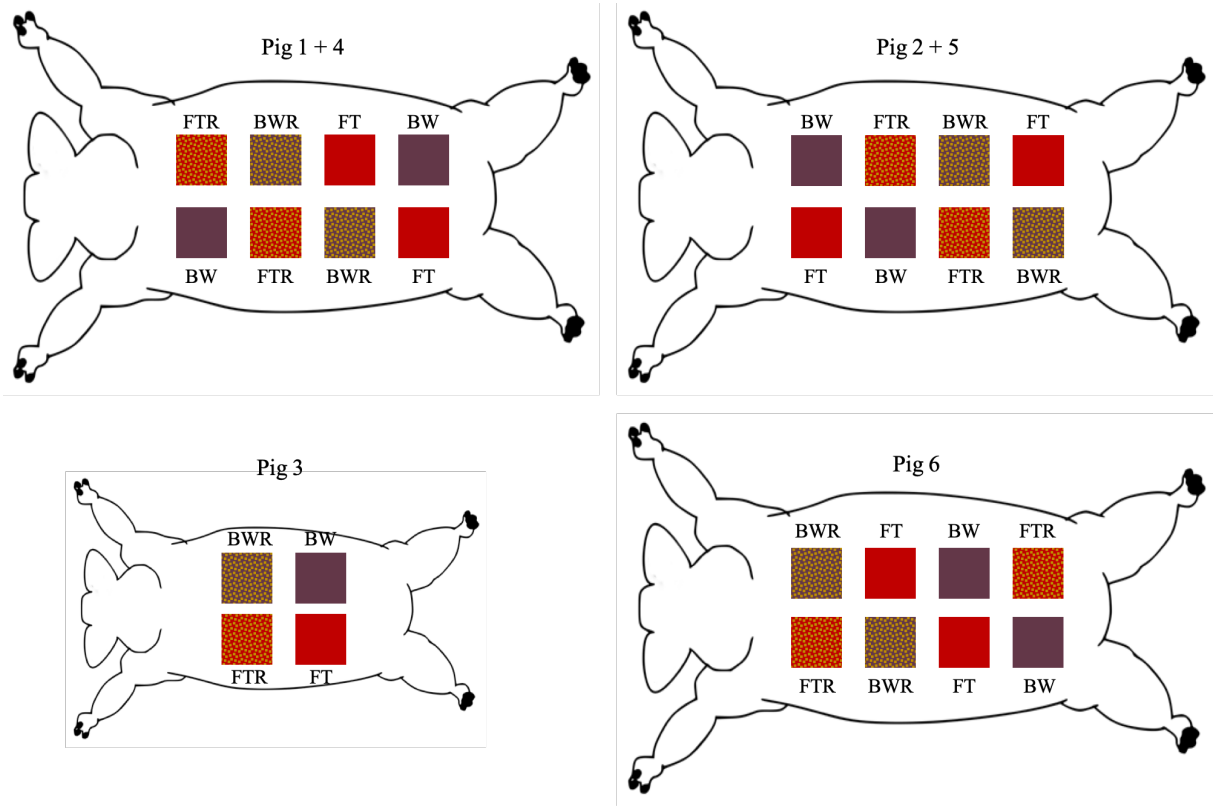

Figure 2: *Wound localizations on the different pigs. To avoid confounding effects by wound localizations, these were altered on the different pigs. Pig 3 received only four wounds due to its smaller bearing. FT = Full-thickness wound, FTR = Full-thickness wound with resiquimod, BW = Burn wound, BWR = Burn wound with resiquimod.*

2.1.3 Wound care

Either 1g of ointment containing the active ingredient (resiquimod, as described in section 2.1.3.1) or 1g of ointment without the active ingredient was administered to the wounds immediately after wounding and during daily dressing changes for the first six consecutive days after wounding (FTR = Full-thickness excisional wound induced with resiquimod, BWR = Burn wound induced with resiquimod). Prior to ointment application, wounds were cleaned by using polyhexamethylene biguanide solution Lavasorb (Fresenius Kabi AG, Bad Homburg vor der Höhe, Germany), assessed, and photographed (see 2.2). Wound dressings were applied using Mepilex lite (Mölnlycke Health Care, Gothenburg, Sweden), Opsite transparent adhesive film (Smith & Nephew plc, Watford, England, UK), and Leukotape K (BSN medical, Hamburg, Germany). If the pigs started scratching their wound dressing, additional overalls (Model Dog & Cat Body, Henry Schein Vet, Melville, New York, USA) were applied.

After the first six days, the wounds were only cleaned and dressed as above. After collecting the punch biopsies (see 2.1.4), the wounds were treated with a silver aluminum aerosol (Henry Schein, Melville, NY, USA). No further dressing changes were conducted after complete re-epithelialization.

2.1.3.1 Ointment preparation

Half of the wounds were treated with an ointment with an active ingredient (resiquimod), and the other half were treated with the same ointment without an active ingredient. Resiquimod was formulated into a cream following patent US 2007/0264317 A1 [171]. 0.45 mg resiquimod was dissolved in endotoxin-free water under vortexing to prepare 1g ointment. The aqueous phase further comprised 0.5% (w/w) xanthan gum (Lactan, Graz, Austria) and 3.4% (w/w) polysorbate 60 (Sigma Aldrich, Munich, Austria). Resiquimod was substituted with water in equal parts for the placebo ointment. The lipophilic phase, consisting of 8.85% (w/w) oleic acid (Merck, Darmstadt, Germany), 3.6% (w/w) stearic acid, 2.63% (w/w) cetyl alcohol, 3.71% (w/w) stearyl alcohol, 3.59% (w/w) Vaseline white, 0.72% (w/w) sorbitan monostearate, and 2.39% (w/w) glycerol was heated to 70°C. Both phases were mixed at the same temperature, stirred cold, and the preservative consisting of 0.2% (w/w) methylparaben, 0.02% (w/w) propylparaben, and 2% (w/w) benzyl alcohol was added. Unless otherwise stated, the materials were purchased from Herba Chemosan (Graz, Austria).

2.1.4 Biopsy procedures

Eight-millimeter punch biopsies were collected at different time points for further histological (see 2.3) and gene expression analysis (see 2.4). All biopsies were collected under analgosedation using the above-mentioned drugs. On the day of the wounding (day 1), biopsies were taken from the excised skin only (no biopsies of burnt wounds). On days 7, 19 (second three pigs only), 21 (first three pigs only), 49, 77, 105, and 133, biopsies of all wounds were taken. Furthermore, to serve as control samples, a single punch biopsy of healthy skin was taken both cranially and caudally to the wounds, resulting in a total of ten biopsies per pig per day. The biopsies were cut in half, and one half was put in a container and stored in formaldehyde until histological preparation (see 2.3), whereas the other half was placed in a container and immediately frozen in liquid nitrogen. These halves were stored in a -80°C freezer until being used for gene expression analysis (see 2.4).

2.2 Wound assessment

2.2.1 Photography and macroscopic wound scoring

Photographs of the wounds have been taken at every dressing change and after healing every time an intervention was conducted. Until healing, wounds were scored in an adapted manner, as published in [95]. This wound score includes assessment of wound size (0-2 points), presence of granulation tissue (0-2 points), pus (0-1 point), erythema (0-3 points), crust (0-3 points), swelling (0-2 points) and necrosis (0-3 points). A maximum of 16 points could be reached, with higher numbers indicating a more intense presence of inflammatory phenotype.

All assessments were conducted by two examiners independently, that were blinded to the actual wound type. If no concordance was reached, the mean of the respective parameter's score was used; if a parameter's score diverged more than 1 point, the examiners were asked to reassess the parameter – however this was necessary only once.

2.2.2 Scar Scoring

After complete epithelialization and once distinct scar features started to form, scars were assessed using a modified version of the Vancouver Scar Scale (VSS). Using this score, scars could reach a score of 15 points maximum with pigmentation (0-2 points), vascularity (0-3 points), pliability (0-4 points), height (0-3 points), and size (0-3 points) being assessed. All assessments were conducted by two examiners independently, that were blinded to the actual wound type. If no concordance was reached, the mean of the respective parameter's score was used; if a parameter's score diverged more than 1 point, it was intended to ask the examiners to reassess the parameter – however this was not necessary in scar scoring. Since distinct scar features only appeared on day 77, scar scoring was done on days 77, 105, and 133.

2.2.3 Thermal imaging

Thermal imaging of the wounds was done before and after wounding, as well as during each time point when wound/scar manipulation was conducted. Thermal imaging was performed non-invasively using the FLIR One® Pro for iOS Attachment for iOS Smartphones. (FLIR Systems, Inc., Wilsonville, OR, USA). This device can detect temperature differences of up to 0.07 °C, enabling a distinction between burnt and non-burnt tissues as well as

temperature changes during the recovery phase. Specifications of the device can be found on the manufacturer's website [172]. The FLIR One® App was used to assess the images.

2.2.4 Hyperspectral imaging

Hyperspectral imaging of the wounds was done before and after wounding, as well as during each time point when wound/scar manipulation was conducted. For hyperspectral imaging, the TIVITA® Wound (500–1000nm, Diaspective Vision GmbH, Am Salzhof-Pepelow, Germany) was utilized. This technology assesses parameters such as perfusion, oxygen saturation, and hemoglobin content via the remission of light of various wavelengths from illuminated tissues. There is no direct contact between the device and the subject, and color-coded computer images display the results using several different parameters. The Tissue Oxygenation parameter (TO) can assess the tissue oxygenation on the wound surface. The Near Infrared Perfusion Index (NIR) is another output parameter of thermal imaging that indicates the blood's relative oxygen saturation in the microcirculation of deeper tissue layers (4-6mm) as an index value. These two parameters were used to evaluate tissue oxygenation in the different wounds. The device's specifications are available on the manufacturer's website [173].

2.3 Histology

The histological examination was performed as outlined in [1,95]. Before embedding them in paraffin, biopsies were fixed in a 10% formaldehyde solution (see 2.1.4). Three micrometer-thick sections were cut and stained with hematoxylin and eosin. These histological sections were assessed for typical scar features.

Additionally, inflammatory activity was assessed by quantifying the number of neutrophils and lymphocytes present in the dermal scar region of each stained tissue section. The cells were counted using a microscope with a 0.5 mm ocular field diameter and 400 magnification (Nikon MICROPHOT-FXA, Nikon, Tokyo, Japan). Each ocular field corresponded to a high-power field (HPF). Four randomly selected HPF within the dermis were evaluated for each case. The sum of the counts of each cell type resulted in the respective cell counts/mm^2. A trained pathologist blinded to the various scar etiologies conducted the counting and data collection. Sections containing air pockets were omitted from the analysis.

2.4 Gene expression analysis

Biopsies of porcine wound/scar tissue were homogenized in QIAzol using innuSPEED Lysis tubes and the Speedmill Plus instrument (Analytik Jena GmbH, Jena, Germany). Ribonucleic acid (RNA) was extracted from the homogenized tissue using the RNeasy Mini Kit (Qiagen, Hilden, Germany) per the manufacturer's instructions. RNA was quantified using a NanoDrop One microvolume spectrophotometer (Thermo Fisher Scientific, Waltham, MA, USA). For gene expression analysis, 1 g of total RNA was reverse transcribed into single-stranded cDNA using the iScriptTM Reverse Transcription Supermix (Bio-Rad Laboratories, Inc., Hercules, CA, USA). Bio-Rad supplied PrimePCRTM probe assays for the genes of interest and the housekeeping gene (Table 2), and Thermo Fisher Scientific provided the TaqManTM Gene Expression Master Mix. On a Bio-Rad CFX384 cycler, real-time PCR was performed. Using the Cq method, relative target gene expression was normalized with respect to the reference gene YWHAZ. All samples were calibrated using a blank (non-treated and healthy) skin sample. Duplicate Cq values that differed by more than one cycle were excluded from subsequent analysis. The investigated genes are listed in Table 2; they are further explained below:

Table 2: *Probe Assays used for qPCR (Bio-Rad Laboratories, Inc., Hercules, CA, USA; adapted from [1] with permission of the copyright holders).*

Gene	Name, commonly used aliases	Cat. No.
ACTA2	actin alpha 2, smooth muscle; alpha smooth muscle actin (aSMA)	qSscCIP0033051
COL1	collagen type I alpha 1 chain	qSscCEP0041702
COL3	collagen type III alpha 1 chain	qSscCIP0024827
HIF1a	hypoxia inducible factor 1 subunit alpha	qSscCIP0025745
HSPA4	heat shock protein family A (Hsp70) member 4; HSP70	qSscCIP0027641
IL6	interleukin 6	qSscCEP0035848
IL8	interleukin 8	qSscCEP0028429
IL10	interleukin 10	qSscCEP0032327
MMP1	matrix metallopeptidase 1	qSscCEP0032832
TGFB1	transforming growth factor beta 1	qSscCIP0039450
TGFB2	transforming growth factor beta 2	qSscCIP0040930
TGFB3	transforming growth factor beta 3	qSscCIP0040113
YWHAZ	tyrosine 3-monooxygenase/tryptophan 5-monooxygenase activation protein zeta	qSscCIP0027700

ACTA2: ACTA2 is the gene that encodes the alpha-smooth muscle actin protein. This protein is primarily expressed in smooth muscle cells and plays a role in cell contraction, motility, and hypertrophic scar formation.

COL1: COL1 is the gene that encodes the alpha 1 chain of collagen 1. Collagen 1 is the most abundant protein in the extracellular matrix of connective tissues.

COL3: COL3 is the gene that encodes the alpha 1 chain of collagen 3. Collagen 3 is found in various tissues, including skin, blood vessels, and internal organs.

HIF1a: HIF1a is the gene encoding the transcription factor HIF-1α that plays a central role in cellular responses to low oxygen levels (hypoxia). It regulates the expression of genes involved in oxygen homeostasis, angiogenesis, and energy metabolism. Dysregulation of HIF1a has been implicated in various diseases, including cancer, cardiovascular disorders, and ischemic conditions.

HSPA4: HSPA4 (Heat shock protein family A member 4) encodes the gene for a heat shock protein that assists in protein folding, assembly, and transport. It plays a role in cellular stress response and helps protect cells from damage caused by various stressors, including heat, toxins, and oxidative stress.

IL6: IL6 encodes for IL-6, a pro-inflammatory cytokine involved in immune responses and inflammation regulation. It plays a crucial role in the immune system's defense against infections and in the acute phase response. Dysregulated IL6 expression has been associated with various inflammatory and autoimmune diseases.

IL8: IL8 encodes for IL-8, another pro-inflammatory cytokine that promotes the recruitment and activation of neutrophils, a type of white blood cell involved in immune responses. It plays a role in inflammation, wound healing, and certain disease processes, including cancer and chronic inflammatory conditions.

IL10: IL10 encodes for IL-10, an anti-inflammatory cytokine that helps regulate immune responses and maintain immune homeostasis. It suppresses excessive inflammation and modulates the activity of various immune cells. Dysregulation of IL10 has been implicated in autoimmune diseases, inflammatory bowel disease, and other immune-related disorders.

MMP1: MMP1 encodes for MMP-1, also known as collagenase-1, an enzyme that degrades extracellular matrix components, including collagen. It plays a role in tissue remodeling, wound healing, and various physiological and pathological processes. Dysregulated MMP1 activity has been associated with tissue damage, fibrosis, and cancer progression.

TGFB1, TGFB2, TGFB3: These genes encode different isoforms of TGF-ß proteins. TGF-ß is a multifunctional cytokine that regulates cell growth, differentiation, and tissue development. It plays critical roles in embryogenesis, immune response modulation, wound healing, and tissue repair. Dysregulation of TGF-ß signaling has been implicated in various diseases, including cancer, fibrosis, and autoimmune disorders.

YWHAZ: YWHAZ (Tyrosine 3-monooxygenase/tryptophan 5-monooxygenase activation protein zeta) encodes a member of the 14-3-3 protein family. This gene was used as a housekeeping gene.

It is important to note that the functions and associations described here are based on current scientific understanding. Still, ongoing research may uncover additional roles or nuances for these genes in different contexts.

2.5 Statistical analysis

The statistical analysis was conducted using Prism 9 (GraphPad Software, San Diego, California, United States). The calculation of arithmetic means, medians, resulting standard deviations, and other variables of descriptive statistics were used to make meaningful and summarizing statements about the measurements. ANOVA, Kruskal–Wallis, and Tukey's/Holm-Šídák's post hoc tests were utilized to characterize inferential statistics. Correlation was measured using Spearman's correlation coefficient. The significance level was set at $p = 0.05$. Given that statistical significance can only be achieved with a sufficiently large sample size and that this study was of exploratory character, p values must be interpreted descriptively and non-conclusively. To make valid statements without omitting significances that could not be reached due to the small sample size, Cohen's d was used to compute the effect size. This additional value permits an estimation of the actual effect for groups with small sample sizes [174].

3 Results

Parts of these results have been published in [1], which is hereby referenced.

3.1 Wound Healing process and scar formation

3.1.1 Macroscopic wound healing

Forty-four wounds were created on the six Duroc pigs, resulting in a total of eleven wounds per type. All wounds achieved full epithelization after 25 days, with the wounds induced with resiquimod (BWR, FTR) displaying a higher level of inflammatory reaction during the healing process than their non-induced counterparts. Exemplary wound photographs captured during the healing process and the resulting scars, as well as the final scars in bigger scale are presented in Figures 3 and 4.

Only slight differences were observed in burn wounds during the initial stages of wound healing. On day 14, the BW showed healthy granulation tissue, while the BWR still exhibited signs of wound necrosis. The FT followed a regular healing pattern characterized by fibrin deposition and wound contracture, resulting in a minimal scar. On the other hand, the FTR wound showed a slow granulation tendency with almost no wound contracture, leading to the development of a larger scar.

3.1.2 Wound score

During the wound healing (until re-epithelialization), wounds were assessed by a wound score to allow estimation of the inflammatory reaction. The wound score shows higher values for the respective wounds that were induced with resiquimod. A difference between resiquimod-induced and non-induced wounds became visible on day 4 for FT and FTR ($p < 0.0001$), and for BW and BWR wounds ($p = 0.01$). The highest difference was seen on day 7 between the previous-mentioned wound types. The difference became less visible on days 10 and 14, but stayed statistically significant throughout the evaluations. Table 3 and Figure 5 display detailed results of the wound scoring.

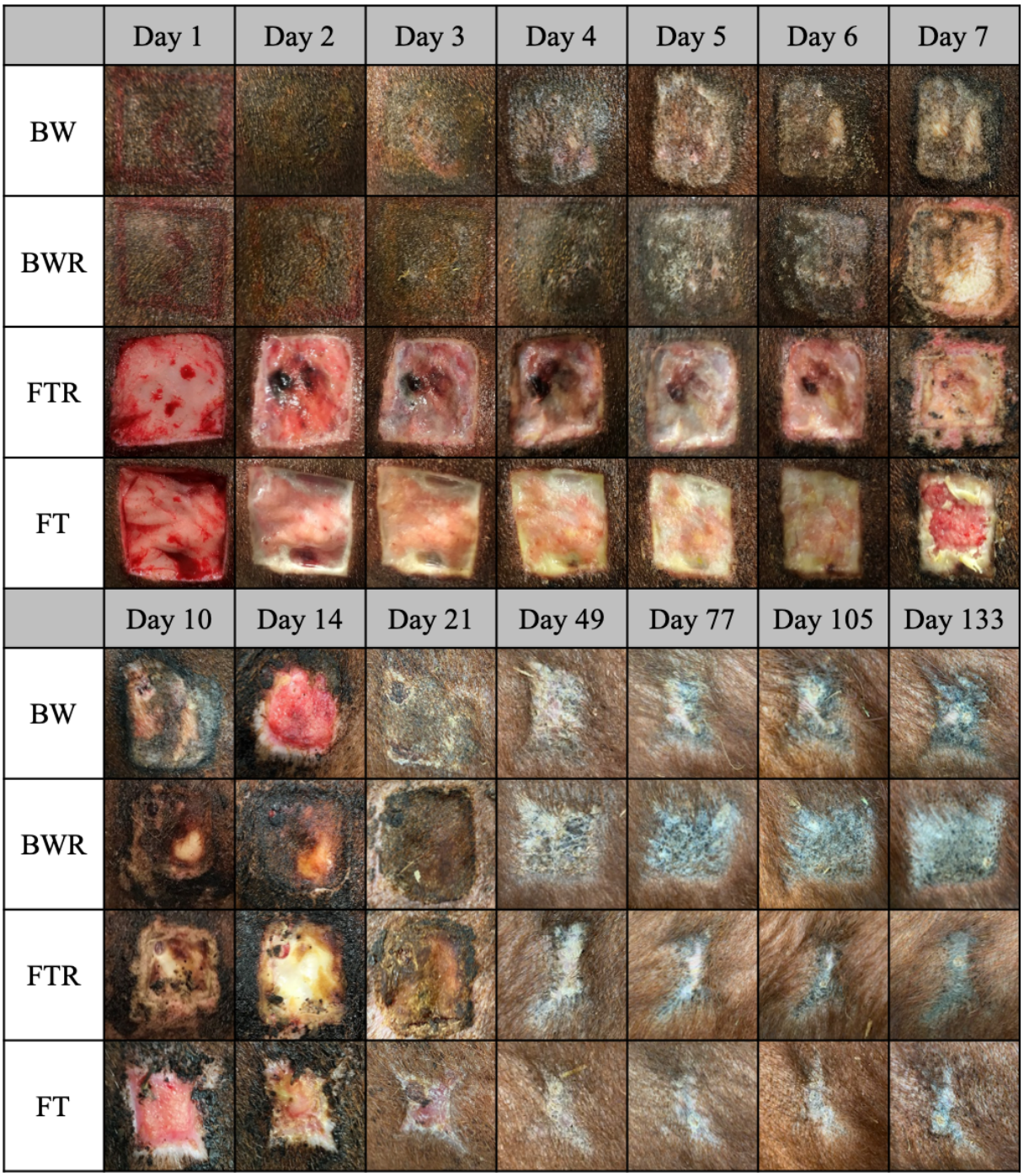

Figure 3: *Wound healing throughout the study course. While in burn wounds almost no differences could be seen initially, thick scabs, prolonged necrosis and less wound contraction were seen starting day 7. Full-thickness wounds without inflammatory induction took a physiological healing course with fibrin deposition, which was reduced in resiquimod-induced wounds that on the other hand showed prolonged necrotic areas as well. The resulting scars were thicker and less pliable than the non-induced ones. FT = Full-thickness wound, FTR = Full-thickness wound with resiquimod, BW = Burn wound, BWR = Burn wound with resiquimod (adapted from [1] with permission of the copyright-holders).*

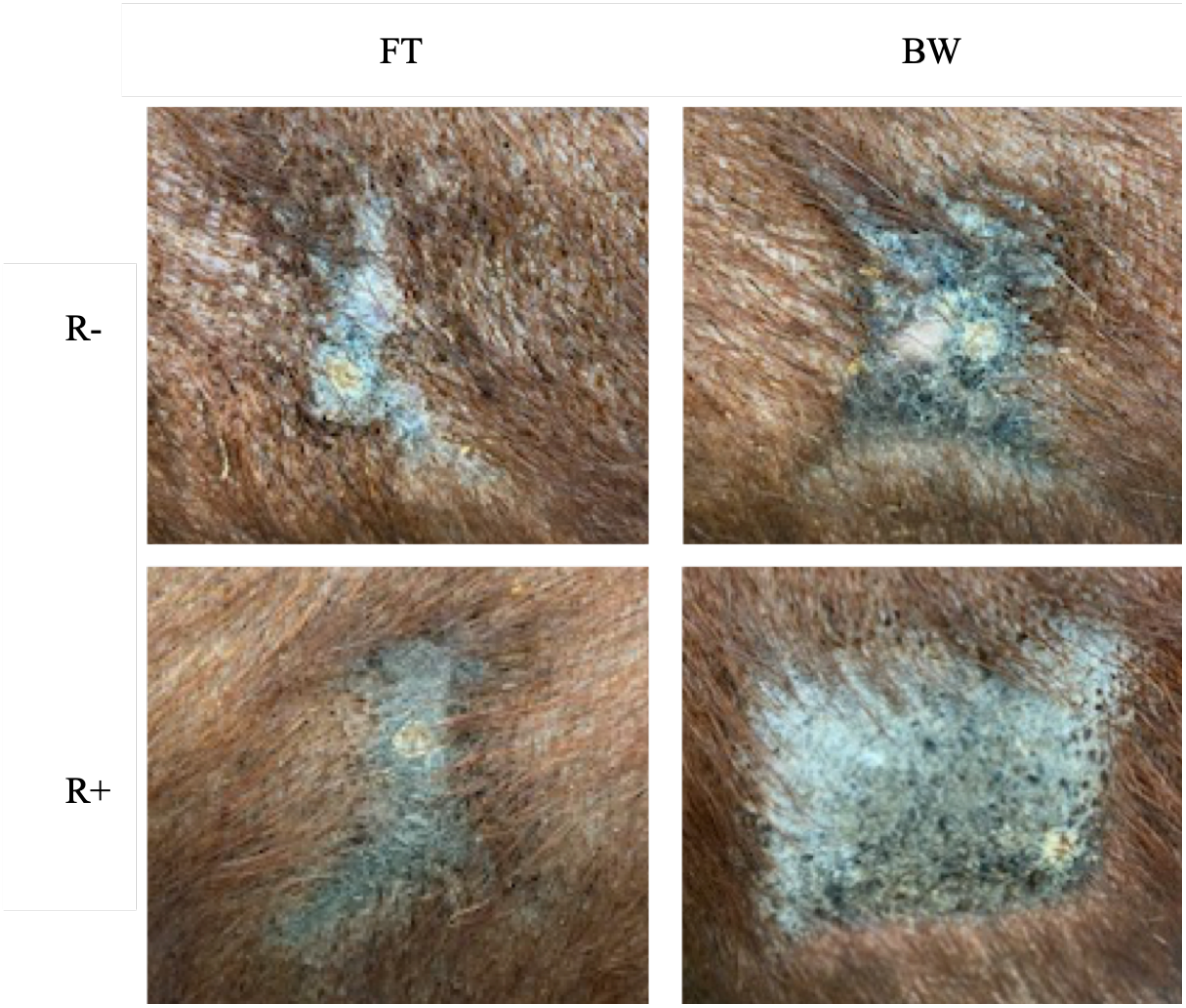

Figure 4: *Larger scale photographs of the final scars. Day 133: Burn scars show clearly less wound size contraction, as did induced full-thickness wound scars. All scars were stiff, non-pliable and showed a hypertrophic relief. FT = Full-thickness wound, BW = Burn wound, R+ = Resiquimod-induced wounds, R- = Non-induced wounds.*

Table 3: *Wound score results. Values are dimensionless and given in means and standard deviation (+/-). FT = Full-thickness wound, FTR = Full-thickness wound with resiquimod, BW = Burn wound, BWR = Burn wound with resiquimod.*

	Day 2	Day 4	Day 7	Day 10	Day 14
FT	6.4 (+/- 1.4)	6.6 (+/- 0.5)	3.0 (+/- 1.2)	2.8 (+/- 0.6)	2.1 (+/- 0.7)
FTR	6.5 (+/- 0.8)	10.1 (+/- 1.4)	9.8 (+/- 2.4)	7.6 (+/- 1.0)	6.8 (+/- 0.7)
p	0.97	< 0.0001	< 0.0001	< 0.0001	< 0.0001
BW	4.7 (+/- 0.8)	3.0 (+/- 1.0)	2.8 (+/- 1.3)	1.8 (+/- 0.7)	1.4 (+/- 0.8)
BWR	4.8 (+/- 0.4)	4.3 (+/- 1.2)	6.6 (+/- 2.6)	3.4 (+/- 0.8)	3.0 (+/- 1.3)
p	0.97	0.01	0.0004	0.0005	0.0019

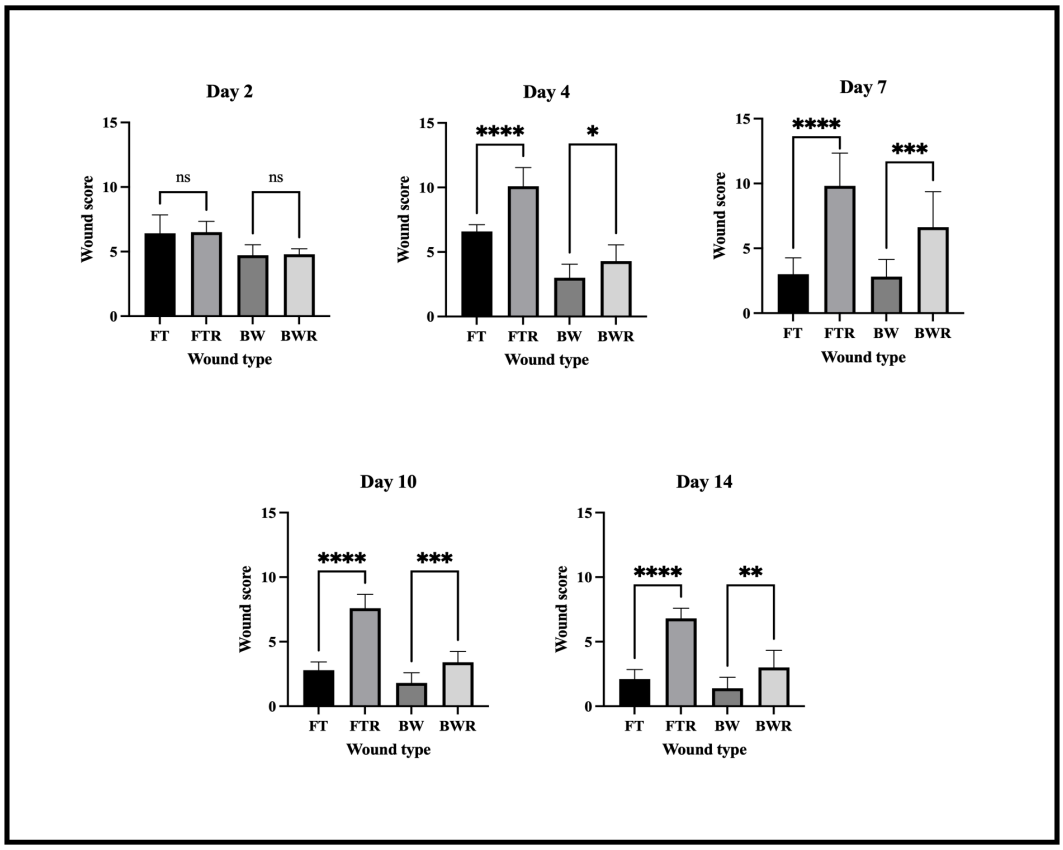

Figure 5: *Wound score results. Initially, no differences between induced and non-induced wounds were seen. Differences started to be significant by day 4 and remained throughout the assessment phase. Full-thickness wounds showed larger differences than burn wounds. FT = Full-thickness wound, FTR = Full-thickness wound with resiquimod, BW = Burn wound, BWR = Burn wound with resiquimod, ns = not significant, * = p < 0.05, ** = p < 0.01, *** = p < 0.001, **** = p < 0.0001. Results are reported as means (bars) and standard deviation (whiskers). No cross-comparisons between burn and full-thickness wounds were conducted as wound scores differed between the wound types.*

3.1.3 Scar score

Following wound closure, pronounced scarring became evident, and by day 77, signs of hypertrophy were visible. On days 77, 105, and 133, the scars were evaluated using a modified VSS. As early as day 77, resiquimod-induced lesions attained significantly higher scores (BWR vs. FT: $p = 0.0012$; FTR vs. FT: $p = 0.036$) than their non-induced counterparts. On day 105, additional differences between non-induced wounds emerged, with BW achieving higher scores than FT (BW vs. FT: $p = 0.0019$; BWR vs. FT: $p = 0.0002$; FTR vs. FT: $p = 0.0080$). These differences persisted until the conclusion of the investigation on day 133 (BW vs. FT: $p = 0.0150$; BWR vs. FT: p 0.0001; FTR vs. FT: $p = 0.0002$). Due to the small sample size, the effect size was calculated for BW vs. BWR: Cohen's d of 0.55 (day 77), 0.38 (day 105), and 0.75 (day 133) was seen. Table 4 and Figure 6 depict detailed results of the scar scoring.

3.1.3.1 Correlation of scar and wound score

The correlation of scar (day 133) and wound score (day 7) was calculated and yielded a significant correlation ($p = 0.0327$) with a correlation coefficient of $r = 0.3225$.

Table 4: *Scar score values of the different wound types. FT = Full-thickness wound, FTR = Full-thickness wound with resiquimod, BW = Burn wound, BWR = Burn wound with resiquimod. Values are dimensionless and given as means and standard deviation (+/-).*

	Day 77	Day 105	Day 133
FT	3.7 (+/- 1.9)	6.1 (+/- 1.0)	5.9 (+/- 1.0)
FTR	6.27 (+/- 1.7)	7.9 (+/- 1.1)	8.3 (+/- 0.8)
BW	5.9 (+/- 1.7)	8.0 (+/- 0.8)	7.7 (+/- 0.9)
BWR	6.8 (+/- 1.6)	8.3 (+/- 0.7)	8.5 (+/- 1.0)

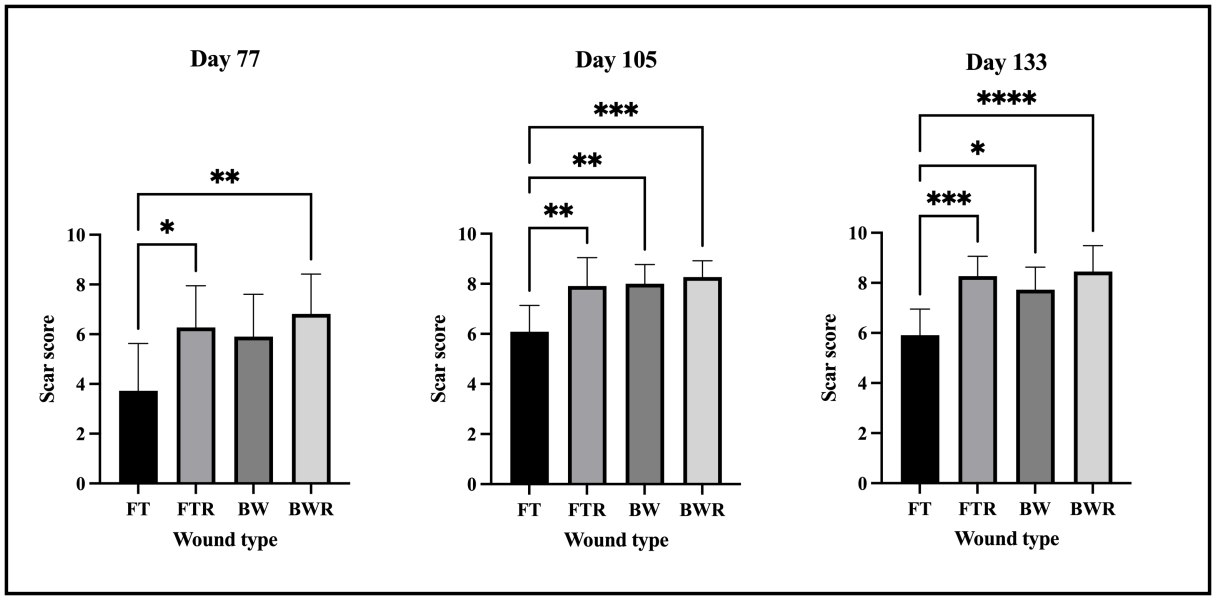

Figure 6: *Scar score results as assessed by a modified Vancouver Scar Scale. Resiquimod-induced wound scars showed significantly different results compared to non-induced full-thickness wound scars by day 77, and thereby earlier than non-induced burn wound scars that showed significantly different phenotype by day 105. These differences remained apparent until the study conclusion. FT = Full-thickness wound, FTR = Full-thickness wound with resiquimod, BW = Burn wound, BWR = Burn wound with resiquimod, * = $p < 0.05$, ** = $p < 0.01$, *** = $p < 0.001$, **** = $p < 0.0001$. Results are reported as means (bars) and standard deviation (whiskers). Only significant differences are shown. Adapted from [1] with permission from the copyright holders.*

3.2 Imaging

3.2.1 Thermal Imaging

Thermal imaging was employed for the optical evaluation of the surface temperature of the wounds. Pre-wounding and post-wounding photographs were taken, along with images captured during each dressing change. Initial differences in temperature were observed among the different wound types. The wound perimetry showed higher temperatures in burn and induced wounds (FTR, BWR, BW), but not in FT wounds. Quantification of the images were not possible due to software issues. Therefore, no further evaluation with thermal imaging was conducted. Figure 7 depicts an exemplary thermal image of one pig before and after wounding. Figure 8 shows the thermal image of pig 1 on day 7 alongside its pictogram for wound mapping.

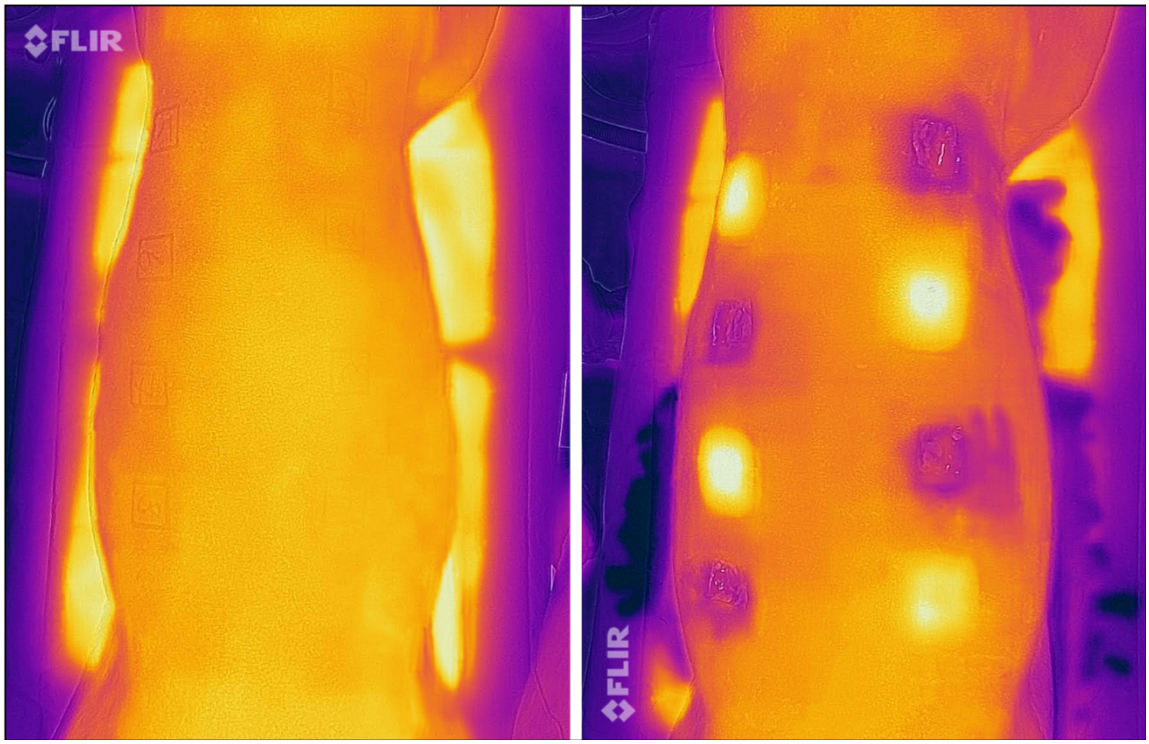

Figure 7: *Thermal imaging of a pig before and immediately after wounding. Yellow color indicates warmer temperatures, blue/purple indicates colder temperatures. Burn wounds can clearly be seen as warmer wounds than excisional wounds. For technical reasons, no quantification was possible.*

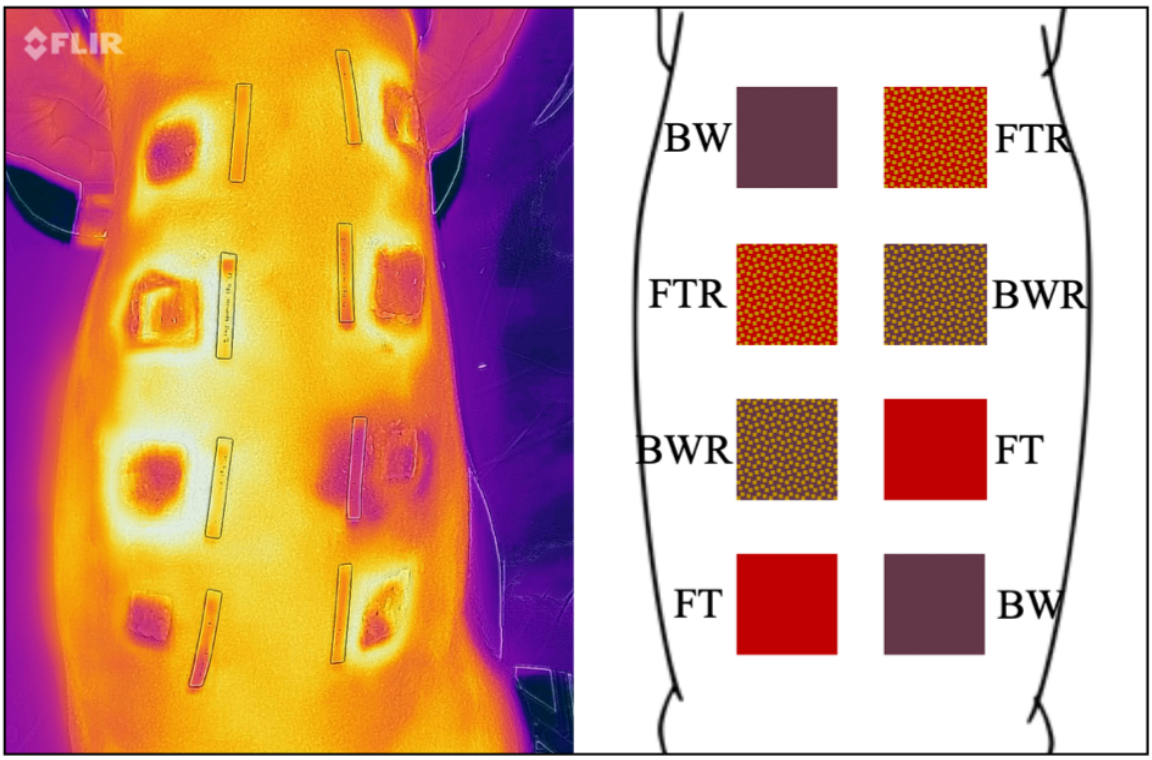

Figure 8: *Thermal image of pig 1 on day 7 alongside its pictogram. In the thermal image (left) it can clearly be seen that one day after resiquimod induction burn as well as induced wounds show warmer temperatures than non-induced full-thickness wounds (compare to pictogram on the right) in the area around the wounds. Yellow color indicates warmer temperatures, blue/purple indicates colder temperatures. For technical reasons, no quantification was possible. FT = Full-thickness wound, FTR = Full-thickness wound with resiquimod, BW = Burn wound, BWR = Burn wound with resiquimod.*

3.2.2 Hyperspectral Imaging

Hyperspectral imaging allows the evaluation of tissue oxygenation on and below the wound surface. An immediate decrease in tissue oxygenation was observed after the infliction of burn wounds, whereas an increase was observed in full-thickness wounds. The application of resiquimod on the full-thickness wound led to a quicker decrease of tissue oxygenation, approximating the burn wounds' curves. Similar courses can be described for tissue oxygenation on the surface (TO) and below the wound surface (NIR). The tissue oxygenation course is depicted in Figure 9.

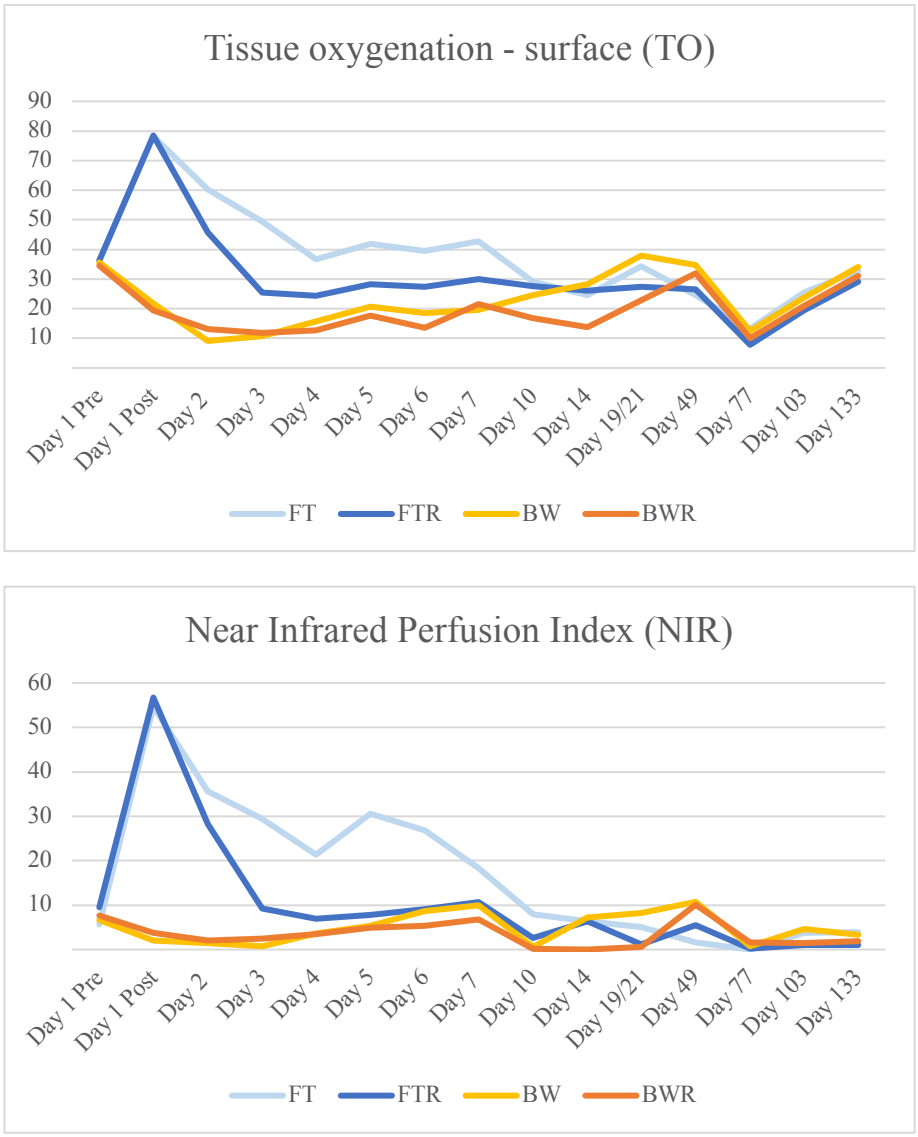

Figure 9: *Oxygenation course as measured by hyperspectral imaging. The tissue oxygenation on the surface (TO, above) and the oxygenation below the surface (NIR, below) show similar courses. Induced full-thickness wounds' oxygenation quickly approximates the relative hypoxia of burn wounds after resiquimod induction. FT = Full-thickness wound, FTR = Full-thickness wound with resiquimod, BW = Burn wound, BWR = Burn wound with resiquimod.*

Given the similar courses and an assumed stronger validity of perfusion below the wound surface, statistical analysis was only performed for NIR values. While no significant differences were observed in the tissue oxygenation on day 3 between BW and BWR ($p > 0.05$), and FT and FTR ($p > 0.05$), the difference between FT and FTR became significant on day 4 ($p = 0.032$) with then no significant difference between FTR and BW, FTR and BWR, and BW

and BWR was observable anymore ($p > 0.05$). All tissue oxygenation curves have approximated each other, with no significant differences being observable anymore on day 14 ($p > 0.05$). Tissue oxygenation values are presented in Table 5, and statistical analysis of NIR values is presented in Figure 10.

Table 5: *Hyperspectral imaging results. Tissue Oxygenation (TO; top) and Near Infrared Perfusion Index (NIR; bottom) in the different wound types (dimensionless values). FT = Full-thickness wound, FTR = Full-thickness wound with resiquimod, BW = Burn wound, BWR = Burn wound with resiquimod. Values are given as means and standard deviation (+/-).*

TO	Day 1 Pre-Wounding	Day 1 Post-Wounding	Day 3	Day 4	Day 14
FT	36.17 (+/- 6.82)	78.18 (+/- 6.28)	49.45 (+/- 10.82)	36.73 (+/- 14.35)	24.60 (+/- 6.25)
FTR	36.17 (+/- 7.06)	78.45 (+/- 6.37)	25.36 (+/- 8.84)	24.45 (+/- 10.57)	26.00 (+/- 9.51)
BW	35.50 (+/- 9.48)	21.73 (+/- 11.85)	10.82 (+/- 8.28)	15.73 (+/- 11.42)	28.20 (+/- 12.64)
BWR	34.50 (+/- 10.19)	19.45 (+/- 11.24)	11.82 (+/- 7.74)	12.64 (+/- 6.50)	13.80 (+/- 3.71)

NIR	Day 1 Pre-Wounding	Day 1 Post-Wounding	Day 3	Day 4	Day 14
FT	5.67 (+/- 5.91)	54.64 (+/- 11.01)	29.45 (+/- 8.74)	21.27 (+/- 6.28)	6.40 (+/- 3.44)
FTR	9.50 (+/- 7.32)	56.73 (+/- 15.63)	9.18 (+/- 3.93)	6.91 (+/- 4.50)	6.40 (+/- 8.21)
BW	6.67 (+/- 6.37)	2.09 (+/- 4.44)	0.73 (+/- 1.60)	3.55 (+/- 4.94)	7.20 (+/- 9.02)
BWR	7.67 (+/- 7.45)	3.73 (+/- 7.12)	2.45 (+/- 5.16)	3.45 (+/- 6.30)	0.00 (+/- 0.00)

3.2.2.1 Correlation of NIR oxygenation and scar score

A correlation between NIR oxygenation (days 3 and 7) and scar score was calculated: On day 3 a significant correlation ($p < 0.0001$) with a correlation coefficient of $r = -0.6450$ was yielded; day 7 yielded no significant result ($p = 0.0918$, $r = -0.2573$).

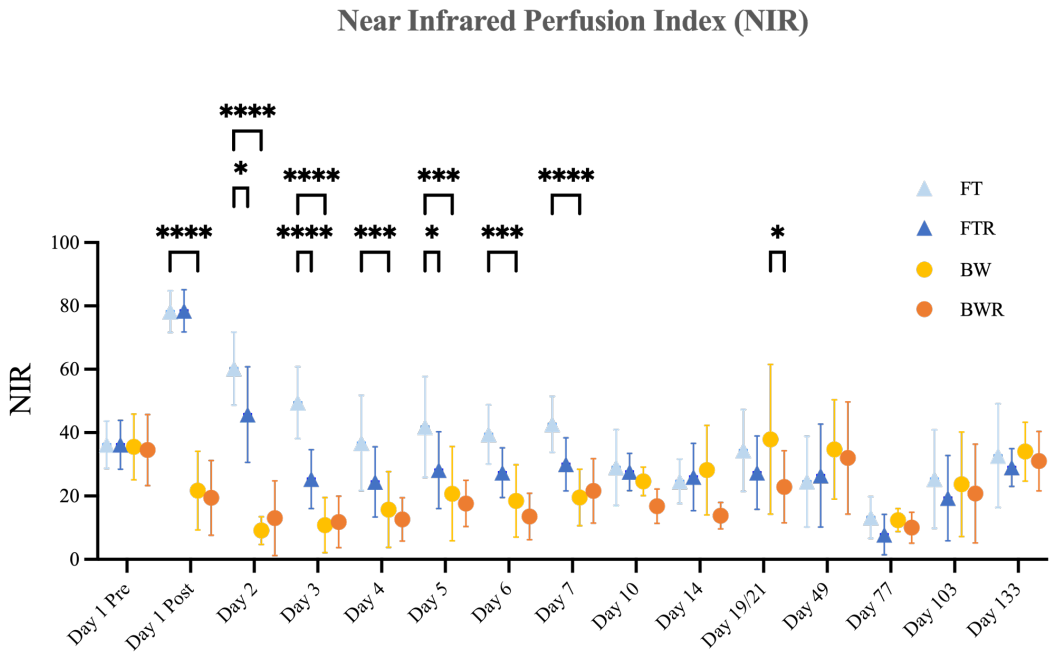

Figure 10: *Statistical results of tissue oxygenation below the wound surface. An initial hyperoxygenation is seen in full-thickness wounds, that is quickly dampened in resiquimod-induced wounds, approximating the relative hypoxia of burn wounds. Ten days after wounding, oxygenation levels converged. NIR = Near Infrared Perfusion Index, FT = Full-thickness wound, FTR = Full-thickness wound with resiquimod, BW = Burn wound, BWR = Burn wound with resiquimod, * = $p < 0.05$, *** = $p < 0.001$, **** = $p < 0.0001$. Results are reported as means (circles and triangles) and standard deviation (whiskers). Only significant differences are shown. Adapted from [1] with permission of the copyright holders.*

3.3 Histology

Eight-millimeter punch biopsies were collected at different times for further histological analysis (see 2.1.4). On the day of the wounding (day 1), biopsies were taken from the excised skin only (no biopsies of burnt wounds). On days 7, 19/21, 49, 77, 105, and 133, biopsies of all wounds were taken. Additionally, one punch biopsy of healthy skin was collected cranially and caudally of the wounds and served as blank samples, resulting in a total of ten biopsies per pig per day. Biopsies were then stained and assessed for their morphology and inflammatory cell infiltration. Figure 11 summarizes the findings described below and shows exemplary sections.

3.3.1 Microscopic scar description

All four wound types formed scars – the below-mentioned description refers to the final histological assessment on day 105. The epidermis of FT scars showed comparable features to the epidermis in control biopsies regarding thickness and epidermal rete ridges morphology with a slight thickening of the epidermis. In induced wounds (FTR, BW, BWR), the epidermal thickness was relevantly increased. Epidermal rete ridges in induced wounds reached deeper into the dermis. The epidermal thickness increased during the healing process. In the control biopsies, the dermis showed wavy, parallel-oriented collagen patterns along with sebaceous glands and hair follicles located deep within dermis. Similarly, the FT scars displayed wavy and mostly parallel collagen organization, which appeared denser than the control samples, but without the presence of hair follicles or sebaceous glands. BW scars also showed a wavy collagen organization, yet less organized than FT scars. The resiquimod-induced scars showed completely disorganized collagen patterns with some insinuated whorl-like patterns (FTR more than BWR) but no nodules. All scars, including controls, showed inflammatory cell infiltration (see 3.2.2). Table 6 summarizes the histological characteristics.

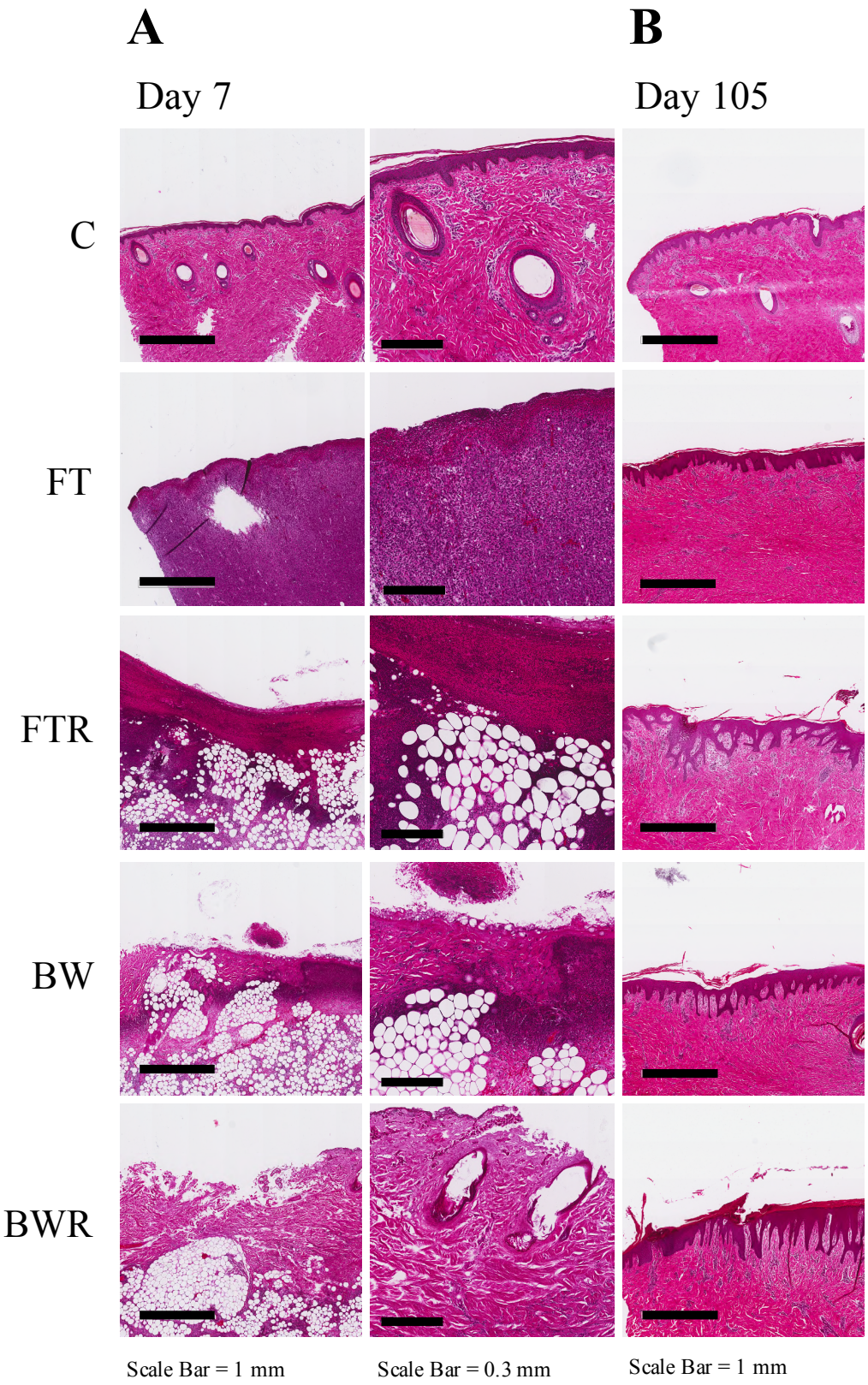

Figure 11: *Exemplary histologic sections of wounds (A) and scars (B) in hematoxylin/eosin staining. Inflammatory cell invasion was significantly higher in resiquimod-induced full-thickness wounds compare to all other wound types. Hyperinflammatory wounds showed adipocyte clusters within the dermis and thickened epidermis with deep dermal ridges in the scars by day 105, as well as insinuated whorl-like collagen deposition as is typical in hypertrophic scars.*

Table 6: *Summary of histologic characteristics found in this project. C = Control biopsies, FT = Full-thickness wound, FTR = Full-thickness wound with resiquimod, BW = Burn wound, BWR = Burn wound with resiquimod, the number of + indicates the relative manifestation.*

	C	FT	FTR	BW	BWR
Epidermal thickness	Normal	+	+++	++	+++
Epidermal rete ridges	Normal	Normal	Deeper	Deeper	Deeper
Dermal collagen organization	Wavy, parallel	Wavy, parallel, dense	Scattered, disorganized, insinuated whorl-like patterns	Less organized, insinuated wavy parallel	Scattered, disorganized, insinuated whorl-like patterns
Inflammatory cells	Some	+	+++	+	+
Skin appendages	Present	Absent	Absent	Absent	Absent

3.3.2 Inflammatory scar assessment

Microscopic analysis of the wounds on days 7, 21, 49, and 105 was performed to evaluate possible infiltration of neutrophils and lymphocytes in the dermis. According to this quantitative histological analysis, the dermis of FTR wounds contained substantially more neutrophils on days 7 and 21. On day 7, FT, FTR, and BW wounds demonstrated substantially greater neutrophil infiltration than the control group (p = 0.0409, < 0.0001, and = 0.001, respectively), and BWR showed no significantly increased neutrophil infiltration (p = 0.12). In addition, the FTR group had substantially more neutrophils than the FT, BW, and BWR groups ($p < 0.0001$ for all comparisons); the other comparisons did not differ significantly. On day 21, the dermis of the FTR group contained noticeably more neutrophils than that of the control, FT, BW, and BWR groups ($p < 0.0001$ for C, FT, and BW, and $p = 0.0002$ for BWR). Other than FTR, there were no significant differences between wound varieties. On day 21, there were differences in the mean number of lymphocytes in the dermis of FTR wounds (21.2 cells/mm^2) versus BWR wounds (8.25 cells/mm^2) and control specimens (9.83 cells/mm^2) (p = 0.0016; p = 0.0023). None of the remaining results regarding the number of lymphocytes were statistically significant. Figure 12 and Table 7 summarize these findings.

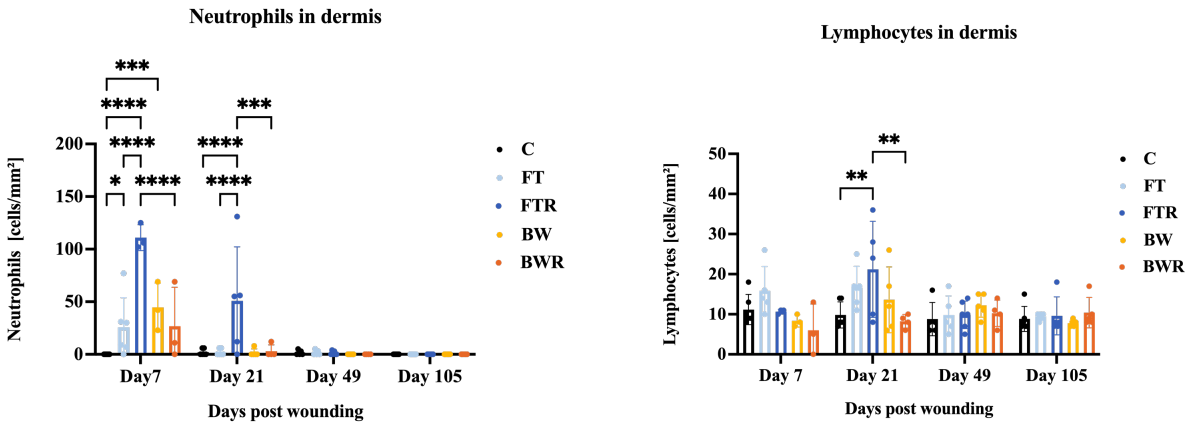

Figure 12: *Microscopical inflammatory cell count in wounds and scars. Burn injury and resiquimod-induced inflammation led to increased neutrophil (left) and lymphocyte (right) counts in biopsies. Induced full-thickness wounds showed significantly more neutrophils and lymphocytes. The other wound types had higher cell counts than control biopsies but no differences among them. C = Control biopsies, FT = Full-thickness wound, FTR = Full-thickness wound with resiquimod, BW = Burn wound, BWR = Burn wound with resiquimod, * = $p < 0.05$, ** = $p < 0.01$, *** = $p < 0.001$, **** = $p < 0.0001$, mm^2 = square millimeter. Results are reported as means (bars) and standard deviation (whiskers). Only significant differences are shown. Adapted from [1] with permission of the copyright holders.*

Table 7: *Histologic inflammatory cell counts. Neutrophils (above) and lymphocytes (below) were counted in high-power fields and are indicated in absolutes as means and standard deviation (+/-). C = Control biopsies, FT = Full-thickness wound, FTR = Full-thickness wound with resiquimod, BW = Burn wound, BWR = Burn wound with resiquimod.*

Neutrophils	Day 7	Day 21	Day 49	Day 105
C	0	2.00 (+/- 2.83)	1.60 (+/- 2.06)	0
FT	30.80 (+/- 25.20)	1.20 (+/- 2.40)	0	0
FTR	111.00 (+/- 10.03)	50.80 (+/- 45.96)	1.17 (+/- 1.67)	0
BW	44.67 (+/- 18.87)	1.60 (+/- 3.20)	0	0
BWR	26.67 (+/- 30.27)	3.00 (+/- 5.20)	0	0

Lymphocytes	Day 7	Day 21	Day 49	Day 105
C	11.17 (+/- 3.44)	9.83 (+/- 2.97)	8.80 (+/- 3.71)	8.83 (+/- 2.85)
FT	15.80 (+/- 5.46)	16.60 (+/- 4.80)	9.80 (+/- 4.26)	9.40 (+/- 0.80)
FTR	10.67 (+/- 0.47)	21.20 (+/- 10.70)	9.83 (+/- 3.13)	9.60 (+/- 4.22)
BW	8.33 (+/- 1.25)	13.60 (+/- 7.34)	12.20 (+/- 2.64)	7.80 (+/- 0.75)
BWR	6.00 (+/- 5.35)	8.25 (+/- 1.48)	10.25 (+/- 2.86)	10.40 (+/- 3.38)

3.3.2.1 Effect size of BWR vs. C and FTR vs. C

Due to small sample size in the BWR group (several slides showed air inclusions and had to be excluded), effect size was calculated. An effect size of 1.25 was obtained.

3.4 Gene expression analysis

Eight-millimeter punch biopsies were collected at different time points for gene expression analysis (see 2.1.4). On the day of the wounding (day 1), biopsies were taken from the excised skin only (no biopsies of burnt wounds). On days 7, 19/21, 49, 77, 105, and 133, biopsies of all wounds were taken. Additionally, to serve as blank samples, one punch biopsy of healthy skin was obtained cranially and caudally to the wounds, resulting in a total of ten biopsies per pig per day. The mean (bar) and standard deviation (whiskers) for N-fold expression levels are depicted in the respective figures.

3.4.1 Inflammatory gene expression

Inflammatory gene expression was investigated at all time points indicated above. The most relevant results were expected and seen during the initial phase; therefore, only days 7, 19/21, and 133 as final values are further described below. All other time points did not yield relevant results.

The pro-inflammatory mediator gene IL6 showed significantly higher expression in resiquimod-induced wounds (FTR, BWR) than in placebo-treated BW wounds ($p = 0.039$ and 0.027, respectively) and placebo-treated FT wounds ($p = 0.001$ and $p = 0.001$, respectively). No significant difference was observed between induced wound categories ($p > 0.05$). These distinctions were only apparent during the initial investigation phase (day 7) and gradually disappeared over time. None of the non-induced burn lesions differed significantly from the controls ($p > 0.05$ for both). On day 7, the anti-inflammatory mediator IL10 was expressed marginally higher in FTR than in the control group ($p = 0.006$). Further analysis of IL10 and IL8 revealed no additional differences. Figure 13 summarizes these findings.

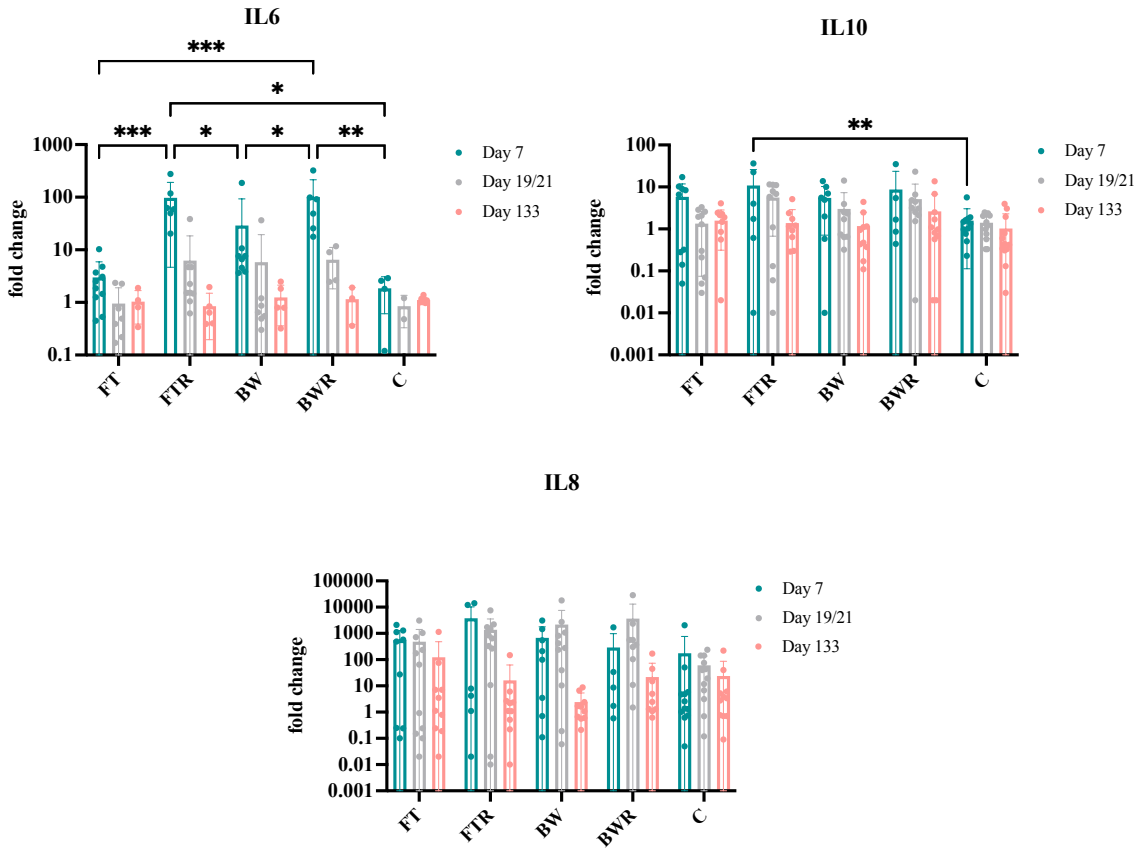

Figure 13: *Gene expression analysis of inflammatory genes. Burn and resiquimod induction significantly increased the IL6 expression, had only a moderate effect on IL10 (induced full-thickness wounds), and showed no effect on IL8 at the investigated time points. C = Control biopsies, FT = Full-thickness wound, FTR = Full-thickness wound with resiquimod, BW = Burn wound, BWR = Burn wound with resiquimod, * = $p < 0.05$, *** = $p < 0.001$. Results are reported as means (bars) and standard deviation (whiskers). Only significant differences are shown. Adapted from [1] with permission of the copyright holders.*

3.4.2 Remodeling gene expression

Remodeling gene expression was investigated at all time points indicated above. The most relevant results were expected and seen during the late (remodeling) phase; therefore, only days 19/21, 77, and 133 as final values are further described below. All other time points did not yield relevant results.

Only TGFB1 gene expression increased significantly in resiquimod-induced wound types compared to controls (FTR vs. C: $p < 0.0001$; BWR vs. C: $p = 0.0224$), as determined by gene expression analysis. Compared to non-induced full-thickness and burn wounds, resiquimod-induced full-thickness wounds also demonstrated significant overexpression on day 19/21 ($p = 0.0002$ and $p = 0.0101$, respectively). MMP1 expression was also markedly elevated in resiquimod-induced wounds compared to controls (FTR vs. C: $p < 0.0063$; BWR vs. C: $p = 0.0351$). TGFB2 expression was significantly higher in FTR than in FT wounds on day 19/21 ($p = 0.0146$). The expression patterns of ACTA2, TGFB3, COL1, and COL3 were not significantly different at any time points examined. Figure 14 summarizes these findings.

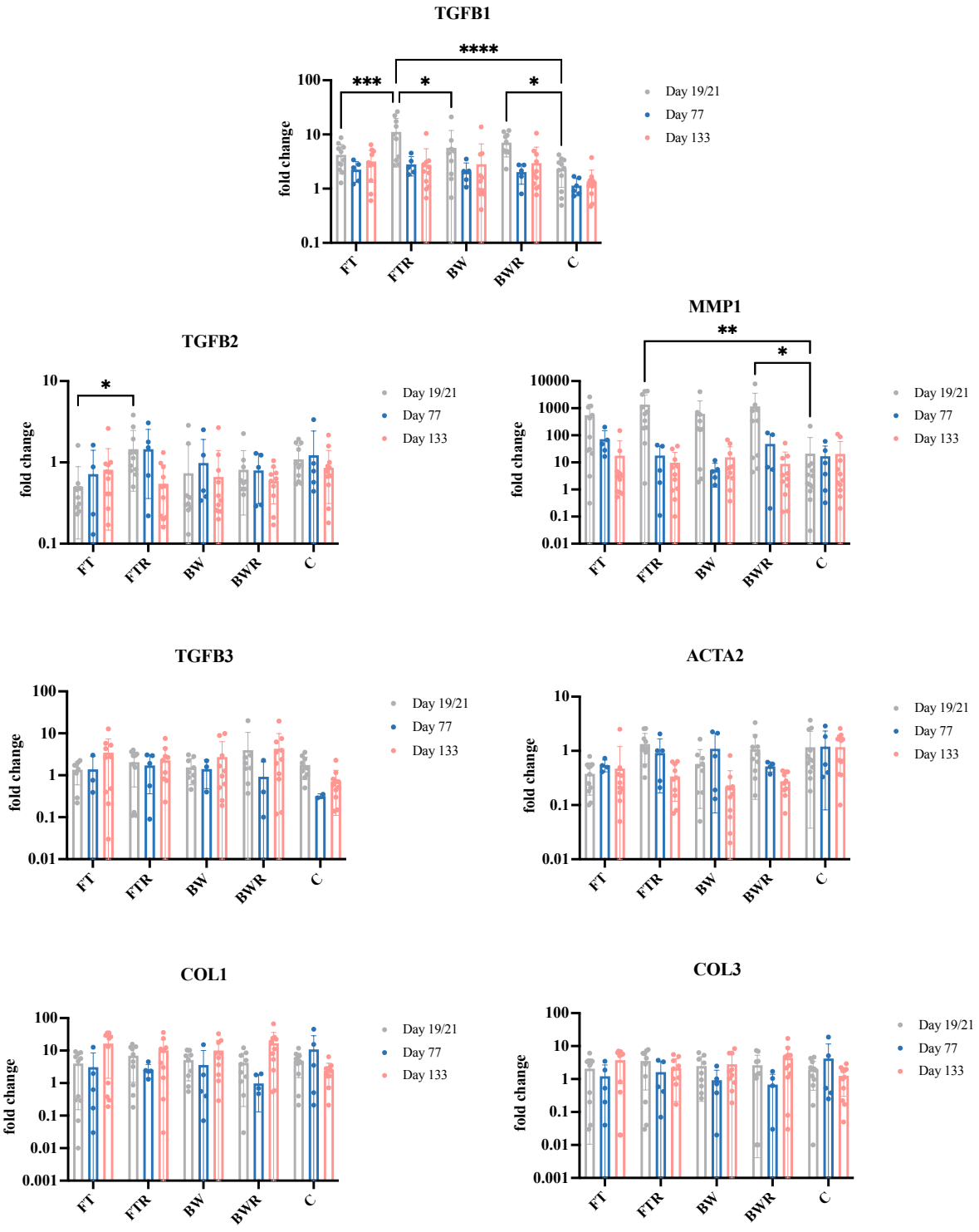

Figure 14: *Gene expression analysis of remodeling-associated genes. Resiquimod-induced wounds showed a significant upregulation compared to non-induced wounds and control in TGFB1, less also in TGFB2 and MMP1. C = Control biopsies, FT = Full-thickness wound, FTR = Full-thickness wound with resiquimod, BW = Burn wound, BWR = Burn wound with resiquimod, * = $p < 0.05$, *** = $p < 0.001$, * = $p < 0.0001$. Results are reported as means (bars) and standard deviation (whiskers). Only significant differences are shown. Adapted from [1] with permission of the copyright holders.*

3.4.3 Oxidative stress response gene expression

Oxidative stress response gene expression was investigated at all time points indicated above. The most relevant results were expected and seen during the early (inflammation) phase; therefore, only days 7, 19/21, and 133 as final values are further described below. All other time points did not yield relevant results.

HIF1a expression exhibited significant upregulation in resiquimod-induced wounds compared to their respective non-induced counterparts (FTR vs. FT: $p = 0.0223$; BWR vs. BW: $p = 0.0118$) as well as in cross-comparisons (FTR vs. BW: $p = 0.0065$; BWR vs. FT: $p = 0.0066$) and in relation to the control biopsies ($p < 0.0001$ for FTR and BWR vs. C respectively). FT wounds showed only slight upregulation compared to control biopsies ($p = 0.0160$). The higher HIF1a expression remained significant in FTR wounds compared to FT wounds and controls until day 19/21 after wounding ($p = 0.0485$ and $p = 0.0220$), whereas expression levels in the other wound types had normalized by that time.

Regarding HSPA4 expression, significant differences were only observed on day 7, with FTR showing marked overexpression compared to all other groups (vs. FT: $p < 0.0001$; vs. C: $p < 0.0001$; vs. BWR: $p = 0.0235$; vs. BW: $p < 0.0001$). BWR biopsies also yielded significant overexpression compared to FT ($p = 0.0083$) and C biopsies ($p = 0.0003$). All other comparisons did not reach statistical significance. Figure 15 summarizes these findings.

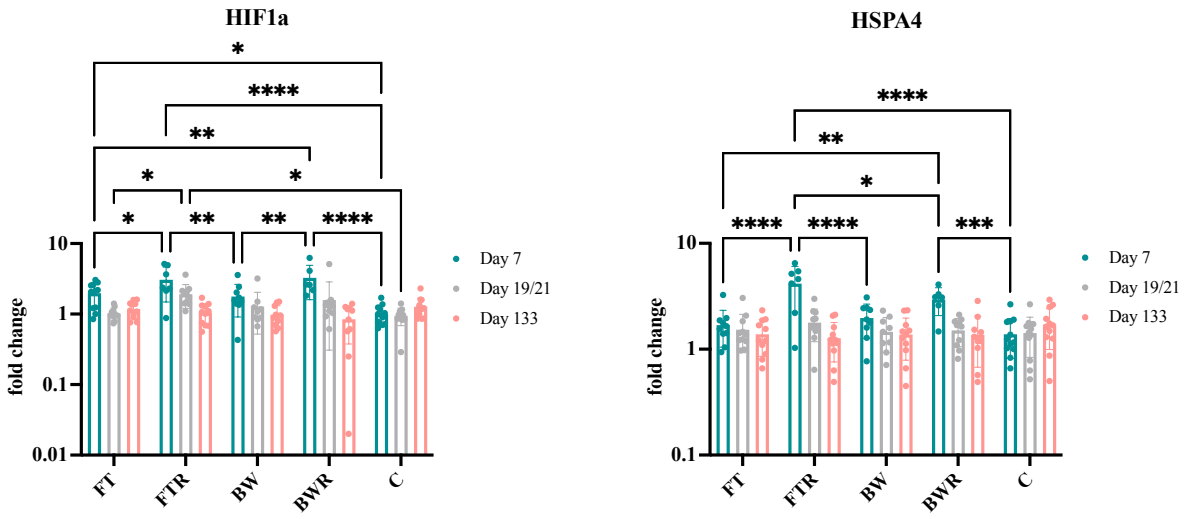

Figure 15: *Gene expression analysis of stress-associated genes. Resiquimod-induced full-thickness and burn wounds showed significantly higher stress response by the increased expression of HIF1a and HSPA4. The upregulation of HIF1a in induced full-thickness wounds lasted until day 19/21. C = Control biopsies, FT = Full-thickness wound, FTR = Full-thickness wound with resiquimod, BW = Burn wound, BWR = Burn wound with resiquimod, * = $p < 0.05$, *** = $p < 0.001$, **** = $p < 0.0001$. Results are reported as means (bars) and standard deviation (whiskers). Only significant differences are shown. Adapted from [1] with permission of the copyright holders.*

4 Discussion

When immersing into scar research, the respective clinical aspects of the research question need to be considered. Recently, a valuable model simulating chronic wounds has been developed by applying the TLR7/8 agonist resiquimod, an immunomodulatory drug used to treat various dermatological conditions. The application of resiquimod to fresh wounds in pigs has shown to produce a hyperinflammatory environment and impede the wound healing process [95]. Leveraging this chronic wound, this project was conceived in light of the fact that hyperinflammation and prolonged healing are regarded as significant risk factors contributing to hypertrophic scar formation [175,176].

Despite the high cost and elaborate animal welfare considerations, the Duroc pig was selected as the experimental animal model as it is considered one of the best suitable animals for scar research [169,177]. The primary objective of this project was two-fold: firstly, to investigate differences between scars of different etiologies, and secondly, to establish a practical and standardized hypertrophic scar model that permits further research into the scarring process and the possible exploration of the working mechanisms of treatment modalities.

The scars subjected to analysis encompassed those resulting from full-thickness wounds and burn injuries, along with their corresponding resiquimod-induced hyperinflammatory counterparts. While all but the non-induced full-thickness wound yielded signs of hyperinflammation and hypoxia, the resiquimod-induced full-thickness wound showed the earliest and most pronounced response in terms of macroscopical, microscopical, and gene expression analysis. In other words, the resiquimod-induced full-thickness wound exhibited the earliest and most conspicuous responses in terms of macroscopic, microscopic, and gene expression analyses, highlighting its use for further scar research.

4.1 The Duroc pig as a suitable animal model

Duroc pigs have been used as hypertrophic scar models since the 1970s [166]. Most studies involving the Duroc pig used dermatome wounds due to their reliable reproducibility and controlled depth characteristics. Although reproducible wound types were used, researchers in subsequent studies encountered varied degrees of success in inducing macroscopic hypertrophic scars in Duroc pigs [167–170]. Several studies, however, showed histological characteristics and/or genetic expression patterns comparable to those in human hypertrophic

scars, which is why the model remained revisited over time: For example, Zhu *et al.* found similar insulin-like growth factor-1 expression to that in humans, yet TGFB1 expression was comparably reduced [169]. In histological analysis, they showed disorganized collagen fibers in a whorl-like pattern comparable to the human phenotype. The same research group could confirm their results in a follow-up study, and similar results were obtained by another group, indicating the superiority of the red Duroc pig over other pig breeds for use as a hypertrophic scar model [178,179].

Apart from dermatome wounds, previous studies have described excisional wounds (in Yorkshire or Clawn miniature pigs [180–182]), as well as thermal wounds induced by different techniques [183–185]. However, it is noteworthy that only a limited number of studies have used burn wounds in Duroc pigs with distinct hypertrophic scar features [177,186,187]. Yet, no study was found using both excisional full-thickness (only dermatome [177]) and burn wounds in Duroc pigs. We believe that with adequate manual dexterity and a standardized technique, excisional full-thickness, and particularly burn wounds, hold substantial importance as wound etiologies in pathological scar formation [188–190]. The wound conditions caused by full-thickness (burn) wounds are already known to induce hypertrophic scarring. In our research, we were able to demonstrate and amplify these effects.

The wounding technique in this study was standardized as much as possible. One board-certified plastic surgeon performed all wounding procedures, and the technique remained consistent throughout the study. Similarly, burn wounds were inflicted in a standardized manner with a stringent process of double-checking to ensure precise control over the temperature and duration of burns. This rigorous approach guaranteed stable and reproducible parameters as opposed to other techniques, as reviewed by Mistry *et al.* [191]. To minimize potential biases arising from variations in skin thickness and other parameters, wound positions were varied across the different pigs; nevertheless, previous studies have reported no significant impact on analysis by the wound position [179,192].

In the present research project, castrated male Duroc pigs were chosen for practical reasons, in contrast to the more commonly used female red Duroc pigs in previous studies. This decision aimed at avoiding potential confounding effects due to the hormonal cycle in females, although Gallant et al. reported no relevant differences in scarring and wound healing between females and castrated males [179]. Furthermore, the procurement of purebred Duroc pigs in the study group’s region posed a considerable challenge due to the scarcity of breeders and the

requirement for larger space and higher husbandry standards to accommodate their size. As a result, breeders had only the required number of castrated males available at the time of the project. Furthermore, the responsible veterinarians anticipated greater ease in handling castrated males as the pigs increase in size during the study (up to 350kg in fully grown pigs) and the castration process allows for easier handling since animals become calmer [193].

In our study, we successfully used Duroc pigs as a suitable model to induce hypertrophic scars by inflicting full-thickness excisional and burn wounds, as well as inducing inflammation by using resiquimod. However, it is essential to acknowledge that this approach necessitates elaborate handling of the Duroc pigs.

4.2 The effect of resiquimod on macroscopic wound healing

4.2.1 Macroscopic observations

All wounds had epithelialized after 25 days. During initial wound healing, resiquimod-induced wounds showed higher inflammatory reactions, less granulation tissue, delayed re-epithelialization, and prolonged presence of necrotic tissues, whereas non-induced wounds already demonstrated healthy granulation tissue on day 7 (FT wounds) and day 14 (BW). Resiquimod-induced wounds exhibited an adherent scab until complete re-epithelialization, as illustrated in Figure 3 on day 19/21. The same reaction (thick scab adherent to the wound) has been reported in previous experiments; furthermore, a similar inhibited reduction of wound size in resiquimod-induced wounds was observed in our study [95]. These wound healing aberrations can be expected when inducing wounds with resiquimod, as several studies have shown and emphasized the importance of TLR pathways in wound healing [94,194–196]. TLR activation prolongs inflammation by inducing and upholding physiological inflammatory pathways. TLR7, for example, suppresses anti-inflammatory T-cells while activating dendritic cells and amplifying interferon expression. While a study conducted by Holzer-Geissler *et al.* constituted, to our knowledge, the inaugural account of impeded wound contraction, it has also been shown that resiquimod is capable of inhibiting smooth muscle contraction in the lung, making it a potential substance for asthma therapy as well [197–200]. Thus, the activation of TLR7/8 supposedly leads to reduced smooth muscle contraction yielding ultimately less contracted wounds and finally scars.

4.2.2 Wound score

To assess wound healing quantitatively, a wound score adapted from Holzer-Geissler *et al.* was employed [95]. While this scoring system is routinely used in wound healing studies by JOANNEUM RESEARCH Forschungsgesellschaft mbH, it necessitated modifications for the present study owing to the examination of two different wound etiologies (excision and burn) and the unique wound healing characteristics exhibited by Duroc pigs compared to other porcine breeds [201–203].

The inflammatory-induced wounds (FTR and BWR) showed significantly higher scores from day 4 to the final assessment on day 14. The statistically non-significant differences up to day 4 can be attributed to the time required for resiquimod to induce the inflammatory process.

Performing a single induction only once would likely be insufficient, probably rendering the model useless.

Over time, the inflammatory wound score course revealed the biggest differences subsequent to the last day of induction (day 6), specifically on day 7. These results concord with the findings previously reported in another study [95]. Therefore, this statistical development can be seen as proof of the model's and score's validity.

As two different wound etiologies characterized by divergent pathophysiology and healing dynamics (see chapters 1.1.2 and 1.1.3) were assessed using the same scoring system, no cross-comparisons (excision vs. burns) have been conducted. One might expect that burn wounds reach relatively higher scores than excisional full-thickness wounds. However, the scoring system does not consider variations in macroscopic wound healing that arise when a wound is necrotic from the beginning (full-thickness burn wound) or not (full-thickness excisional wound). Furthermore, due to the ordinal nature of the data used in the scoring system, the intermediary steps between the scores are not appropriately reflected, and the parameters are not weighted. While the scoring system appears appropriate for a relative comparison of a single wound type, its ability to evaluate distinctions between different wound types – particularly within the context of the Duroc pig model in our study – proves inadequate and fails to reflect relative differences between these wound types sufficiently.

The purpose of calculating the correlation between scar and wound scores was to assess whether macroscopic alterations in wound healing, i.e. inflammation signs, could be used to predict the final scar severity. The wound score on day 7 (with the most remarkable differences in wound scores) and the final scar score (day 133) showed a significant but only low correlation ($r = 0.3225$). Consequently, one might be inclined to propose that inflammatory signs in wound healing do not correlate with pathologic scarring. However, it is important to note that the wound score does not unequivocally reflect inflammation during wound healing. Therefore, the observed low correlation implies that the wound score may not be a reliable means to predict the likelihood of the occurrence of pathologic scarring – especially since two different wound etiologies were assessed.

4.3 Scarring

One of the primary objectives was to induce hypertrophic scars in Duroc pigs, as demonstrated in several previous studies [167–169,177–179,186,201,204]. All wounds formed distinct, raised, prominent, firm, and partially hypervascularized scars, macroscopically resembling human hypertrophic scars.

4.3.1 Quantitative assessment

Signs of hypertrophy became apparent by day 77. Other authors have reported comparable timeframes until hypertrophic scar formation [170,177,186,205]. However, in our study, the scars were not fully mature but only started to show signs of hypertrophy as opposed to some of the previous-mentioned studies that described scar maturation at that time point. As depicted in Figure 6, the scar scores of hyperinflammatory wounds (FTR, BW, BWR) showed similar values throughout the assessment without attaining significant differences. Notably, the distinction from excisional full-thickness wounds (FT) became apparent by day 77 for FTR and BWR, and day 105 for BW. Hence, hyperinflammation – either induced by a burn, resiquimod, or both – can be considered a trigger for pathologic (more intense) scarring.

Furthermore, the observed scores suggest that resiquimod-induced hyperinflammation allows for an earlier distinction of a more intense scar compared to regular excisional wounds. Owing to the small sample size, Cohen's *d* was additionally calculated for the comparison between BW and BWR to determine the effect size. An effect size of 0.75 was observed at day 133, indicating a large effect of resiquimod on the scar score, aligning with the conventional understanding that effect sizes > 0.5 indicate a large effect [174,206]. Thus, we could achieve an even more pronounced reaction to the pre-existing hyperinflammation resulting from the burn.

In conclusion, our study demonstrates that inducing hyperinflammation using resiquimod represents a valid approach for triggering pathologic scarring. These findings contribute to advancing future animal research on hypertrophic scars by potentially obviating the need for burn injuries, thereby signifying a substantial improvement aligned with the principles of the 3Rs (Replacement, Reduction, Refinement).

4.3.2 Evaluation of the scoring system

A scoring system adapted from the VSS was implemented for the assessment of the scarring outcome. The VSS was introduced by Sullivan *et al.* in 1990 [207] and it is still one of the most frequently used rating tools for evaluating burn scars [208]. However, several drawbacks have been reported, including a lack of patient perspective on itch/pain and other symptoms, as well as the partial use of a nominal scale to record the VSS parameters: For example, the nominal scale assigns lower scores to hypopigmented scars (1 point) compared to hyperpigmented scars (3 points), even though no evidence can be found that hyperpigmented scars are more severe than hypopigmented scars [209,210]. Although various authors have proposed adaptions to the VSS, a consensus on a universally accepted gold standard adaption has yet to be reached.

Moreover, the VSS is not specifically designed for hypertrophic scars, let alone the evaluation of scars in Duroc pigs that cannot evaluate pain or itch [208,209]. As a result, the VSS was adapted in the present study to assess hypertrophy-related characteristics such as pliability and height appropriately. While pigmentation was weighted less than in the original VSS, it was not entirely excluded in our study, as an increase in hyperpigmentation has been observed in Duroc pigs the deeper and more severe the wound [169,177,179]. Notably, neither the VSS nor our modified version clearly delineated a threshold score for classifying a scar as hypertrophic. Therefore, the reported values should be interpreted within a relative context rather than considered absolute indicators.

To mitigate potential bias stemming from the subjectivity of the score, two independent examiners conducted scar scoring blinded to the wound etiology [209,211]. In light of this, we believe that our modification of the used scar score is appropriate in the given setting and can be considered valid.

4.4 Imaging

4.4.1 Thermal imaging as tool do detect inflammation

We employed the FLIR One thermal imaging device to monitor differences in wound healing. The rationale behind this device was the increase in skin temperature in inflamed/infected wounds (as already postulated by Aulus Cornelius Celsus in his work *De Medicina* around 47 CE [212,213]) that can be measured by thermal imaging nowadays [214-216]. We observed an initial difference in the images immediately after burn-induced wounding. After 24 hours (day 2), the surface temperature of the wound areas ceased to be distinguishable, which is in concordance with another study that found that the temperature in a contact burn returned to physiological levels after approximately 6 hours in a human *ex vivo* burn model [217].

After induction of inflammation by either resiquimod, burn, or both, we were able to show that the periwound area around the inflammatory-induced wounds (BW, BWR, and FTR) exhibited increased temperature on the skin surface on day 7 (see Figure 8); unfortunately, technical constraints precluded the quantitative analysis of the thermal images. Nevertheless, a discernible trend was evident, with higher temperatures (indicated as yellow in the figures) during wound healing in the (peri)wound area, which was not observed in FT wounds. A thermal image from day 7 was chosen as an exemplary representation because, without visual quantification (to the naked eye), this appeared to be the time point with the greatest difference between wounds. This concurs with the observed wound scores, which also showed the biggest differences on day 7 – right after resiquimod-induced hyperinflammation. After scar formation, discernible differences perceptible to the unaided eye were unapparent.

The higher periwound temperatures observed in inflamed wounds corroborate the findings of Fierheller & Sibbald, who detected higher periwound temperatures in chronic, infected (not inflamed) wounds [218]. Interestingly, another study reported that elevated periwound temperatures are associated with an enhanced healing tendency in chronic ulcers [219]. Since temperature seems to be a relevant factor, as detailed in previous studies [220–223], thermal imaging has considerable potential within the domain of wound healing research [224].

Nevertheless, the full extent of its potential remains to be harnessed. Further exploration through quantitative analyses [223–226] is necessary to detect the smallest differences, possibly

extending to decimals and hundredths, which could be of decisive importance [225,226]. Unfortunately, this study falls short in offering additional depth to this topic. Therefore, future studies should prioritize an in-depth exploration of thermal imaging in wound healing and scar formation. Further limitations of the technique include the restriction of the measurement to the immediate surface, which could potentially be affected by wound healing products, such as scabs or fibrin.

4.4.2 Hyperspectral imaging as tool for prospective scar development

In response to the aforementioned surface measurement limitation inherent in thermal imaging, we employed hyperspectral imaging to evaluate tissue oxygenation both on the wound surface and, more importantly, below it. The reactive hyperoxygenation that can be seen in excisional full-thickness wounds indicated an increased blood flow and blood pooling that can be considered part of the physiological initiation of wound healing which requires oxygen for its proper function [227,228] (see chapter 1.2.1.4). While the oxygenation in non-induced FT wounds slowly decreased with progressing wound healing, relative hypoxia was seen in hyperinflammatory wounds (BWR, BW, FTR), beginning immediately following wounding in burns due to coagulation-related perfusion impairment and hence oxygenation deficit [229] (see chapter 1.1.3). In FTR wounds, it was observed after three days, with the oxygenation curve quickly aligning closely with that of burn wounds. The notably steep oxygenation reduction in FTR wounds relative to FT wounds may be attributed to the inflammatory induction prompted by resiquimod.

An additional rise of oxygenation was seen in FT wounds between days 4 and 5, coinciding with the inflammation phase. Notably, resiquimod induction (or inflammation in general, as the same goes for BW and BWR wounds) seems to inhibit this oxygen peak, thereby substantially interfering with wound healing. The activation of TLRs (as induced by resiquimod in this study) can prolong wound healing time [94,95,194,196]. In essence, resiquimod replicates the wound healing physiology of burns, resulting in extended healing time akin to burn wounds, which is considered a key element in the development of pathological scars.

Except for day 19/21, during which non-induced wounds displayed non-significant higher oxygenation as early as day 14, no significant difference was evident between BW and BWR wounds. We consider this difference as an earlier “return-to-normal” with progressing wound healing that is inhibited in BWR wounds by the additionally induced inflammation by

resiquimod for six days at that time. BWR wounds' oxygenation can therefore only return to normal levels a few days later when the hyperinflammatory effect of resiquimod has worn off.

Thus, our work substantiates not only the hyperinflammatory effect induced by resiquimod, akin to burns, but also underscores the agonistic mechanism of TLR7/8 to induce hypoxia or, at the very least, suppress the reactive hyperperfusion of excisional wounds, thereby leading to a state of relative hypoxia. Several publications have explored the role of hypoxia in myofibroblast differentiation and scar formation [116,118–120], and the relationship between hypoxia and inflammation is also well-established [230–232]. In conjunction with the increased scar score levels in underperfused wounds, our findings of relative hypoxia postulate hypoxia as a triggering factor that fosters enhanced and persistent inflammation, eventually culminating in hypertrophic scarring.

This hypothesis is further supported by the calculated correlation between NIR oxygenation on day 3 and the final scar score (day 133); with a correlation coefficient of $r = -0.6450$, it implies that lower oxygenation levels in the wound correspond to higher final scar scores (and therefore "the more pathologic" scars). Hence, hypoxia emerges as a crucial condition and even a predictor of pathologic scarring. Future studies could therefore focus on hyperspectral imaging as a non-invasive tool to prospectively evaluate fresh scars concerning their risk of developing a hypertrophic scar.

4.5 Histological findings

4.5.1 Microscopic evaluation

Our histologic analysis revealed hallmark features of hypertrophic scars, most notably in BWR, FTR, and BW wounds. These typical characteristics encompassed a thicker epidermis and the presence of disordered collagen as well as collagen nodules. Similar observations have also been described in earlier studies [167,178,179,204], corroborating the validity of our presented model in inducing hypertrophic scarring not only macroscopically but also at the microscopic level.

Interestingly, our findings diverged from prior studies regarding rete ridge morphology. The rete ridges in the present study showed a significant deepening, with further intensification observed in hyperinflammatory wounds (BW, BWR, FTR), where these rete ridges displayed branch-like ramifications. Considering that rete ridges are at least co-responsible for the mechanical integrity of the epidermal-dermal junction, a deeper and more branched network thereof could offer an explanation for less pliable and more firm scars [233–235].

Contrary to our observations, Limandjaja *et al.* and Carney *et al.* both reported that the epidermis in the scars analyzed was thickened but no or decreased rete ridges were present [236,237]. It is noteworthy that while the first mentioned group investigated hypertrophic and keloidal scars, and the second explored post-burn hypertrophic scars, both studies involved human subjects. Another group investigated the histology not in a Duroc pig but in a porcine scar (Göttingen mini pig): They found rete ridge restoration 21 days post-wounding [238], suggesting the possibility of further deepening with progressing time as a consequence of continued wound healing. This is also insinuated by Gallant *et al.*, who state "[…] the rete ridges were not complete […]" at day 28 of their experiments (in Durocs) [179]. Moreover, these early scars cannot be considered actual hypertrophic scars, as other groups also described hypertrophic scars in their experiments at later time points (as mentioned above). Most other studies investigating histology in Duroc pig scars at later time points did not make statements about rete ridges in their publications [167,170,178,204,205]. Yet Blackstone *et al.* described "[…] at day 90 displayed a lack of elongated rete ridges […]", which could not be confirmed in this present study. The flattening of rete ridges is also described as a sign of skin aging [239], which might explain the observed variations compared to other studies on "older" human scars.

Through histological examination, especially the analysis of rete ridges, our study confirmed the induction of hypertrophic scars with extensively pronounced rete ridges, contributing to the non-pliability of hypertrophic scars at day 133. In full-thickness wounds in Duroc pigs, rete ridges can therefore be restored as compared to human full-thickness wounds [235,239].

4.5.2 Inflammatory cell invasion

An analysis of inflammatory cell invasion was performed to evaluate local inflammation [240]. As expected, increased neutrophil infiltration was observed in FT, FTR, and BW wounds compared to non-wounded controls after day 7. Unexpectedly, BWR wounds did not show a significant increase in infiltration. Further investigation unveiled that several BWR slides had to be excluded from analysis due to air inclusions. This led to a low sample size in the BWR group regarding slides, necessitating an additional effect size calculation, which yielded a very strong effect of 1.25. Consequently, it can be inferred that BWR wounds would likely exhibit significantly different results than controls if a larger sample size was available. This conjecture aligns with expectations, as neutrophils are a key cell type in the early inflammation phase and should therefore be present in the dermis.

The significantly higher cell counts in FTR wounds compared to FT wounds indicate a relevantly higher inflammatory reaction in resiquimod-induced wounds, as reported by Holzer-Geissler et al. [95]. This emphasizes the involvement of the TLR7/8 agonist resiquimod in activating and priming neutrophils, which is further supported by the progression observed on day 21, as well as the presence of lymphocyte infiltration [241,242], which was also expressed highest in FTR wound types. However, temporal considerations are crucial in this context, as we found the most meaningful changes in neutrophil infiltration on day 7, whereas Holzer-Geissler et al. observed immune cell infiltration on day 16. In our study, the initially apparent changes already started to subside on day 21, with lymphocytes remaining the dominant (and significantly different) cell type. Therefore, future studies should potentially explore additional time points, which could be of high importance, to comprehensively scrutinize the ramifications of hyperinflammation on altered wound healing.

The immune cells examined in this study, along with other cell types such as mast cells, which play a relevant albeit not yet completely elucidated role in scarring, merit focused attention [243–246]. Furthermore, our findings' reported significances have to be interpreted with caution, given the divergence and reduced sample size within this assessment.

4.6 Findings of gene expression analysis

4.6.1 Inflammatory gene expression

The pro-inflammatory mediator IL-6 is a crucial component in wound healing and showed significantly higher expression (IL6) in resiquimod-induced wounds than in placebo-treated wounds (BW and FT) as well as controls [21,247]. This confirms the above-reported findings of increased inflammatory reaction in resiquimod-induced wounds. Previous reports have already discovered increased levels of IL6 in non-healing wounds [248–250]; therefore, the observed increase in FTR and BWR wounds (and also slightly higher, but not significant in BW) might indicate a less advanced state of wound healing compared to FT wounds. This is further supported by the levels observed at day 19/21, which, although non-significant, were elevated in FTR, BWR, and BW wounds relative to FT wounds (see Figure 13), suggesting a progression in wound healing that is not as advanced as in FT wounds. Therefore, the upregulation of inflammatory parameters such as IL6 aligns with what has been shown to be mediated by resiquimod [251,252].

Resiquimod thereby shows a "burn-mimicking" impact which may be seen in the enhanced and extended relative hyperinflammation caused by a burn or, in this example, by the inflammatory induction triggered by resiquimod. The fact that persistent hyperinflammation was observed seven days post-wounding underscores the imperative of early surgical intervention to remove the tissue causing the inflammation in a clinical setting of burn treatment. Early excision has been found to dramatically minimize the amount of scarring burn patients experience and enhance their chances of survival [253–255]. Alternatively, in cases where surgery is either contraindicated or not feasible, burn wounds should not be left to heal on their own. Instead, at the very least to slow down the excessive hyperinflammation, subsequent conservative care involving the application of burn-wound-specific dressings is necessary.

Interestingly, aside from an elevated IL10 level in FTR wounds compared to controls, the only substantial result drawn from the analysis of inflammatory gene expression pertains to IL6. Serving as an anti-inflammatory regulating counterpart, IL-10 plays a pivotal role in the downregulation of inflammation during wound healing [256,257]. Studies have shown that increased IL10 expression can improve scarring in animal and human studies, thereby assigning a particular role to this cytokine in the context of post-hyperinflammatory

conditions [67,258-260]. Since several investigations have confirmed that TLR7/8 activation (as induced by resiquimod in this study) induces IL-10 production [261-264], the observed findings deviated from expectations. Possible explanations may reside in the timing of the gene expression analysis or a rather systemic reaction driving the anti-inflammatory expression. However, this slight upregulation could potentially result from a compensatory overexpression of anti-inflammatory cytokines due to the increased inflammatory reaction.

4.6.2 Remodeling gene expression

Remodeling genes have been investigated to try and mirror the clinical impact by gene expression analysis. Despite the macroscopic hyperproliferative nature of scars, the expected overexpression of profibrotic parameters could not be detected. Resiquimod-induced wounds exhibited a significant overexpression of TGFB1 compared to controls, and FTR also demonstrated elevated expression when compared to BW and FT wounds on day 19/21. Although this overexpression might suggest a predisposition to hypertrophic scar development, the macroscopic appearance of scars did not exhibit substantial differentiation in the early stages after completed re-epithelialization. Furthermore, one might expect the upregulation to be sustained through the remodeling phase of wound healing, and before the manifestation of hypertrophic signs, given the fundamental role of TGF-β pathways in this context [22,51,265]. In contrast, MMP1, a fibrotic regulator and counterpart, showed only modest modifications characterized by a mild upregulation that rapidly reverted to normal levels, as reported in previous studies [179,205].

However, this model could not confirm significantly elevated (or decreased) levels of other remodeling factors, including TGFB2, TGFB3, COL1, COL3, or even ACTA2. Particularly noteworthy is the case of ACTA2, the coding gene for smooth muscle actin, which was expected to be upregulated in FT wounds compared to other wounds. This expectation was rooted in the reported inhibition of wound contraction in resiquimod-induced wounds, as could be seen in macroscopic wound description and further described by Holzer-Geissler *et al.* [95]. Possible reasons for this include the timing of biopsy collection and flaws during handling or the methodology *per se* [266,267], but other aspects, such as scar heterogeneity or relatively small sample sizes, could also invoke bias.

4.6.3 Hypoxia-related genes

Among the genes investigated in the gene expression analysis, HIF1a and HSPA4 showed the most pronounced reaction in this study setup. Notably, HIF1a was indeed the only gene that remained pronouncedly overexpressed until day 19/21. While the initial upregulations observed in resiquimod-induced wounds parallel the measured oxygenation in the wounds, BW wound samples did not overexpress HIF1a. Possible explanations for this divergence encompass sampling errors or, more plausibly, may be attributed to the fact that TLR activation leads to increased HIF1a accumulation even under normoxic conditions [268–270], which remained present one day after the end of the induction cycle in induced wounds, whereas it dissipated in non-induced wounds in this study. The sustained overexpression of HIF1a in FTR wounds relative to FT and control biopsies, but not compared to BWR and BW wounds, supports the impact of TLR-triggered mechanisms underlying this overexpression.

While HSPA4 is not a hypoxia-indicating marker *per se*, it serves as a significant marker in situations of cellular stress, encompassing scenarios marked by heat-, toxin-, or hypoxia-associated conditions, and contributes to neo-angiogenesis [271,272]. Again, compared to other wound types, FTR wounds showed the highest expression of HSPA4, indicative of the highest stress situation. Despite observations indicating that the expression of HSPA4 may delay healing in gastric ulcers [273], and that heat shock proteins in general are supposed to have their share in cancer and fibrotic diseases [274,275], further research is necessary to elucidate the exact role of HSPA4 in skin wound healing.

Ultimately, it is deducible from these cellular stress response gene expressions that resiquimod induces a hypoxic stress situation that inhibits wound healing processes.

4.7 Final evaluation

4.7.1 Contributing factors to pathological scarring

When summarizing all investigated parameters, we were able to establish the significance of hypoxia and inflammation as relevant parameters contributing to scarring. While the interrelation between these two processes is well-known [230], yet, within this particular setup, a conundrum reminiscent of the "chicken-or-egg" dilemma emerges: Does hyperinflammation trigger hypoxia [276], or does hypoxia trigger hyperinflammation [277,278]? Generally speaking, existing literature tends to focus on inflammation as the impetus driving pathologic scarring [63,99]. While this assumption may hold validity and offers a credible foundation for designing therapeutic modalities targeting hyperinflammation, it is imperative to acknowledge that such treatments are possibly merely symptomatic, intervening in a running process caused by an alternate condition.

Evidently, hyperinflammation warrants attention and intervention, particularly given its potential to lead to more severe problems, especially in burns [279–281]. However, this present study insinuates a correlation between early hypoxia after wounding and the severity of the final scar, as assessed through scar scoring. Furthermore, parameters indicating hypoxic conditions were far more pronounced than those indicating inflammation. Based on these findings, the hypothesis that hypoxia is the leading condition in hypertrophic scar formation, induced by TLR activation (resiquimod) or burns, leading to inflammation can be convincingly argued. This is further supported by the contention that skin tension significantly influences pathologic scarring dynamics [112,282]. In the realm of plastic surgery, it is a well-known fact that too much tension on a wound ultimately leads to necrosis. In cases where tension is moderate and does not culminate in necrosis, compromised skin perfusion ensues, consequently impairing oxygenation [283]. While the physiological consequence of too much tension is inflammation [284], the driving force behind this inflammatory cascade and, ultimately, pathologic scarring, could be attributed to relative hypoxia. Another possible argument for this hypothesis is the inflammaging paradox: While in elderly patients, inflammatory parameters seem to be increased (inflammaging, [285]), the occurrence of pathologic scars appears to be reduced [286,287]. Attributing the occurrence of hypertrophic scars, thereby solely to inflammation, would not be coherent reasoning.

These considerations, while not asserting absolute certainty, warrant attention in future therapeutic developments, suggesting that a quick restoration of normal oxygenation levels could be an avenue of exploration, potentially alongside (or in addition to?) symptomatic inflammation reduction. Evidently, to gain deeper insights into the process of scarring, it is imperative for future research to focus on these aspects, conducting more extensive investigations to determine the pivotal pathways, parameters, and variables that hold relevance at distinct time points.

Although a definitive resolution of the causative sequence to what came first remains elusive, with the truth likely lying somewhere in between, this study provided valuable insights into the dynamics of scarring processes following various wound inflictions.

4.7.2 Establishment of a new model

In addition to the explorative nature of this study to investigate local alterations in scars, our primary objective encompassed the establishment of a new model for future scar research. We were able to induce scars with features of human hypertrophic scars by the addition of resiquimod to excisional full-thickness wounds. This advancement holds the potential to obviate the need for more ethically challenging burn infliction methods in future animal studies. Furthermore, signs of scar hypertrophy (as evaluated by the scar score) appeared earlier than in regular burn wounds. Future refinement of the model is definitely necessary and should focus on intensifying the scars and shifting the timepoint of hypertrophic scar formation towards the wounding. This could be achieved by a second inflammatory (or hypoxic?) booster, such as infiltration of LPS into the just healed wounds.

While the overall attainment of a new hypertrophic scar model within the Duroc pig is undoubtedly a significant accomplishment, it is again crucial to emphasize the paramount importance of aligning the chosen model with the respective research question to ensure the most suitable model and optimal experimental congruence.

4.8 Limitations

This research was subject to several inherent limitations that were beyond our control. Firstly, we conducted two separate sets of studies, each with three Duroc pigs as subjects. Because the breeder who delivered the first series of Duroc pigs went out of business due to the coronavirus pandemic 2019, the Duroc pigs used in the second series were delivered by a different breeder. Although all six Duroc pigs were of purebred lineage, we observed modest variations in the macroscopic appearance of scars, as well as in the histological and gene expression analyses between the two series. Therefore, the possibility of genetic variation being a significant confounding factor in this experiment should not be discounted, especially since genetic variation in (even purebred) Duroc pigs has some significant impact on the phenotype [288].

Another limitation was imposed by the scheduling of tests and examinations. Given the lengthy and cost-intensive nature of the experimental protocol, the timing of these assessments was restricted, potentially resulting in the oversight of significant information or insights that would have been evident at other time points. Considering the scope of our investigations, it is self-evident that additional pertinent factors that could have yielded intriguing perspectives were not included in this project.

4.9 Outlook & Clinical Impact

Upon completing a project, it becomes imperative to reflect on the research's impact and chart the course for the next steps. While we've gained insightful glimpses into the underlying mechanisms of scar formation following induced inflammation, a comprehensive understanding still eludes us. To delve deeper into this phenomenon, it would be prudent to start a fresh phase of the project, involving the selection of different time points for histological and gene expression analyses. This tweak is rooted in the sometimes unexpected variations in gene expression patterns that were shown, defying our initial expectations.

In the context of our exploratory study, intriguing indications have surfaced, suggesting a plausible link between relative hypoxia and pathological scar formation. This insight encourages a clear imperative for future investigations to delve deeper into this relationship. To refine our model, an appealing adaption involves introducing another inflammatory stimulus at a later stage, coinciding with the remodeling phase, investigating the impact of not only prolonged, but an additional inflammatory trigger on the final scar. Moreover, given our current findings, it would be insightful to explore whether (an artificial) hypoxia alone and without additional inflammatory trigger holds the potential to initiate pathologic scar formation.

Once scar formation is complete, the scars can further be used as model for therapeutic approaches. This potential extends beyond treatment strategies in final scars, encompassing preventive measures in early stages as well. It is worth investigating whether optimizing wound oxygenation post-injury could influence the subsequent course of scar formation.

The outcomes of this study, coupled with subsequent concepts, carry significant implications for future clinical therapies. While the standardization, development, and testing of treatment modalities remain crucial to create and increase evidence, it is equally vital to remain receptive to emerging paths. This study emphasizes the importance of timely debridement in burn cases, as the potential consequences of prolonged inflammation not only afflict systemic health but might also lead to severe scarring, further distressing already anguished individuals. Currently, surgical removal of the causing agent stands as the principal means to mitigate inflammation in severely burnt patients. Yet, the observed negative correlation between scar severity and relative hypoxia offers novel insights for scar prevention. If further confirmed, our findings might point towards a paradigm shift, advocating for innovative approaches focused on oxygenating wounds to temper the inflammatory response and potentially obviate (or at least reduce) the need for extended radical surgical interventions. This paradigm would hold true not

only for burn cases but also for patients prone to conspicuous scarring, extending the utility of hyperoxygenating fresh scars post-surgery as a feasible avenue. The proven benefits of hyperbaric oxygen therapy in reducing inflammation and enhancing wound healing are noteworthy [289,290], even though its widespread use, especially perioperatively, is hampered by practical challenges given its challenging availability.

Nevertheless, looking deeper into oxygen's role, spanning wound healing, systemic inflammation, and scar evolution, assumes paramount importance in advancing burn care and enhancing scar management. As previously highlighted, further inquiries are imperative to unravel the nuanced dimensions of this role and consolidate our understanding.

5 Conclusion

In this research project, we were able to create distinct scarring in Duroc pigs after the infliction of burn and excisional full-thickness wounds, of which each half had an additional inflammatory boost by local application of the immunomodulatory drug resiquimod. We observed and confirmed that burns cause local inflammation, which was mimicked in excisional full-thickness and intensified in burn wounds by applying the drug. Scar scoring revealed significantly higher scores in hyperinflammatory wounds, both burn and induced excisional full-thickness wounds. Further investigations revealed histological aspects of human hypertrophic scars with deep dermal ridges that have not been described in the literature before at that time point. Hyperspectral imaging and gene expression analysis revealed pronounced hypoxic states in hyperinflammatory wounds, with the oxygenation levels of induced full-thickness wounds closely approximating the ones of burns. A significant negative correlation was seen between the oxygenation of the wound in the early stages and the final scar score. Inflammatory assessment by histologic immune cell infiltration and gene expression analysis revealed higher inflammation in hyperinflammatory wounds. However, the inflammatory reaction was not as high as the reaction to hypoxia. The inflammation subsided in excisional full-thickness wounds earlier than in burn wounds.

These findings emphasize the need for swift reaction in case of inflammation – be it a deep dermal burn or inflammation due to other prevalent states. The swift reaction includes the removal of the causing agent, like burnt or inflamed tissues, to appropriately regulate the wound environment so that healing can progress normally. We furthermore raised the question of whether targeting inflammatory pathways in scar therapy is a causal therapy or whether this aims at the second to last link in the chain, with the last being fibrosis. Future studies are needed to completely elucidate the pathophysiology of hypertrophic scarring. Potentially, other targets can be unveiled by further advancing scar research and refining models such as the one we have successfully established and presented in this study.

6 Bibliography

[1] Nischwitz SP, Fink J, Schellnegger M, Luze H, Bubalo V, Tetyczka C, et al. The Role of Local Inflammation and Hypoxia in the Formation of Hypertrophic Scars - A New Model in the Duroc Pig. *Int J Mol Sci* 2022;24:316. https://doi.org/10.3390/ijms24010316.

[2] Mosteller RD. Simplified Calculation of Body-Surface Area. *N Engl J Med* 1987;317:1098. https://doi.org/10.1056/nejm198710223171717.

[3] Kolarsick PAJ, Kolarsick MA, Goodwin C. Anatomy and Physiology of the Skin. *J Dermatol Nurses Assoc* 2011;3:203–13. https://doi.org/10.1097/jdn.0b013e3182274a98.

[4] Arda O, Göksügür N, Tüzün Y. Basic Histological Structure and Functions of Facial Skin. *Clin Dermatol* 2014;32:3–13. https://doi.org/10.1016/j.clindermatol.2013.05.021.

[5] Wickett RR, Visscher MO. Structure and Function of the Epidermal Barrier. *Am J Infect Control* 2006;34:S98–110. https://doi.org/10.1016/j.ajic.2006.05.295.

[6] Firooz A, Rajabi-Estarabadi A, Zartab H, Pazhohi N, Fanian F, Janani L. The Influence of Gender and Age on the Thickness and Echo-Density of Skin. *Skin Res Technol* 2017;23:13–20. https://doi.org/10.1111/srt.12294.

[7] Cichorek M, Wachulska M, Stasiewicz A, Tymińska A. Skin Melanocytes: Biology and Development. *Postepy Dermatol Alergol* 2013;30:30–41. https://doi.org/10.5114/pdia.2013.33376.

[8] Jaitley S, Saraswathi TR. Pathophysiology of Langerhans Cells. *J Oral Maxillofac Pathol* 2012;16:239–44. https://doi.org/10.4103/0973-029x.99077.

[9] Briggaman RA, Wheeler CE. The Epidermal-Dermal Junction. *J Invest Dermatol* 1975;65:71–84. https://doi.org/10.1111/1523-1747.ep12598050.

[10] Driskell RR, Lichtenberger BM, Hoste E, Kretzschmar K, Simons BD, Charalambous M, et al. Distinct Fibroblast Lineages Determine Dermal Architecture in Skin Development and Repair. *Nature* 2013;504:277–81. https://doi.org/10.1038/nature12783.

[11] García-Piqueras J, Cobo R, Cárcaba L, García-Mesa Y, Feito J, Cobo J, et al. The Capsule of Human Meissner Corpuscles: Immunohistochemical Evidence. *J Anat* 2020;236:854–61. https://doi.org/10.1111/joa.13139.

[12] Oikarinen A. Aging of the Skin Connective Tissue: How to Measure the Biochemical and Mechanical Properties of Aging Dermis. *Photodermatol Photoimmunol Photomed* 1994;10:47–52.

[13] Ricard-Blum S. The Collagen Family. *Cold Spring Harb Perspect Biol* 2011;3:1–19. https://doi.org/10.1101/cshperspect.A004978.

[14] Meigel WN, Gay S, Weber L. Dermal Architecture and Collagen Type Distribution. *Arch Dermatol Res* 1977;259:1–10. https://doi.org/10.1007/bf00562732.

[15] Lovell CR, Smolenski KA, Duance VC, Light ND, Young S, Dyson M. Type I and III Collagen Content and Fibre Distribution in Normal Human Skin during Ageing. *Br J Dermatol* 1987;117:419–28. https://doi.org/10.1111/j.1365-2133.1987.tb04921.x.

[16] Cheng W, Yan-hua R, Fang-gang N, Guo-an Z. The Content and Ratio of Type I and III Collagen in Skin Differ with Age and Injury. *Afr J Biotechnol* 2011;10:2524–9. https://doi.org/10.5897/ajb10.1999.

[17] Piérard GE, Lapière CM. Microanatomy of the Dermis in Relation to Relaxed Skin Tension Lines and Langer's Lines. *Am J Dermatopathol* 1987;9:219–24. https://doi.org/10.1097/00000372-198706000-00007.

[18] Daly CH, Odland GF. Age-Related Changes in the Mechanical Properties of Human Skin. *J Invest Dermatol* 1979;73:84–7. https://doi.org/10.1111/1523-1747.ep12532770.

[19] Hussain SH, Limthongkul B, Humphreys TR. The Biomechanical Properties of the Skin. *Dermatol Surg* 2013;39:193–203. https://doi.org/10.1111/dsu.12095.

[20] Broughton G, Janis JE, Attinger CE. Wound Healing: An Overview. *Plast Reconstr Surg* 2006;117:1e-S-32e-S. https://doi.org/10.1097/01.prs.0000222562.60260.f9.

[21] Rodrigues M, Kosaric N, Bonham CA, Gurtner GC. Wound Healing: A Cellular Perspective. *Physiol Rev* 2019;99:665. https://doi.org/10.1152/physrev.00067.2017.

[22] Wang PH, Huang BS, Horng HC, Yeh CC, Chen YJ. Wound Healing. *J Chin Med Assoc* 2018;81:94–101. https://doi.org/10.1016/j.jcma.2017.11.002.

[23] Lindley LE, Stojadinovic O, Pastar I, Tomic-Canic M. Biology and Biomarkers for Wound Healing. *Plast Reconstr Surg* 2016. https://doi.org/10.1097/prs.0000000000002682.

[24] Wilgus TA, Roy S, McDaniel JC. Neutrophils and Wound Repair: Positive Actions and Negative Reactions. *Adv Wound Care* 2013;2:379. https://doi.org/10.1089/wound.2012.0383.

[25] Wilkinson HN, Hardman MJ. Wound Healing: Cellular Mechanisms and Pathological Outcomes. *Open Biol* 2020;10. https://doi.org/10.1098/rsob.200223.

[26] Hassanshahi A, Moradzad M, Ghalamkari S, Fadaei M, Cowin AJ, Hassanshahi M. Macrophage-Mediated Inflammation in Skin Wound Healing. *Cells* 2022;11. https://doi.org/10.3390/cells11192953.

[27] Martin CW, Muir IFK. The Role of Lymphocytes in Wound Healing. *Br J Plast Surg* 1990;43:655–62. https://doi.org/10.1016/0007-1226(90)90185-3.

[28] Martin P. Wound Healing--Aiming for Perfect Skin Regeneration. *Science* 1997;276:75–81. https://doi.org/10.1126/science.276.5309.75.

[29] Fisher G, Rittié L. Restoration of the Basement Membrane after Wounding: A Hallmark of Young Human Skin Altered with Aging. *J Cell Commun Signal* 2018;12:401. https://doi.org/10.1007/s12079-017-0417-3.

[30] Singer AJ, Clark RAF. Cutaneous Wound Healing. *N Engl J Med* 1999;341:738–46. https://doi.org/10.1056/nejm199909023411006.

[31] Kandhwal M, Behl T, Singh S, Sharma N, Arora S, Bhatia S, et al. Role of Matrix Metalloproteinase in Wound Healing. *Am J Transl Res* 2022;14:4391. https://doi.org/10.31838/ijpr/2020.sp2.087.

[32] Levenson SM, Geever EF, Crowley L V., Oates JF, Berard CW, Rosen H. The Healing of Rat Skin Wounds. *Ann Surg* 1965;161:293–308. https://doi.org/10.1097/00000658-196502000-00019.

[33] Keck M, Herndon DH, Kamolz LP, Frey M, Jeschke MG. Pathophysiology of Burns. *Wien Med Wochenschr* 2009;159:327–36. https://doi.org/10.1007/s10354-009-0651-2.

[34] Ladak A, Tredget EE. Pathophysiology and Management of the Burn Scar. *Clin Plast Surg* 2009;36:661–74. https://doi.org/10.1016/j.cps.2009.05.014.

[35] Jackson DM. The Diagnosis of the Depth of Burning. *Br J Surg* 2005;40:588–96. https://doi.org/10.1002/bjs.18004016413.

[36] Evers LH, Bhavsar D, Mailänder P. The Biology of Burn Injury. *Exp Dermatol* 2010;19:777–83. https://doi.org/10.1111/j.1600-0625.2010.01105.x.

[37] Nielson CB, Duethman NC, Howard JM, Moncure M, Wood JG. Burns: Pathophysiology of Systemic Complications and Current Management. *J Burn Care Res* 2017;38:e469–81. https://doi.org/10.1097/bcr.0000000000000355.

[38] Kao CC, Garner WL. Acute Burns. *Plast Reconstr Surg* 2000;101:2482–93. https://doi.org/10.1097/00006534-200006000-00028

[39] Aulick LH, Wilmore DW, Mason AD, Pruitt BA. Influence of the Burn Wound on Peripheral Circulation in Thermally Injured Patients. *Am J Physiol Heart Circ Physiol* 1977;233:H520–6. https://doi.org/10.1152/ajpheart.1977.233.4.h520.

[40] Demling RH. Fluid Replacement in Burned Patients. *Surg Clin North Am* 1987;67:15–30. https://doi.org/10.1016/s0039-6109(16)44130-7.

[41] Settle JA. Fluid Therapy in Burns. *J R Soc Med* 1982;75:6–11.

[42] Shin C, Kinsky MP, Thomas JA, Traber DL, Kramer GC. Effect of Cutaneous Burn Injury and Resuscitation on the Cerebral Circulation in an Ovine Model. *Burns* 1998;24:39–45. https://doi.org/10.1016/s0305-4179(97)00057-0.

[43] Chrysopoulo MT, Jeschke MG, Dziewulski P, Barrow RE, Herndon DN. Acute Renal Dysfunction in Severely Burned Adults. *J Trauma* 1999;46:141–4. https://doi.org/10.1097/00005373-199901000-00024.

[44] Jeschke MG, Gauglitz GG, Kulp GA, Finnerty CC, Williams FN, Kraft R, et al. Long-Term Persistance of the Pathophysiologic Response to Severe Burn Injury. *PLoS One* 2011;6. https://doi.org/10.1371/journal.pone.0021245.

[45] Mulder PPG, Vlig M, Boekema BKHL, Stoop MM, Pijpe A, van Zuijlen PPM, et al. Persistent Systemic Inflammation in Patients with Severe Burn Injury Is Accompanied by Influx of Immature Neutrophils and Shifts in T Cell Subsets and Cytokine Profiles. *Front Immunol* 2021;11. https://doi.org/10.3389/fimmu.2020.621222.

[46] Verhaegen PDHM, Van Zuijlen PPM, Pennings NM, Van Marle J, Niessen FB, Van Der Horst CMAM, et al. Differences in Collagen Architecture between Keloid, Hypertrophic Scar, Normotrophic Scar, and Normal Skin: An Objective Histopathological Analysis. *Wound Repair Regen* 2009;17:649–56. https://doi.org/10.1111/j.1524-475x.2009.00533.x.

[47] Almine JF, Wise SG, Weiss AS. Elastin Signaling in Wound Repair. *Birth Defects Res* 2012;96:248–57. https://doi.org/10.1002/bdrc.21016.

[48] Amadeu TP, Braune AS, Porto LC, Desmoulière A, Costa AMA. Fibrillin-1 and Elastin Are Differentially Expressed in Hypertrophic Scars and Keloids. *Wound Repair Regen* 2004;12:169–74. https://doi.org/10.1111/j.1067-1927.2004.012209.x.

[49] Darby IA, Laverdet B, Bonté F, Desmoulière A. Fibroblasts and Myofibroblasts in Wound Healing. *Clin Cosmet Investig Dermatol* 2014;7:301. https://doi.org/10.2147/ccid.s50046.

[50] Finnson KW, McLean S, Di Guglielmo GM, Philip A. Dynamics of Transforming Growth Factor Beta Signaling in Wound Healing and Scarring. *Adv Wound Care* 2013;2:195–214. https://doi.org/10.1089/wound.2013.0429.

[51] Berman B, Maderal A, Raphael B. Keloids and Hypertrophic Scars: Pathophysiology, Classification, and Treatment. *Dermatol Surg* 2017;43 Suppl 1:S3–18. https://doi.org/10.1097/dss.0000000000000819.

[52] Gauglitz GG, Korting HC, Pavicic T, Ruzicka T, Jeschke MG. Hypertrophic Scarring and Keloids: Pathomechanisms and Current and Emerging Treatment Strategies. *Mol Med* 2011;17:113. https://doi.org/10.2119/molmed.2009.00153.

[53] Boen M, Jacob C. A Review and Update of Treatment Options Using the Acne Scar Classification System. *Dermatol Surg* 2019;45:411–22. https://doi.org/10.1097/dss.0000000000001765.

[54] Huang C, Murphy GF, Akaishi S, Ogawa R. Keloids and Hypertrophic Scars: Update and Future Directions. *Plast Reconstr Surg Glob Open* 2013;1. https://doi.org/10.1097/gox.0b013e31829c4597.

[55] Glass DA. Current Understanding of the Genetic Causes of Keloid Formation. *J Invest Dermatol* 2017;18:S50–3. https://doi.org/10.1016/j.jisp.2016.10.024.

[56] Köse O, Waseem A. Keloids and Hypertrophic Scars: Are They Two Different Sides of the Same Coin? *Dermatol Surg* 2008;34:336–46. https://doi.org/10.1111/j.1524-4725.2007.34067.x.

[57] Burd A, Huang L. Hypertrophic Response and Keloid Diathesis: Two Very Different Forms of Scar. *Plast Reconstr Surg* 2005;116. https://doi.org/10.1097/01.prs.0000191977.51206.43.

[58] Huang C, Akaishi S, Hyakusoku H, Ogawa R. Are keloid and Hypertrophic Scar Different Forms of the Same Disorder? A Fibroproliferative Skin Disorder Hypothesis Based on Keloid Findings. *Int Wound J* 2014;11:517–22. https://doi.org/10.1111/j.1742-481x.2012.01118.x.

[59] Butzelaar L, Ulrich MMW, Mink Van Der Molen AB, Niessen FB, Beelen RHJ. Currently Known Risk Factors for Hypertrophic Skin Scarring: A Review. *J Plast Reconstr Aesthet Surg* 2016;69:163–9. https://doi.org/10.1016/j.bjps.2015.11.015.

[60] Bombaro KM, Engrav LH, Carrougher GJ, Wiechman SA, Faucher L, Costa BA, et al. What Is the Prevalence of Hypertrophic Scarring Following Burns? *Burns* 2003;29:299–302. https://doi.org/10.1016/s0305-4179(03)00067-6.

[61] Arno AI, Gauglitz GG, Barret JP, Jeschke MG. Up-to-Date Approach to Manage Keloids and Hypertrophic Scars: a Useful Guide. *Burns* 2014;40:1255–66. https://doi.org/10.1016/j.burns.2014.02.011.

[62] Ogawa R. The Most Current Algorithms for the Treatment and Prevention of Hypertrophic Scars and Keloids: A 2020 Update of the Algorithms Published 10 Years Ago. *Plast Reconstr Surg* 2022;149:79E-94E. https://doi.org/10.1097/prs.0000000000008667.

[63] Wang ZC, Zhao WY, Cao Y, Liu YQ, Sun Q, Shi P, et al. The Roles of Inflammation in Keloid and Hypertrophic Scars. *Front Immunol* 2020;11. https://doi.org/10.3389/fimmu.2020.603187.

[64] Longaker MT, Whitby DJ, Adzick NS, Crombleholme TM, Langer JC, Duncan BW, et al. Studies in Fetal Wound Healing, VI. Second and Early Third Trimester Fetal Wounds Demonstrate Rapid Collagen Deposition without Scar Formation. *J Pediatr Surg* 1990;25:63–9. https://doi.org/10.1016/s0022-3468(05)80165-4.

[65] Lo DD, Zimmermann AS, Nauta A, Longaker MT, Lorenz HP. Scarless Fetal Skin Wound Healing Update. *Birth Defects Res* 2012;96:237–47. https://doi.org/10.1002/bdrc.21018.

[66] Liechty KW, Adzick NS, Crombleholme TM. Diminished Interleukin 6 (IL-6) Production during Scarless Human Fetal Wound Repair. *Cytokine* 2000;12:671–6. https://doi.org/10.1006/cyto.1999.0598.

[67] Kieran I, Knock A, Bush J, So K, Metcalfe A, Hobson R, et al. Interleukin-10 Reduces Scar Formation in Both Animal and Human Cutaneous Wounds: Results of Two Preclinical and Phase II Randomized Control Studies. *Wound Repair Regen* 2013;21:428–36. https://doi.org/10.1111/wrr.12043.

[68] Duncan MR, Berman B. Stimulation of Collagen and Glycosaminoglycan Production in Cultured Human Adult Dermal Fibroblasts by Recombinant Human Interleukin 6. *J Invest Dermatol* 1991;97:686–92. https://doi.org/10.1111/1523-1747.ep12483971.

[69] Ghazizadeh M, Tosa M, Shimizu H, Hyakusoku H, Kawanami O. Functional Implications of the IL-6 Signaling Pathway in Keloid Pathogenesis. *J Invest Dermatol* 2007;127:98–105. https://doi.org/10.1038/sj.jid.5700564.

[70] Wulff BC, Parent AE, Meleski MA, Dipietro LA, Schrementi ME, Wilgus TA. Mast Cells Contribute to Scar Formation during Fetal Wound Healing. *J Invest Dermatol* 2012;132:458–65. https://doi.org/10.1038/jid.2011.324.

[71] Chen X, Thibeault SL. Role of TNF–α in Wound Repair in Human Vocal Fold Fibroblasts. *Laryngoscope* 2010;120:1819. https://doi.org/10.1002/lary.21037.

[72] Mariani TJ, Sandefur S, Roby JD, Pierce RA. Collagenase-3 Induction in Rat Lung Fibroblasts Requires the Combined Effects of Tumor Necrosis Factor-Alpha and 12-Lipoxygenase Metabolites: a Model of Macrophage-Induced, Fibroblast-Driven Extracellular Matrix Remodeling during Inflammatory Lung Injury. *Mol Biol Cell* 1998;9:1411–24. https://doi.org/10.1091/mbc.9.6.1411.

[73] Yan C, Grimm WA, Garner WL, Qin L, Travis T, Tan N, et al. Epithelial to Mesenchymal Transition in Human Skin Wound Healing is Induced by Tumor Necrosis Factor-Alpha through Bone Morphogenic Protein-2. *Am J Pathol* 2010;176:2247–58. https://doi.org/10.2353/ajpath.2010.090048.

[74] Ghahary A, Shen YJ, Nedelec B, Wang R, Scott PG, Tredget EE. Collagenase Production Is Lower in Post-Burn Hypertrophic Scar Fibroblasts than in Normal Fibroblasts and Is Reduced by Insulin-Like Growth Factor-1. *J Invest Dermatol* 1996;106:476–81. https://doi.org/10.1111/1523-1747.ep12343658.

[75] Lee HJ, Jang YJ. Recent Understandings of Biology, Prophylaxis and Treatment Strategies for Hypertrophic Scars and Keloids. *Int J Mol Sci* 2018;19. https://doi.org/10.3390/ijms19030711.

[76] Ghazawi FM, Zargham R, Gilardino MS, Sasseville D, Jafarian F. Insights into the Pathophysiology of Hypertrophic Scars and Keloids: How Do They Differ? *Adv Skin Wound Care* 2018;31:582–95. https://doi.org/10.1097/01.asw.0000527576.27489.0f.

[77] Shao DD, Suresh R, Vakil V, Gomer RH, Pilling D. Pivotal Advance: Th-1 Cytokines Inhibit, and Th-2 Cytokines Promote Fibrocyte Differentiation. *J Leukoc Biol* 2008;83:1323–33. https://doi.org/10.1189/jlb.1107782.

[78] Wynn TA. Fibrotic Disease and the T(H)1/T(H)2 Paradigm. *Nat Rev Immunol* 2004;4:583–94. https://doi.org/10.1038/nri1412.

[79] Wang JF, Jiao H, Stewart TL, Shankowsky HA, Scott PG, Tredget EE. Increased TGF-Beta-Producing CD4+ T Lymphocytes in Postburn Patients and Their Potential Interaction with Dermal Fibroblasts in Hypertrophic Scarring. *Wound Repair Regen* 2007;15:530–9. https://doi.org/10.1111/j.1524-475x.2007.00261.x.

[80] Gawronska-Kozak B, Bogacki M, Rim JS, Monroe WT, Manuel JA. Scarless Skin Repair in Immunodeficient Mice. *Wound Repair Regen* 2006;14:265–76. https://doi.org/10.1111/j.1743-6109.2006.00121.x.

[81] Short WD, Wang X, Keswani SG. The Role of T Lymphocytes in Cutaneous Scarring. *Adv Wound Care* 2022;11:121–31. https://doi.org/10.1089/wound.2021.0059.

[82] Mikhal'Chik E v., Piterskaya JA, Budkevich LY, Pen'Kov LY, Facchiano A, de Luca C, et al. Comparative Study of Cytokine Content in the Plasma And Wound Exudate from Children With Severe Burns. *Bull Exp Biol Med* 2009;148:771–5. https://doi.org/10.1007/s10517-010-0813-7.

[83] Bergquist M, Hästbacka J, Glaumann C, Freden F, Huss F, Lipcsey M. The Time-Course of the Inflammatory Response to Major Burn Injury and Its Relation to Organ Failure and Outcome. *Burns* 2019;45:354–63. https://doi.org/10.1016/j.burns.2018.09.001.

[84] Prager MD, Sabeh F, Baxter CR, Atiles L, Hartline B. Dipeptidyl Peptidase IV and Aminopeptidase in Burn Wound Exudates: Implications for Wound Healing. *J Trauma* 1994;36:629–33. https://doi.org/10.1097/00005373-199405000-00005.

[85] Midwood KS, Piccinini AM. DAMPening Inflammation by Modulating TLR Signalling. *Mediators Inflamm* 2010;2010. https://doi.org/10.1155/2010/672395.

[86] Janeway CA, Medzhitov R. Innate Immune Recognition. *Annu Rev Immunol* 2002;20:197–216. https://doi.org/10.1146/annurev.immunol.20.083001.084359.

[87] Kenny EF, O'Neill LAJ. Signalling Adaptors Used by Toll-Like Receptors: An Update. *Cytokine* 2008;43:342–9. https://doi.org/10.1016/j.cyto.2008.07.010.

[88] Seki E, de Minicis S, Österreicher CH, Kluwe J, Osawa Y, Brenner DA, et al. TLR4 Enhances TGF-Beta Signaling and Hepatic Fibrosis. *Nat Med* 2007;13:1324–32. https://doi.org/10.1038/nm1663.

[89] Isayama F, Hines IN, Kremer M, Milton RJ, Byrd CL, Perry AW, et al. LPS Signaling Enhances Hepatic Fibrogenesis Caused by Experimental Cholestasis in Mice. *Am J Physiol Gastrointest Liver Physiol* 2006;290. https://doi.org/10.1152/ajpgi.00405.2005.

[90] Watanabe A, Hashmi A, Gomes DA, Town T, Badou A, Flavell RA, et al. Apoptotic Hepatocyte DNA Inhibits Hepatic Stellate Cell Chemotaxis via Toll-Like Receptor 9. *Hepatology* 2007;46:1509–18. https://doi.org/10.1002/hep.21867.

[91] Wang JF, Hori K, Ding J, Huang Y, Kwan P, Ladak A, et al. Toll-Like Receptors Expressed by Dermal Fibroblasts Contribute to Hypertrophic Scarring. *J Cell Physiol* 2011;226:1265–73. https://doi.org/10.1002/jcp.22454.

[92] Crompton R, Williams H, Ansell D, Campbell L, Holden K, Cruickshank S, et al. Oestrogen Promotes Healing in a Bacterial LPS Model of Delayed Cutaneous Wound Repair. *Lab Invest* 2016;96:439–49. https://doi.org/10.1038/labinvest.2015.160.

[93] Qian LW, Fourcaudot AB, Yamane K, You T, Chan RK, Leung KP. Exacerbated and Prolonged Inflammation Impairs Wound Healing and Increases Scarring. *Wound Repair Regen* 2016;24:26–34. https://doi.org/10.1111/wrr.12381.

[94] Akira S, Takeda K. Toll-Like Receptor Signalling. *Nature Rev Immunol* 2004 4:7 2004;4:499–511. https://doi.org/10.1038/nri1391.

[95] Holzer-Geissler JCJ, Schwingenschuh S, Zacharias M, Einsiedler J, Kainz S, Reisenegger P, et al. The Impact of Prolonged Inflammation on Wound Healing. *Biomedicines* 2022;10. https://doi.org/10.3390/biomedicines10040856.

[96] van der Fits L, Mourits S, Voerman JSA, Kant M, Boon L, Laman JD, et al. Imiquimod-Induced Psoriasis-Like Skin Inflammation in Mice Is Mediated via The IL-23/IL-17 Axis. *J Immunol* 2009;182:5836–45. https://doi.org/10.4049/jimmunol.0802999.

[97] Monguió-Tortajada M, Franquesa M, Sarrias MR, Borràs FE. Low Doses of LPS Exacerbate the Inflammatory Response and Trigger Death on TLR3-Primed Human Monocytes. *Cell Death Dis* 2018;9. https://doi.org/10.1038/s41419-018-0520-2.

[98] Kamp DW. Idiopathic Pulmonary Fibrosis: the Inflammation Hypothesis Revisited. *Chest* 2003;124:1187–90. https://doi.org/10.1378/chest.124.4.1187.

[99] Armour A, Scott PG, Tredget EE. Cellular and Molecular Pathology of HTS: Basis for Treatment. *Wound Repair Regen* 2007;15 Suppl 1. https://doi.org/10.1111/j.1524-475x.2007.00219.x.

[100] Bullard KM, Longaker MT, Lorenz HP. Fetal Wound Healing: Current Biology. *World J Surg* 2003;27:54–61. https://doi.org/10.1007/s00268-002-6737-2.

[101] Lichtman MK, Otero-Vinas M, Falanga V. Transforming Growth Factor Beta (TGF-β) Isoforms in Wound Healing and Fibrosis. *Wound Repair Regen* 2016;24:215–22. https://doi.org/10.1111/wrr.12398.

[102] Xia W, Phan TT, Lim IJ, Longaker MT, Yang GP. Complex Epithelial-Mesenchymal Interactions Modulate Transforming Growth Factor-Beta Expression in Keloid-Derived Cells. *Wound Repair Regen* 2004;12:546–56. https://doi.org/10.1111/j.1067-1927.2004.012507.x.

[103] Schmid P, Itin P, Cherry G, Bi C, Cox DA. Enhanced Expression of Transforming Growth Factor-Beta Type I and Type II Receptors in Wound Granulation Tissue and Hypertrophic Scar. *Am J Pathol* 1998;152:485.

[104] Bock O, Yu H, Zitron S, Bayat A, Ferguson MWJ, Mrowietz U. Studies of Transforming Growth Factors Beta 1-3 and Their Receptors I and II in Fibroblast of Keloids and Hypertrophic Scars. *Acta Derm Venereol* 2005;85:216–20. https://doi.org/10.1080/00015550410025453.

[105] Lu L, Saulis AS, Liu WR, Roy NK, Chao JD, Ledbetter S, et al. The Temporal Effects of Anti-TGF-Beta1, 2, and 3 Monoclonal Antibody on Wound Healing and Hypertrophic Scar Formation. *J Am Coll Surg* 2005;201:391–7. https://doi.org/10.1016/j.jamcollsurg.2005.03.032.

[106] Shah M, Foreman DM, Ferguson MW. Neutralisation of TGF-Beta 1 and TGF-Beta 2 or Exogenous Addition of TGF-Beta 3 to Cutaneous Rat Wounds Reduces Scarring. *J Cell Sci* 1995;108 (Pt 3):985–1002. https://doi.org/10.1242/jcs.108.3.985.

[107] Shah M, Foreman DM, Ferguson MWJ. Control of Scarring in Adult Wounds by Neutralising Antibody to Transforming Growth Factor Beta. *Lancet* 1992;339:213–4. https://doi.org/10.1016/0140-6736(92)90009-r.

[108] Su CW, Alizadeh K, Boddie A, Lee RC. The Problem Scar. *Clin Plast Surg* 1998;25:451–65. https://doi.org/10.1016/s0094-1298(20)32476-7.

[109] Bran GM, Goessler UR, Hormann K, Riedel F, Sadick H. Keloids: Current Concepts of Pathogenesis (Review). *Int J Mol Med* 2009;24:283–93. https://doi.org/10.3892/ijmm_00000231.

[110] Uchida G, Yoshimura K, Kitano Y, Okazaki M, Harii K. Tretinoin Reverses Upregulation of Matrix Metalloproteinase-13 in Human Keloid-Derived Fibroblasts. *Exp Dermatol* 2003;12 Suppl 2:35–42. https://doi.org/10.1034/j.1600-0625.12.s2.6.x.

[111] Ogawa R. Mechanobiology of Scarring. *Wound Repair Regen* 2011;19 Suppl 1:s2–9. https://doi.org/10.1111/j.1524-475x.2011.00707.x.

[112] Ogawa R, Okai K, Tokumura F, Mori K, Ohmori Y, Huang C, et al. The Relationship between Skin Stretching/Contraction and Pathologic Scarring: The Important Role of Mechanical Forces in Keloid Generation. *Wound Repair Regen* 2012;20:149–57. https://doi.org/10.1111/j.1524-475x.2012.00766.x.

[113] Aarabi S, Bhatt KA, Shi Y, Paterno J, Chang EI, Loh SA, et al. Mechanical Load Initiates Hypertrophic Scar Formation through Decreased Cellular Apoptosis. *FASEB J* 2007;21:3250–61. https://doi.org/10.1096/fj.07-8218com.

[114] Akaishi S, Akimoto M, Ogawa R, Hyakusoku H. The Relationship between Keloid Growth Pattern and Stretching Tension: Visual Analysis Using The Finite Element Method. *Ann Plast Surg* 2008;60:445–51. https://doi.org/10.1097/sap.0b013e3181238dd7.

[115] Huang C, Akaishi S, Ogawa R. Mechanosignaling Pathways in Cutaneous Scarring. *Arch Dermatol Res* 2012;304:589–97. https://doi.org/10.1007/s00403-012-1278-5.

[116] Sen CK, Roy S. Oxygenation State As A Driver of Myofibroblast Differentiation and Wound Contraction: Hypoxia Impairs Wound Closure. *J Invest Dermatol* 2010;130:2701–3. https://doi.org/10.1038/jid.2010.316.

[117] Nauta TD, van Hinsbergh VWM, Koolwijk P. Hypoxic Signaling During Tissue Repair and Regenerative Medicine. *Int J Mol Sci* 2014;15:19791. https://doi.org/10.3390/ijms151119791.

[118] Steinbrech DS, Mehrara BJ, Chau D, Rowe NM, Chin G, Lee T, et al. Hypoxia Upregulates VEGF Production in Keloid Fibroblasts. *Ann Plast Surg* 1999;42:514–20. https://doi.org/10.1097/00000637-199905000-00009.

[119] Ueda K, Yasuda Y, Furuya E, Oba S. Inadequate Blood Supply Persists in Keloids. *Scand J Plast Reconstr Surg Hand Surg* 2004;38:267–71. https://doi.org/10.1080/02844310410029552.

[120] Zhao B, Guan H, Liu JQ, Zheng Z, Zhou Q, Zhang J, et al. Hypoxia Drives The Transition of Human Dermal Fibroblasts to A Myofibroblast-Like Phenotype via The TGF-β1/Smad3 Pathway. *Int J Mol Med* 2017;39:153–9. https://doi.org/10.3892/ijmm.2016.2816.

[121] Nischwitz SP, Rauch K, Luze H, Hofmann E, Draschl A, Kotzbeck P, et al. Evidence-Based Therapy in Hypertrophic Scars: An Update of A Systematic Review. *Wound Repair and Regen* 2020;28:656. https://doi.org/10.1111/wrr.12839.

[122] American Society of Plastic Surgeons. ASPS Evidence Rating Scales. Accessed on: AUG 11th 2023 via: https://www.plasticsurgery.org/documents/medical-professionals/health-policy/evidence-practice/ASPS-Scale-for-Grading-Recommendations.pdf.

[123] Evans D. Hierarchy of Evidence: A Framework for Ranking Evidence Evaluating Healthcare Interventions. *J Clin Nurs* 2003;12:77–84. https://doi.org/10.1046/j.1365-2702.2003.00662.x.

[124] Kafka M, Collins V, Kamolz LP, Rappl T, Branski LK, Wurzer P. Evidence of Invasive and Noninvasive Treatment Modalities for Hypertrophic Scars: A Systematic Review. *Wound Repair Regen* 2017;25:139–44. https://doi.org/10.1111/wrr.12507.

[125] Ogawa R. The Most Current Algorithms for The Treatment and Prevention of Hypertrophic Scars and Keloids. *Plast Reconstr Surg* 2010;125:557–68. https://doi.org/10.1097/prs.0b013e3181c82dd5.

[126] Mustoe TA, Cooter RD, Gold MH, Hobbs FDR, Ramelet AA, Shakespeare PG, et al. International Clinical Recommendations on Scar Management. *Plast Reconstr Surg* 2002;110:560–71. https://doi.org/10.1097/00006534-200208000-00031.

[127] Abedini R, Sasani P, Mahmoudi HR, Nasimi M, Teymourpour A, Shadlou Z. Comparison of Intralesional Verapamil Versus Intralesional Corticosteroids in Treatment of Keloids and Hypertrophic Scars: A Randomized Controlled Trial. *Burns* 2018;44:1482–8. https://doi.org/10.1016/j.burns.2018.05.005.

[128] Ali K, Tayyaba F, Tabassum HM. Comparison between The Efficacy of Intra-Lesional Triamcenolone and Combination of Triamcinolone with 5-Fluorouracil in The Treatment of Keloid and Hypertrophic Scars. *Pak J Med Health Sci* 2016;10:578–81.

[129] Khan MA, Bashir MM, Khan FA. Intralesional Triamcinolone Alone and in Combination with 5-Fluorouracil for The Treatment of Keloid and Hypertrophic Scars. *J Pak Med Assoc* 2014;64:1003–7.

[130] Khalid FA, Mehrose MY, Saleem M, Yousaf MA, Mujahid AM, Rehman SU, et al. Comparison of Efficacy and Safety of Intralesional Triamcinolone and Combination of Triamcinolone with 5-Fluorouracil in The Treatment of Keloids and Hypertrophic Scars: Randomised Control Trial. *Burns* 2019;45:69–75. https://doi.org/10.1016/j.burns.2018.08.011.

[131] Li-Tsang CWP, Zheng YP, Lau JCM. A Randomized Clinical Trial to Study The Effect of Silicone Gel Dressing and Pressure Therapy on Posttraumatic Hypertrophic Scars. *J Burn Care Res* 2010;31:448–57. https://doi.org/10.1097/bcr.0b013e3181db52a7.

[132] Nedelec B, Couture MA, Calva V, Poulin C, Chouinard A, Shashoua D, et al. Randomized Controlled Trial of The Immediate and Long-Term Effect of Massage on Adult Postburn Scar. *Burns* 2019;45:128–39. https://doi.org/10.1016/j.burns.2018.08.018.

[133] Mohammadi AA, Parand A, Kardeh S, Janati M, Mohammadi S. Efficacy of Topical Enalapril in Treatment of Hypertrophic Scars. *World J Plast Surg* 2018;7:326–31. https://doi.org/10.29252/wjps.7.3.326.

[134] Momeni M, Hafezi F, Rahbar H, Karimi H. Effects of Silicone Gel on Burn Scars. *Burns* 2009;35:70–4. https://doi.org/10.1016/j.burns.2008.04.011.

[135] Blome-Eberwein S, Gogal C, Weiss MJ, Boorse D, Pagella P. Prospective Evaluation of Fractional CO2 Laser Treatment of Mature Burn Scars. *J Burn Care Res* 2016;37:379–87. https://doi.org/10.1097/bcr.0000000000000383.

[136] Park GS, An MK, Yoon JH, Park SS, Koh SH, Mauro TM, et al. Botulinum Toxin Type A Suppresses Pro-Fibrotic Effects via The JNK Signaling Pathway in Hypertrophic Scar Fibroblasts. *Arch Dermatol Res* 2019;311:807–14. https://doi.org/10.1007/s00403-019-01975-0.

[137] Zhibo X, Miaobo Z. Intralesional Botulinum Toxin Type A Injection as A New treatment Measure for Keloids. *Plast Reconstr Surg* 2009;124. https://doi.org/10.1097/prs.0b013e3181b98ee7.

[138] Xiao Z, Zhang F, Cui Z. Treatment of Hypertrophic Scars with Intralesional Botulinum Toxin Type A Injections: A Preliminary Report. *Aesthetic Plast Surg* 2009;33:409–12. https://doi.org/10.1007/s00266-009-9334-z.

[139] Wang X, Chen X, Xiao Z. Effects of Botulinum Toxin Type A on Expression of Genes in Keloid Fibroblasts. *Aesthet Surg J* 2014;34:154–9. https://doi.org/10.1177/1090820x13482938.

[140] Ojeh N, Bharatha A, Gaur U, Forde AL. Keloids: Current and Emerging Therapies. *Scars Burn Heal* 2020;6:205951312094049. https://doi.org/10.1177/2059513120940499.

[141] Bojanic C, To K, Hatoum A, Shea J, Seah KTM, Khan W, et al. Mesenchymal Stem Cell Therapy in Hypertrophic and Keloid Scars. *Cell Tissue Res* 2021;383:915–30. https://doi.org/10.1007/s00441-020-03361-z.

[142] Sawhney CP. Amniotic Membrane as A Biological Dressing in The Management of Burns. *Burns* 1989;15:339–42. https://doi.org/10.1016/0305-4179(89)90015-6.

[143] Ravishanker R, Bath AS, Roy R. "Amnion Bank" - The Use of Long Term Glycerol Preserved Amniotic Membranes in The Management of Superficial and Superficial Partial Thickness Burns. *Burns* 2003;29:369–74. https://doi.org/10.1016/s0305-4179(02)00304-2.

[144] Simon F, Bergeron D, Larochelle S, Lopez-Vallé CA, Genest H, Armour A, et al. Enhanced Secretion of TIMP-1 by Human Hypertrophic Scar Keratinocytes Could Contribute to Fibrosis. *Burns* 2012;38:421–7. https://doi.org/10.1016/j.burns.2011.09.001.

[145] Mohammadi A, Eskandari S, Johari H, Rajabnejad A. Using Amniotic Membrane as A Novel Method to Reduce Post-Burn Hypertrophic Scar Formation: A Prospective Follow-up Study. *J Cutan Aesthet Surg* 2017;10:13–7. https://doi.org/10.4103/jcas.jcas_109_16.

[146] Williams EA, Thaller SR. The Role of Fat Grafting in the Treatment of Keloid Scars and Venous Ulcers. *J Craniofac Surg* 2019;30:696–7. https://doi.org/10.1097/scs.0000000000005208.

[147] Lee G, Hunter-Smith DJ, Rozen WM. Autologous Fat Grafting in Keloids and Hypertrophic Scars: A Review. *Scars Burn Heal* 2017;3:205951311770015. https://doi.org/10.1177/2059513117700157.

[148] da Silva VZ, Neto AA, de Souza Horácio G, de Andrade GAM, Procópio LD, Coltro PS, et al. Evidences of Autologous Fat Grafting for The Treatment of Keloids and Hypertrophic Scars. *Rev Assoc Med Bras* 2016;62:862–6. https://doi.org/10.1590/1806-9282.62.09.862.

[149] Pallua N, Baroncini A, Alharbi Z, Stromps JP. Improvement of Facial Scar Appearance and Microcirculation by Autologous Lipofilling. *J Plast Reconstr Aesthet Surg* 2014;67:1033–7. https://doi.org/10.1016/j.bjps.2014.04.030.

[150] Fan C, Dong Y, Xie Y, Su Y, Zhang X, Leavesley D, et al. Shikonin Reduces TGF-β1-Induced Collagen Production and Contraction in Hypertrophic Scar-Derived Human Skin Fibroblasts. *Int J Mol Med* 2015;36:985–91. https://doi.org/10.3892/ijmm.2015.2299.

[151] Shi-Wen X, Thompson K, Khan K, Liu S, Murphy-Marshman H, Baron M, et al. Focal Adhesion Kinase and Reactive Oxygen Species Contribute to The Persistent Fibrotic Phenotype of Lesional Scleroderma Fibroblasts. *Rheumatology (Oxford)* 2012;51:2146–54. https://doi.org/10.1093/rheumatology/kes234.

[152] Ramos MLC, Gragnani A, Ferreira LM. Is There An Ideal Animal Model to Study Hypertrophic Scarring? *J Burn Care Res* 2008;29:363–8. https://doi.org/10.1097/bcr.0b013e3181667557.

[153] Finnerty CC, Jeschke MG, Branski LK, Barret JP, Dziewulski P, Herndon DN. Hypertrophic Scarring: The Greatest Unmet Challenge after Burn Injury. *Lancet* 2016;388:1427–36. https://doi.org/10.1016/s0140-6736(16)31406-4.

[154] Luze H, Kotzbeck P, Nischwitz SP, Kamolz LP. Importance of Accurate and Reproducible Animal Models for Burn Wounds. *Burns* 2020;46:1479–80. https://doi.org/10.1016/j.burns.2020.04.010.

[155] van den Broek LJ, Limandjaja GC, Niessen FB, Gibbs S. Human Hypertrophic and Keloid Scar Models: Principles, Limitations and Future Challenges from A Tissue Engineering Perspective. *Exp Dermatol* 2014;23:382–6. https://doi.org/10.1111/exd.12419.

[156] Derderian CA, Bastidas N, Lerman OZ, Bhatt KA, Lin SE, Voss J, et al. Mechanical Strain Alters Gene Expression in An in Vitro Model of Hypertrophic Scarring. *Ann Plast Surg* 2005;55:69–75. https://doi.org/10.1097/01.sap.0000168160.86221.e9.

[157] Ahlfors JEW, Billiar KL. Biomechanical and Biochemical Characteristics of A Human Fibroblast-Produced and Remodeled Matrix. *Biomaterials* 2007;28:2183–91. https://doi.org/10.1016/j.biomaterials.2006.12.030.

[158] Butler PD, Ly DP, Longaker MT, Yang GP. Use of Organotypic Coculture to Study Keloid Biology. *Am J Surg* 2008;195:144–8. https://doi.org/10.1016/j.amjsurg.2007.10.003.

[159] van den Broek LJ, Niessen FB, Scheper RJ, Gibbs S. Development, Validation and Testing of A Human Tissue Engineered Hypertrophic Scar Model. *ALTEX* 2012;29:389–402. https://doi.org/10.14573/altex.2012.4.389.

[160] Rössler S, Nischwitz SP, Luze H, Holzer-Geissler JCJ, Zrim R, Kamolz LP. In Vivo Models for Hypertrophic Scars - A Systematic Review. Medicina (Kaunas) 2022;58. https://doi.org/10.3390/medicina58060736.

[161] Russell WMS, Burch RL. The Principles of Humane Experimental Technique. *Med J Austral* 1960;1:500. https://doi.org/10.5694/j.1326-5377.1960.tb73127.x.

[162] Flecknell P. Replacement, Reduction and Refinement. *ALTEX* 2002;19:73–8.

[163] Aksoy MH, Vargel I, Canter IH, Erk Y, Sargon M, Pinar A, et al. A New Experimental Hypertrophic Scar Model in Guinea Pigs. *Aesthetic Plast Surg* 2002;26:388–96. https://doi.org/10.1007/s00266-002-1121-z.

[164] Kimura T. Hairless Descendants of Mexican Hairless Dogs: An Experimental Model for Studying Hypertrophic Scars. *J Cutan Med Surg* 2011;15:329–39. https://doi.org/10.2310/7750.2011.10081.

[165] Sullivan TP, Eaglstein WH, Davis SC, Mertz P. The Pig as A Model for Human Wound Healing. *Wound Repair Regen* 2001;9:66–76. https://doi.org/10.1046/j.1524-475x.2001.00066.x.

[166] Silverstein P, Goodwin MN, Raulston GL, Pruitt BA. The Ultrastructure of Collagen: Its Relation to The Healing of Wounds and to The Management of Hypertrophic Scar. *Arch Surg* 1977:213–36. https://doi.org/10.1001/archsurg.1977.01370010105034.

[167] Harunari N, Zhu KQ, Armendariz RT, Deubner H, Muangman P, Carrougher GJ, et al. Histology of The Thick Scar on The Female, Red Duroc Pig: Final Similarities to Human Hypertrophic Scar. *Burns* 2006;32:669. https://doi.org/10.1016/j.burns.2006.03.015.

[168] Zhu KQ, Carrougher GJ, Gibran NS, Isik FF, Engrav LH. Review of The Female Duroc/Yorkshire Pig Model of Human Fibroproliferative Scarring. *Wound Repair Regen* 2007;15:S32. https://doi.org/10.1111/j.1524-475x.2007.00223.x.

[169] Zhu KQ, Engrav LH, Gibran NS, Cole JK, Matsumura H, Piepkorn M, et al. The Female, Red Duroc Pig as An Animal Model of Hypertrophic Scarring and The Potential Role of The Cones of Skin. *Burns* 2003;29:649–64. https://doi.org/10.1016/s0305-4179(03)00205-5.

[170] Travis TE, Mino MJ, Moffatt LT, Mauskar NA, Prindeze NJ, Ghassemi P, et al. Biphasic Presence of Fibrocytes in A Porcine Hypertrophic Scar Model. *J Burn Care Res* 2015;36:e125. https://doi.org/10.1097/bcr.0000000000000097.

[171] Yosha I, Tsahor H, Tikhonenko T, Naim R. Imiquimod Cream Formulation. *US Patents* US2007/0264317A1, 2007.

[172] FLIR ONE Pro Thermal Imaging Camera for Smartphones | Teledyne FLIR. Accessed on AUG 11th 2021 via: https://www.flir.eu/products/flir-one-pro/.

[173] TIVITA® Wound - Diaspective Vision. Accessed on AUG 11th 2023 via: https://diaspective-vision.com/en/produkt/tivita-wound/.

[174] Cohen J. A Power Primer. *Psychol Bull* 1992;112:155–9. https://doi.org/10.1037/0033-2909.112.1.155.

[175] Ogawa R, Dohi T, Tosa M, Aoki M, Akaishi S. The Latest Strategy for Keloid and Hypertrophic Scar Prevention and Treatment: The Nippon Medical School (NMS) Protocol. *J Nippon Med Sch* 2021;88. https://doi.org/10.1272/jnms.jnms.2021_88-106.

[176] Tredget EE, Levi B, Donelan MB. Biology and Principles of Scar Management and Burn Reconstruction. *Surg Clin North Am* 2014;94:793–815. https://doi.org/10.1016/j.suc.2014.05.005.

[177] Blackstone BN, Kim JY, McFarland KL, Sen CK, Supp DM, Bailey JK, et al. Scar Formation Following Excisional and Burn Injuries in A Red Duroc Pig Model. *Wound Repair Regen* 2017;25:618. https://doi.org/10.1111/wrr.12562.

[178] Zhu KQ, Engrav LH, Tamura RN, Cole JA, Muangman P, Carrougher GJ, et al. Further Similarities between Cutaneous Scarring in The Female, Red Duroc Pig and Human Hypertrophic Scarring. *Burns* 2004;30:518–30. https://doi.org/10.1016/j.burns.2004.02.005.

[179] Gallant CL, Olson ME, Hart DA. Molecular, Histologic, and Gross Phenotype of Skin Wound Healing in Red Duroc Pigs Reveals An Abnormal Healing Phenotype of Hypercontracted, Hyperpigmented Scarring. *Wound Repair Regen* 2004;12:305–19. https://doi.org/10.1111/j.1067-1927.2004.012311.x.

[180] Yun IS, Jeon YR, Lee WJ, Lee JW, Rah DK, Tark KC, et al. Effect of Human Adipose Derived Stem Cells on Scar Formation and Remodeling in A Pig Model: A Pilot Study. *Dermatol Surg* 2012;38:1678–88. https://doi.org/10.1111/j.1524-4725.2012.02495.x.

[181] Jimi S, Matsumura H. Effect of Chymase Activity on Skin Thickness in The Clawn Miniature Pig Hypertrophic Scarring Model. *J Plast Surg Hand Surg* 2017;51:446–52. https://doi.org/10.1080/2000656x.2017.1310733.

[182] Yun IS, Kang E, Ahn HM, Kim YO, Rah DK, Roh TS, et al. Effect of Relaxin Expression from An Alginate Gel-Encapsulated Adenovirus on Scar Remodeling in a Pig Model. *Yonsei Med J* 2019;60:854. https://doi.org/10.3349/ymj.2019.60.9.854.

[183] Chan QE, Harvey JG, Graf NS, Godfrey C, Holland AJA. The Correlation between Time to Skin Grafting and Hypertrophic Scarring Following an Acute Contact Burn in A Porcine Model. *J Burn Care Res* 2012;33:e43–8. https://doi.org/10.1097/bcr.0b013e31823356ce.

[184] Jandera V, Hudson DA, De Wet PM, Innes PM, Rode H. Cooling The Burn Wound: Evaluation of Different Modalities. *Burns* 2000;26:265–70. https://doi.org/10.1016/s0305-4179(99)00133-3.

[185] Cuttle L, Kempf M, Phillips GE, Mill J, Hayes MT, Fraser JF, et al. A Porcine Deep Dermal Partial Thickness Burn Model with Hypertrophic Scarring. *Burns* 2006;32:806–20. https://doi.org/10.1016/j.burns.2006.02.023.

[186] Rodriguez-Menocal L, Davis SS, Becerra S, Salgado M, Gill J, Valdes J, et al. Assessment of Ablative Fractional CO2 Laser and Er:YAG Laser to Treat Hypertrophic Scars in A Red Duroc Pig Model. J Burn Care Res 2018;39:954–62. https://doi.org/10.1093/jbcr/iry012.

[187] Nguyen JQ, Sanjar F, Rajasekhar Karna SL, Fourcaudot AB, Wang LJ, Silliman DT, et al. Comparative Transcriptome Analysis of Superficial and Deep Partial-Thickness Burn Wounds in Yorkshire vs Red Duroc Pigs. *J Burn Care Res* 2022;43:1299–311. https://doi.org/10.1093/jbcr/irac028.

[188] Mony MP, Harmon KA, Hess R, Dorafshar AH, Shafikhani SH. An Updated Review of Hypertrophic Scarring. *Cells* 2023;12:678. https://doi.org/10.3390/cells12050678.

[189] Zhu Z, Ding J, Tredget EE. The Molecular Basis of Hypertrophic Scars. *Burns Trauma* 2016;4:1–12. https://doi.org/10.1186/s41038-015-0026-4.

[190] Li H, Ziemer M, Stojanovic I, Saksida T, Maksimovic-Ivanic D, Mijatovic S, et al. Mesenchymal Stem Cells from Mouse Hair Follicles Reduce Hypertrophic Scarring in A Murine Wound Healing Model. *Stem Cell Rev Rep* 2022;18:2028–44. https://doi.org/10.1007/s12015-021-10288-7.

[191] Mistry R, Veres M, Issa F. A Systematic Review Comparing Animal and Human Scarring Models. *Front Surg* 2022;9. https://doi.org/10.3389/fsurg.2022.711094.

[192] Wang JF, Olson ME, Reno CR, Kulyk W, Wright JB, Hart DA. Molecular and Cell Biology of Skin Wound Healing in A Pig Model. *Connect Tissue Res* 2000;41:195–211. https://doi.org/10.3109/03008200009005290.

[193] Bollen PJA, Hansen AK, Olsen Alstrup AK. The Laboratory Swine. Second Edition. Boca Raton, Florida: CRC Press, Taylor & Francis Group; 2010.

[194] Singh K, Agrawal NK, Gupta SK, Mohan G, Chaturvedi S, Singh K. Increased Expression of Endosomal Members of Toll-Like Receptor Family Abrogates Wound Healing in Patients with Type 2 Diabetes Mellitus. *Int Wound J* 2016;13:927–35. https://doi.org/10.1111/iwj.12411.

[195] D'arpa P, Leung KP. Toll-Like Receptor Signaling in Burn Wound Healing and Scarring. *Adv Wound Care* 2017;6:330–43. https://doi.org/10.1089/wound.2017.0733.

[196] Chen L, Dipietro LA. Toll-Like Receptor Function in Acute Wounds. *Adv Wound Care* 2017;6:344. https://doi.org/10.1089/wound.2017.0734.

[197] Moiseenko A, Kheirollahi V, Chao CM, Ahmadvand N, Quantius J, Wilhelm J, et al. Origin and Characterization of Alpha Smooth Muscle Actin-Positive Cells During Murine Lung Development. *Stem Cells* 2017;35:1566–78. https://doi.org/10.1002/stem.2615.

[198] Camateros P, Tamaoka M, Hassan M, Marino R, Moisan J, Marion D, et al. Chronic Asthma-Induced Airway Remodeling Is Prevented by Toll-Like Receptor-7/8 Ligand S28463. *Am J Respir Crit Care Med* 2007;175:1241–9. https://doi.org/10.1164/rccm.200701-054oc.

[199] Drake MG, Kaufman EH, Fryer AD, Jacoby DB. The Therapeutic Potential of Toll-Like Receptor 7 Stimulation in Asthma. *Inflamm Allergy Drug Targets* 2012;11:484–91. https://doi.org/10.2174/187152812803589967.

[200] Ekman AK, Adner M, Cardell LO. Toll-Like Receptor 7 Activation Reduces The Contractile Response of Airway Smooth Muscle. *Eur J Pharmacol* 2011;652:145–51. https://doi.org/10.1016/j.ejphar.2010.11.009.

[201] Xie Y, Zhu KQ, Deubner H, Emerson DA, Carrougher GJ, Gibran NS, et al. The Microvasculature in Cutaneous Wound Healing in The Female Red Duroc Pig Is Similar to That in Human Hypertrophic Scars and Different from That in The Female Yorkshire Pig. *J Burn Care Res* 2007;28:500–6. https://doi.org/10.1097/bcr.0b013e318053dafe.

[202] Gallant-Behm CL, Tsao H, Reno C, Olson ME, Hart DA. Skin Wound Healing in The First Generation (F1) Offspring of Yorkshire and Red Duroc Pigs: Evidence for Genetic Inheritance of Wound Phenotype. *Burns* 2006;32:180–93. https://doi.org/10.1016/j.burns.2005.10.012.

[203] Germscheid NM, Thornton GM, Hart DA, Hildebrand KA. Wound Healing Differences Between Yorkshire and Red Duroc Porcine Medial Collateral Ligaments Identified by Biomechanical Assessment of Scars. *Clin Biomech* 2012;27:91–8. https://doi.org/10.1016/j.clinbiomech.2011.07.001.

[204] Harunari N, Engrav LH, Armendariz RT, Zhu KQ, Deubner H, Muangman P, et al. Comparison of Collagen Nodules and Mast Cells Between Human Hypertrophic Scar and Thick Scar of The Female Red Duroc Pig. *Wound Repair Regen* 2008;13:A4–27. https://doi.org/10.1111/j.1067-1927.2005.130215cq.x.

[205] Travis TE, Ghassemi P, Prindeze NJ, Moffatt LT, Carney BC, Alkhalil A, et al. Matrix Metalloproteinases Are Differentially Regulated and Responsive to Compression Therapy in A Red Duroc Model of Hypertrophic Scar. *Eplasty* 2018;18:e1.

[206] Gignac GE, Szodorai ET. Effect Size Guidelines for Individual Differences Researchers. *Pers Individ Dif* 2016;102:74–8. https://doi.org/10.1016/j.paid.2016.06.069.

[207] Sullivan T, Smith J, Kermode J, McIver E, Courtemanche DJ. Rating The Burn Scar. *J Burn Care Rehabil* 1990;11:256–60. https://doi.org/10.1097/00004630-199005000-00014.

[208] Tyack Z, Simons M, Spinks A, Wasiak J. A Systematic Review of The Quality of Burn Scar Rating Scales for Clinical and Research Use. *Burns* 2012;38:6–18. https://doi.org/10.1016/j.burns.2011.09.021.

[209] Roques C, Téot L. A Critical Analysis of Measurements Used to Assess and Manage Scars. *Int J Low Extrem Wounds* 2007;6:249–53. https://doi.org/10.1177/1534734607308249.

[210] Nguyen TA, Feldstein SI, Shumaker PR, Krakowski AC. A Review of Scar Assessment Scales. *Semin Cutan Med Surg* 2015;34:28–36. https://doi.org/10.12788/j.sder.2015.0125.

[211] Forbes-Duchart L, Marshall S, Strock A, Cooper JE. Determination of Inter-Rater Reliability in Pediatric Burn Scar Assessment Using A Modified Version of The Vancouver Scar Scale. *J Burn Care Res* 2007;28:460–7. https://doi.org/10.1097/bcr.0b013e318053d3bb.

[212] Celsus AC. De Medicina. *Self-Published* 47AD. Accessed on AUG 11th 2023 via https://www.loc.gov/resource/gdcwdl.wdl_11618/.

[213] Tracy RP. The Five Cardinal Signs of Inflammation: Calor, Dolor, Rubor, Tumor ... and Penuria (Apologies to Aulus Cornelius Celsus, De Medicina, c. A.D. 25). *J Gerontol A Biol Sci Med Sci* 2006;61:1051–2. https://doi.org/10.1093/gerona/61.10.1051.

[214] Monshipouri M, Aliahmad B, Ogrin R, Elder K, Anderson J, Polus B, et al. Thermal Imaging Potential and Limitations to Predict Healing of Venous Leg Ulcers. *Sci Rep* 2021;11. https://doi.org/10.1038/s41598-021-92828-2.

[215] Gethin G, O'Connor GM, Abedin J, Newell J, Flynn L, Watterson D, et al. Monitoring of pH and Temperature of Neuropathic Diabetic and Nondiabetic Foot Ulcers for 12 Weeks: An Observational Study. *Wound Repair Regen* 2018;26:251–6. https://doi.org/10.1111/wrr.12628.

[216] Li S, Mohamedi AH, Senkowsky J, Nair A, Tang L. Imaging in Chronic Wound Diagnostics. *Adv Wound Care* 2020;9:245. https://doi.org/10.1089/wound.2019.0967.

[217] Holzer JCJ, Tiffner K, Kainz S, Reisenegger P, Bernardelli de Mattos I, Funk M, et al. A Novel Human Ex-Vivo Burn Model and The Local Cooling Effect of A Bacterial Nanocellulose-Based Wound Dressing. *Burns* 2020;46:1924–32. https://doi.org/10.1016/j.burns.2020.06.024.

[218] Fierheller M, Sibbald RG. A Clinical Investigation into The Relationship Between Increased Periwound Skin Temperature and Local Wound Infection in Patients with Chronic Leg Ulcers. *Adv Skin Wound Care* 2010;23. https://doi.org/10.1097/01.asw.0000383197.28192.98.

[219] Lin YH, Chen YC, Cheng KS, Yu PJ, Wang JL, Ko NY. Higher Periwound Temperature Associated with Wound Healing of Pressure Ulcers Detected by Infrared Thermography. *J Clin Med* 2021;10. https://doi.org/10.3390/jcm10132883.

[220] Romanelli M, Miteva M, Romanelli P, Barbanera S, Dini V. Use of Diagnostics in Wound Management. *Curr Opin Support Palliat Care* 2013;7:106–10. https://doi.org/10.1097/spc.0b013e32835dc0fc.

[221] Salvo P, Dini V, Kirchhain A, Janowska A, Oranges T, Chiricozzi A, et al. Sensors and Biosensors for C-Reactive Protein, Temperature and pH, and Their Applications for Monitoring Wound Healing: A Review. *Sensors* (Basel) 2017;17. https://doi.org/10.3390/s17122952.

[222] Derwin R, Patton D, Avsar P, Strapp H, Moore Z. The Impact of Topical Agents and Dressing on pH and Temperature on Wound Healing: A Systematic, Narrative Review. *Int Wound J* 2022;19:1397–408. https://doi.org/10.1111/iwj.13733.

[223] Power G, Moore Z, O'Connor T. Measurement of pH, Exudate Composition and Temperature in Wound Healing: A Systematic Review. *J Wound Care* 2017;26:381–97. https://doi.org/10.12968/jowc.2017.26.7.381.

[224] Nischwitz SP, Luze H, Kamolz LP. Thermal Imaging via FLIR One – A Promising Tool in Clinical Burn Care and Research. *Burns* 2020;46:988–9. https://doi.org/10.1016/j.burns.2020.02.017.

[225] Cwajda-Białasik J, Mościcka P, Jawień A, Szewczyk MT. Infrared Thermography to Prognose The Venous Leg Ulcer Healing Process - Preliminary Results of A 12-Week, Prospective Observational Study. *Wound Repair Regen* 2020;28:224–33. https://doi.org/10.1111/wrr.12781.

[226] Derwin R, Patton D, Strapp H, Moore Z. Wound pH and Temperature as Predictors of Healing: An Observational Study. *J Wound Care* 2023;32:302–10. https://doi.org/10.12968/jowc.2023.32.5.302.

[227] Sen CK. Wound Healing Essentials: Let There Be Oxygen. *Wound Repair Regen* 2009;17:1–18. https://doi.org/10.1111/j.1524-475x.2008.00436.x.

[228] Schreml S, Szeimies RM, Prantl L, Karrer S, Landthaler M, Babilas P. Oxygen in Acute and Chronic Wound Healing. *Br J Dermatol* 2010;163:257–68. https://doi.org/10.1111/j.1365-2133.2010.09804.x.

[229] Tsolakidis S, Rosenauer R, Schmidhammer R, Pallua N, Rennekampff HO. Wireless Microcurrent Stimulation Improves Blood Flow in Burn Wounds. *Burns* 2022;48:1230–5. https://doi.org/10.1016/j.burns.2021.09.021.

[230] Eltzschig HK, Carmeliet P. Hypoxia and Inflammation. *N Engl J Med* 2011;364:656. https://doi.org/10.1056/nejmra0910283.

[231] Watts ER, Walmsley SR. Inflammation and Hypoxia: HIF and PHD Isoform Selectivity. *Trends Mol Med* 2019;25:33–46. https://doi.org/10.1016/j.molmed.2018.10.006.

[232] Taylor CT, Colgan SP. Regulation of Immunity and Inflammation by Hypoxia in Immunological Niches. *Nat Rev Immunol* 2017;17:774. https://doi.org/10.1038/nri.2017.103.

[233] Cerqueira MT, Pirraco RP, Santos TC, Rodrigues DB, Frias AM, Martins AR, et al. Human Adipose Stem Cells Cell Sheet Constructs Impact Epidermal Morphogenesis in Full-Thickness Excisional Wounds. *Biomacromolecules* 2013;14:3997–4008. https://doi.org/10.1021/bm4011062.

[234] Yannas I V., Lee E, Orgill DP, Skrabut EM, Murphy GF. Synthesis and Characterization of A Model Extracellular Matrix That Induces Partial Regeneration of Adult Mammalian Skin. *Proc Natl Acad Sci USA* 1989;86:933–7. https://doi.org/10.1073/pnas.86.3.933.

[235] Shen Z, Sun L, Liu Z, Li M, Cao Y, Han L, et al. Rete ridges: Morphogenesis, Function, Regulation, and Reconstruction. *Acta Biomater* 2023;155:19–34. https://doi.org/10.1016/j.actbio.2022.11.031.

[236] Limandjaja GC, van den Broek LJ, Waaijman T, van Veen HA, Everts V, Monstrey S, et al. Increased Epidermal Thickness and Abnormal Epidermal Differentiation in Keloid Scars. *Br J Dermatol* 2017;176:116–26. https://doi.org/10.1111/bjd.14844.

[237] Carney BC, Travis TE, Deldar R, Moffatt LT, Johnson LS, McLawhorn MM, et al. Rete Ridges are Decreased in Dyschromic Burn Hypertrophic Scar: A Histological Study. *J Burn Care Res* 2021;42:S27. https://doi.org/10.1093/jbcr/irab032.038.

[238] Hanson SE, Kleinbeck KR, Cantu D, Kim J, Bentz ML, Faucher LD, et al. Local Delivery of Allogeneic Bone Marrow and Adipose Tissue-Derived Mesenchymal Stromal Cells for Cutaneous Wound Healing in A Porcine Model. *J Tissue Eng Regen Med* 2016;10:E90. https://doi.org/10.1002/term.1700.

[239] Roig-Rosello E, Rousselle P. The Human Epidermal Basement Membrane: A Shaped and Cell Instructive Platform That Aging Slowly Alters. *Biomolecules* 2020;10:1607. https://doi.org/10.3390/biom10121607.

[240] Kotzbeck P, Hofmann E, Nischwitz SP, Kamolz L-P. Differentiating Local and Systemic Inflammatory Responses to Burn Injuries. *Burns* 2019;45:1934–5. https://doi.org/10.1016/j.burns.2018.11.006.

[241] Hattermann K, Picard S, Borgeat M, Leclerc P, Pouliot M, Borgeat P. The Toll-Like Receptor 7/8-Ligand Resiquimod (R-848) Primes Human Neutrophils for Leukotriene B4, Prostaglandin E2 and Platelet-Activating Factor Biosynthesis. *FASEB J* 2007;21:1575–85. https://doi.org/10.1096/fj.06-7457com.

[242] Janke M, Poth J, Wimmenauer V, Giese T, Coch C, Barchet W, et al. Selective and Direct Activation of Human Neutrophils but Not Eosinophils by Toll-Like Receptor 8. *J Allergy Clin Immunol* 2009;123:1026–33. https://doi.org/10.1016/j.jaci.2009.02.015.

[243] Chen H, Xu Y, Yang G, Zhang Q, Huang X, Yu L, et al. Mast Cell Chymase Promotes Hypertrophic Scar Fibroblast Proliferation and Collagen Synthesis by Activating TGF-β1/Smads Signaling Pathway. *Exp Ther Med* 2017;14:4438–42. https://doi.org/10.3892/etm.2017.5082.

[244] Wulff BC, Wilgus TA. Mast Cell Activity in The Healing Wound: More Than Meets The Eye? *Exp Dermatol* 2013;22:507–10. https://doi.org/10.1111/exd.12169.

[245] Kischer CW, Bunce H, Shetlar MR. Mast Cell Analyses in Hypertrophic Scars, Hypertrophic Scars Treated with Pressure and Mature Scars. *J Invest Dermatol* 1978;70:355–7. https://doi.org/10.1111/1523-1747.ep12543553.

[246] Bacci S. Fine Regulation During Wound Healing by Mast Cells, a Physiological Role Not Yet Clarified. *Int J Mol Sci* 2022;23. https://doi.org/10.3390/ijms23031820.

[247] Yussof SJM, Omar E, Pai DR, Sood S. Cellular Events and Biomarkers of Wound Healing. *Indian J Plast Surg* 2012;45:220. https://doi.org/10.4103/0970-0358.101282.

[248] Patel S, Maheshwari A, Chandra A. Biomarkers for Wound Healing and Their Evaluation. *J Wound Care* 2016;25:46–55. https://doi.org/10.12968/jowc.2016.25.1.46.

[249] Chin GC, Diegelmann RF, Schultz GS. Cellular and Molecular Regulation of Wound Healing. In: Falabella Anna F., Kirsner RS (editors). *Wound Healing*, Boca Raton: Taylor & Francis Group; 2005, p. 17–37.

[250] Trengove NJ, Bielefeldt-Ohmann H, Stacey MC. Mitogenic Activity and Cytokine Levels in Non-Healing and Healing Chronic Leg Ulcers. *Wound Repair Regen* 2000;8:13–25. https://doi.org/10.1046/j.1524-475x.2000.00013.x.

[251] Lysa B, Tartler U, Wolf R, Arenberger P, Benninghoff B, Ruzicka T, et al. Gene Expression in Actinic Keratoses: Pharmacological Modulation by Imiquimod. *Br J Dermatol* 2004;151:1150–9.
https://doi.org/10.1111/j.1365-2133.2004.06236.x.

[252] Szeimies RM, Bichel J, Ortonne JP, Stockfleth E, Lee J, Meng TC. A Phase II Dose-Ranging Study of Topical Resiquimod to Treat Actinic Keratosis. *Br J Dermatol* 2008;159:205–10.
https://doi.org/10.1111/j.1365-2133.2008.08615.x.

[253] Herndon DN, Barrow RE, Rutan RL, Rutan TC, Desai MH, Abston S. A Comparison of Conservative Versus Early Excision. Therapies in Severely Burned Patients. *Ann Surg* 1989;209:547.
https://doi.org/10.1097/00000658-198905000-00006.

[254] Cubison TCS, Pape SA, Parkhouse N. Evidence for The Link between Healing Time and The Development of Hypertrophic Scars (HTS) in Paediatric Burns due to Scald Injury. *Burns* 2006;32:992–9.
https://doi.org/10.1016/j.burns.2006.02.007.

[255] Monstrey S, Hoeksema H, Verbelen J, Pirayesh A, Blondeel P. Assessment of Burn Depth and Burn Wound Healing Potential. *Burns* 2008;34:761–9.
https://doi.org/10.1016/j.burns.2008.01.009.

[256] Couper KN, Blount DG, Riley EM. IL-10: The Master Regulator of Immunity to Infection. *J Immunol* 2008;180:5771–7.
https://doi.org/10.4049/jimmunol.180.9.5771.

[257] Ouyang W, Rutz S, Crellin NK, Valdez PA, Hymowitz SG. Regulation and Functions of The IL-10 Family of Cytokines in Inflammation and Disease. *Annu Rev Immunol* 2011;29:71–109.
https://doi.org/10.1146/annurev-immunol-031210-101312.

[258] Peranteau WH, Zhang L, Muvarak N, Badillo AT, Radu A, Zoltick PW, et al. IL-10 Overexpression Decreases Inflammatory Mediators and Promotes Regenerative Healing in An Adult Model of Scar Formation. *J Invest Dermatol* 2008;128:1852–60. https://doi.org/10.1038/sj.jid.5701232.

[259] Gordon A, Kozin ED, Keswani SG, Vaikunth SS, Katz AB, Zoltick PW, et al. Permissive Environment in Postnatal Wounds Induced by Adenoviral-Mediated Overexpression of The Anti-Inflammatory Cytokine Interleukin-10 Prevents Scar Formation. *Wound Repair Regen* 2008;16:70–9. https://doi.org/10.1111/j.1524-475x.2007.00326.x.

[260] Short WD, Steen E, Kaul A, Wang X, Olutoye OO, Vangapandu H V., et al. IL-10 Promotes Endothelial Progenitor Cell Infiltration and Wound Healing via STAT3. *FASEB J* 2022;36. https://doi.org/10.1096/fj.201901024rr.

[261] Liu BS, Cao Y, Huizinga TW, Hafler DA, Toes REM. TLR-Mediated STAT3 and ERK Activation Controls IL-10 Secretion by Human B Cells. *Eur J Immunol* 2014;44:2121–9. https://doi.org/10.1002/eji.201344341.

[262] Lombardi V, Van Overtvelt L, Horiot S, Moingeon P. Human Dendritic Cells Stimulated via TLR7 and/or TLR8 Induce The Sequential Production of Il-10, IFN-gamma, and IL-17A by Naive CD4+ T Cells. *J Immunol* 2009;182:3372–9. https://doi.org/10.4049/jimmunol.0801969.

[263] den Hartog G, van Osch TLJ, Vos M, Meijer B, Savelkoul HFJ, van Neerven RJJ, et al. BAFF Augments IgA2 and IL-10 Production by TLR7/8 Stimulated Total Peripheral Blood B Cells. *Eur J Immunol* 2018;48:283–92. https://doi.org/10.1002/eji.201646861.

[264] Lee MH, Gallo PM, Hooper KM, Corradetti C, Ganea D, Caricchio R, et al. The Cytokine Network Type I Interferon, IL-27 and IL-10 Is Augmented in Murine and Human Lupus. *J Leukoc Biol* 2019;106:967. https://doi.org/10.1002/jlb.3ab0518-180rr.

[265] Zhang T, Wang XF, Wang ZC, Lou D, Fang QQ, Hu YY, et al. Current Potential Therapeutic Strategies Targeting The TGF-β/Smad Signaling Pathway to Attenuate Keloid and Hypertrophic Scar Formation. *Biomed Pharmacother* 2020;129. https://doi.org/10.1016/j.biopha.2020.110287.

[266] de Gonzalo-Calvo D, Marchese M, Hellemans J, Betsou F, Skov Frisk NL, Dalgaard LT, et al. Consensus Guidelines for The Validation of qRT-PCR Assays in Clinical Research by the CardioRNA Consortium. *Mol Ther Methods Clin Dev* 2022;24:171. https://doi.org/10.1016/j.omtm.2021.12.007.

[267] Kamphuis W, Schneemann A, van Beek LM, Smit AB, Hoyng PF, Koya E. Prostanoid Receptor Gene Expression Profile in Human Trabecular Meshwork: A Quantitative Real-Time PCR Approach. *Invest Ophthalmol Vis Sci* 2001;42:3209–15.

[268] Jantsch J, Chakravortty D, Turza N, Prechtel AT, Buchholz B, Gerlach RG, et al. Hypoxia and Hypoxia-Inducible Factor-1 Alpha Modulate Lipopolysaccharide-Induced Dendritic Cell Activation and Function. *J Immunol* 2008;180:4697–705. https://doi.org/10.4049/jimmunol.180.7.4697.

[269] Spirig R, Djafarzadeh S, Regueira T, Shaw SG, von Garnier C, Takala J, et al. Effects of TLR Agonists on The Hypoxia-Regulated Transcription Factor HIF-1Alpha and Dendritic Cell Maturation under Normoxic Conditions. *PLoS One* 2010;5. https://doi.org/10.1371/journal.pone.0010983.

[270] Jantsch J, Wiese M, Schödel J, Castiglione K, Gläsner J, Kolbe S, et al. Toll-Like Receptor Activation and Hypoxia Use Distinct Signaling Pathways to Stabilize Hypoxia-Inducible Factor 1α (HIF1A) and Result in Differential HIF1A-Dependent Gene Expression. *J Leukoc Biol* 2011;90:551–62. https://doi.org/10.1189/jlb.1210683.

[271] Li SC, Lan KC, Hung HN, Huang WT, Lai YJ, Cheng HH, et al. HSPA4 Is a Biomarker of Placenta Accreta and Enhances the Angiogenesis Ability of Vessel Endothelial Cells. *Int J Mol Sci* 2022;23. https://doi.org/10.3390/ijms23105682.

[272] Lichtenauer M, Zimmermann M, Nickl S, Lauten A, Goebel B, Pistulli R, et al. Transient Hypoxia Leads to Increased Serum Levels of Heat Shock Protein-27, -70 and Caspase-Cleaved Cytokeratin 18. *Clin Lab* 2014;60:323–8. https://doi.org/10.7754/clin.lab.2013.130303.

[273] Park JM, Kim JW, Hahm KB. HSPA4, The "Evil Chaperone" of The HSP Family, Delays Gastric Ulcer Healing. *Dig Dis Sci* 2015;60:824–6. https://doi.org/10.1007/s10620-015-3597-9.

[274] Bellaye PS, Burgy O, Causse S, Garrido C, Bonniaud P. Heat Shock Proteins in Fibrosis and Wound Healing: Good or Evil? *Pharmacol Ther* 2014;143:119–32. https://doi.org/10.1016/j.pharmthera.2014.02.009.

[275] Atalay M, Oksala N, Lappalainen J, Laaksonen D, Sen C, Roy S. Heat Shock Proteins in Diabetes and Wound Healing. *Curr Protein Pept Sci* 2009;10:85–95. https://doi.org/10.2174/138920309787315202.

[276] McGarry T, Biniecka M, Veale DJ, Fearon U. Hypoxia, Oxidative Stress and Inflammation. *Free Radic Biol Med* 2018;125:15–24. https://doi.org/10.1016/j.freeradbiomed.2018.03.042.

[277] Semenza GL. Life with Oxygen. *Science* 2007;318:62–4. https://doi.org/10.1126/science.1147949.

[278] Rosenberger P, Schwab JM, Mirakaj V, Masekowsky E, Mager A, Morote-Garcia JC, et al. Hypoxia-Inducible Factor-Dependent Induction of Netrin-1 Dampens Inflammation Caused by Hypoxia. *Nat Immunol* 2009;10:195–202. https://doi.org/10.1038/ni.1683.

[279] Van De Groot F, Krijnen PAJ, Begieneman MPV, Ulrich MMW, Middelkoop E, Niessen HWM. Acute Inflammation Is Persistent Locally in Burn Wounds: A Pivotal Role for Complement and C-Reactive Protein. *J Burn Care Res* 2009;30:274–80. https://doi.org/10.1097/bcr.0b013e318198a252.

[280] Korkmaz HI, Ulrich MMW, Wieringen WN Van, Doğan H, Vlig M, Emmens RW, et al. C1 Inhibitor Administration Reduces Local Inflammation and Capillary Leakage, Without Affecting Long-term Wound Healing Parameters, in a Pig Burn Wound Model. *Antiinflamm Antiallergy Agents Med Chem* 2021;20:150–60. https://doi.org/10.2174/1871523019666200702101513.

[281] Mannes M, Schmidt CQ, Nilsson B, Ekdahl KN, Huber-Lang M. Complement As Driver of Systemic Inflammation and Organ Failure in Trauma, Burn, and Sepsis. *Semin Immunopathol* 2021;43:773. https://doi.org/10.1007/s00281-021-00872-x.

[282] Ogawa R. Keloid and Hypertrophic Scars Are the Result of Chronic Inflammation in The Reticular Dermis. *Int J Mol Sci* 2017;18. https://doi.org/10.3390/ijms18030606.

[283] Krishnan NM, Brown BJ, Davison SP, Mauskar N, Mino M, Jordan MH, et al. Reducing Wound Tension with Undermining or Imbrication - Do They Work? *Plast Reconstr Surg Glob Open* 2016;4. https://doi.org/10.1097/gox.0000000000000799.

[284] Parikh UM, Mentz J, Collier I, Davis MJ, Abu-Ghname A, Colchado D, et al. Strategies to Minimize Surgical Scarring: Translation of Lessons Learned from Bedside to Bench and Back. *Adv Wound Care* 2022;11:311–29. https://doi.org/10.1089/wound.2021.0010.

[285] Ferrucci L, Fabbri E. Inflammageing: Chronic Inflammation in Ageing, Cardiovascular Disease, and Frailty. *Nat Rev Cardiol* 2018;15:505. https://doi.org/10.1038/s41569-018-0064-2.

[286] Colboc H, Meaume S. Scar and Scarring in the Elderly. In: Téot L, Mustoe TA, Middelkoop E, Gauglitz GG, (editors). Textbook on Scar Management, Springer; 2020, p. 379–84. https://doi.org/10.1007/978-3-030-44766-3_44.

[287] Rabello FB, Souza CD, Farina JA. Update on Hypertrophic Scar Treatment. *Clinics* 2014;69:565–73. https://doi.org/10.6061/clinics/2014(08)11.

[288] Zhou S, Ding R, Meng F, Wang X, Zhuang Z, Quan J, et al. A Meta-Analysis of Genome-Wide Association Studies for Average Daily Gain and Lean Meat Percentage in Two Duroc Pig Populations. *BMC Genomics* 2021;22:1–13. https://doi.org/10.1186/s12864-020-07288-1.

[289] Lindenmann J, Kamolz L, Graier W, Smolle J, Smolle-Juettner FM. Hyperbaric Oxygen Therapy and Tissue Regeneration: A Literature Survey. Biomedicines 2022;10:3145. https://doi.org/10.3390/biomedicines10123145.

[290] Slotman GJ. Hyperbaric Oxygen in Systemic Inflammation ... HBO Is Not Just A Movie Channel Anymore. *Crit Care Med* 1998;26:1932-3. https://doi.org/10.1097/00003246-199812000-00002.